



UNIVERSIDADE DE BRASÍLIA
INSTITUTO DE GEOCIÊNCIAS

**COMPARTIMENTAÇÃO GEOLÓGICA E
GEOCRONOLÓGICA DOS TERRENOS DO
EMBASAMENTO NORTE DA FAIXA BRASÍLIA**

Tese de Doutorado

Nº 114

Pedro Filipe de Oliveira Cordeiro

Orientador:

Prof. Dr. CLAUDINEI GOUVEIA DE OLIVEIRA

Brasília, Fevereiro de 2014



UNIVERSIDADE DE BRASÍLIA
INSTITUTO DE GEOCIÊNCIAS

COMPARTIMENTAÇÃO GEOLÓGICA E GEOCRONOLÓGICA DOS TERRENOS DO EMBASAMENTO NORTE DA FAIXA BRASÍLIA

Pedro Filipe de Oliveira Cordeiro

Tese de Doutorado apresentada ao
Instituto de Geociências da Universidade
de Brasília como requisito parcial à
obtenção do título de Doutor em Geologia

Brasília, Fevereiro de 2014



UNIVERSIDADE DE BRASÍLIA
INSTITUTO DE GEOCIÊNCIAS

COMPARTIMENTAÇÃO GEOLÓGICA E GEOCRONOLÓGICA DOS TERRENOS DO EMBASAMENTO NORTE DA FAIXA BRASÍLIA

Tese de Doutorado

Nº 114

Pedro Filipe de Oliveira Cordeiro

Orientador: Prof. Dr. Claudinei Gouveia de Oliveira

Banca examinadora: Prof. Dr. Nilson Francisquini Botelho (UnB)

Prof. Dr. Reinhardt Adolfo Fuck (UnB)

Prof. Dr. Cláudio de Morrison Valeriano (UERJ)

Dr. Evandro Luiz Klein (CPRM)

Brasília, Fevereiro de 2014

“The scientist is not a person who gives the right answers, he's one who asks the right questions.”

Claude Lévi-Strauss

Agradecimentos

Ao glorioso Claudinei Oliveira que adotou um doutorando no meio do caminho e que precisou ouvir muita reclamação e atender inúmeros telefonemas. Obrigado professor pela paciência e, acima de tudo, pela amizade.

Aos meus pais, à minha irmã e ao pessoal da TCS pela torcida e pelo amor.

À Naelyan Wyvern, sem quem eu sequer teria cursado geologia, quanto mais me tornado Doutor nela.

Palavras não servem para expressar minha gratidão, meu respeito e meu amor por você.

Aos Deuses Antigos, especialmente a Hécate, por iluminarem as sendas da minha felicidade.

Resumo

O Maciço de Goiás é composto por terrenos arqueano-paleoproterozoicos que representam o embasamento da Faixa Brasília. O maciço é dividido de sudoeste para nordeste nos domínios Crixás-Goiás, Campinorte, Cavalcante-Arraias e Almas-Conceição do Tocantins com base em critérios petrográficos, geológicos, tectônicos e geocronológicos. Esta tese é dividida de forma a explorar dois tópicos principais: a definição do Arco Paleoproterozoico Campinorte e uma revisão regional do contexto tectônico de formação do Maciço de Goiás.

O Arco Campinorte é um arco de ilhas formado entre 2,19 e 2,07 Ga, pouco exposto, em contato com o Arco Magmático de Goiás pela Falha Rio dos Bois na Faixa Brasília Norte, Brasil Central. O arco é dividido em Suíte Pau de Mel, que inclui metatonalitos a metamonzogranitos, e rochas meta-vulcanossedimentares da Sequência Campinorte. Geoquímica de rocha total da Suíte Pau de Mel indica pelo menos três magmas parentais distintos compatíveis com assinaturas de arco vulcânico e que progridem a composições de termos monzograníticos mais evoluídos. Paragranulitos e granulitos maficos expostos na região também são parte do Arco Campinorte e foram gerados quando a bacia de *back arc* passou por *tectonic switching* e consequente afinamento litosférico de 2,14-2,09 Ga com pico de metamorfismo entre 2,11-2,08 Ga. Proximidade geográfica, idade máxima de sedimentação e a ocorrência de tipos de rocha similares, incluindo vulcanismo félscico, indicam que o Arco Campinorte e as faixas de *greenstone belt* de Crixás e Guarinos podem ter compartilhado a mesma fonte de sedimentos.

A comumente citada hipótese de que os domínios Campinorte e Crixás-Goiás representaram blocos alóctones durante o Ciclo Neoproterozoico Brasiliano é questionada com base em novos dados geocronológicos apresentados nesta tese e na reinterpretação de dados publicados na literatura geológica. Primeiramente, estudos sísmicos e gravimétricos sugerem que o forte contraste entre os domínios Campinorte e Cavalcante-Arraias, marcado em superfície pelo Empurrao Rio Maranhão, podem ser explicados por evento de delaminação Neoproterozoico da crosta inferior, afetando tanto orógenos brasileiros quanto o terreno contra o qual eles foram acrescionados, o Domínio Campinorte. Em segundo lugar, rochas do Arco Campinorte afloram ao longo

do traço do Empurrão Rio Maranhão e nenhuma rocha neoproterozoica sin-collisional foi descrita ao longo deste importante limite geológico. Em terceiro lugar, granitos mesoproterozoicos da Suprovíncia Tocantins intrudiram ambos os lados do Empurrão Rio Maranhão e, portanto, indicam que os dois domínios estavam amalgamados antes do Mesoproterozoico. Eventos de rifte contemporâneos no Maciço de Goiás e no Cráton São Francisco por volta de 1,77 Ga e 1,58 Ga sugerem que maciço e cráton podem ter sido parte do mesmo paleocontinente. A ocorrência de orógenos formados entre 2,2-2,0 Ga com pico metamórfico entre 2,12-2,05 Ga tanto no Maciço de Goiás quanto no Cráton São Francisco podem indicar que não apenas eles eram parte do mesmo paleocontinente como também foram amalgamados no mesmo ciclo tectônico. Essa tese propõe que este evento de amalgamamento responsável pela formação do Paleocontinente São Francisco entre 2,2-2,0 Ga seja chamado Evento Franciscano. O paleocontinente eventualmente tornou-se parte da massa continental Atlântica como um bloco estável durante o amalgamamento do Supercontinente Columbia entre 1,9-1,8 Ga.

Palavras chave: Tectônica do Paleoproterozóico, Maciço de Goiás, Faixa Brasília, Arco Magmático, granulitos

Abstract

The Goiás Massif is composed of Archean-Paleoproterozoic terranes that represent the Brasília Belt basement. The massif is divided from southwest to northeast into the Crixás-Goiás, Campinorte, Cavalcante-Arraias and Almas-Conceição do Tocantins domains based on petrographical and geochronological criteria. This thesis is divided into exploring two main points; the definition of the Paleoproterozoic Campinorte Arc and the regional review of the Goiás Massif tectonic framework.

The Campinorte Arc is a poorly exposed 2.19 to 2.07 Ga Paleoproterozoic island arc in contact with the Goiás Magmatic Arc by the Rio dos Bois Fault in the northern Brasília Belt, Central Brazil. The arc is divided into Pau de Mel Suite, which includes metatonalites to metamonzogranites, and the Campinorte Volcano-sedimentary Sequence. Pau de Mel Suite whole rock geochemistry indicates at least three separate coeval parental magmas compatible with volcanic arc signatures that trend from an intraplate setting toward more evolved monzogranitic composition. Paragranulites and mafic granulites exposed in the region are also part of the Campinorte Arc and were generated when the back arc basin underwent tectonic switching and consequent lithospheric thinning from 2.14 to 2.09 Ga with metamorphic peak from 2.11 to 2.08 Ga. Geographic proximity, coeval maximum sedimentation and the occurrence of similar rock types including felsic volcanism indicate that the Campinorte Arc and the neighbouring Crixás/Guarinos greenstone belts may have shared the same source of sediments.

The commonly cited hypothesis that the Campinorte and Crixás-Goiás domains represented an allochthonous block during the Neoproterozoic Brasiliano Orogeny is questioned in this thesis based on new geochronology and reinterpretation of published data. First, seismic and gravimetric studies that suggest a sharp crustal thickness contrast between the Campinorte and Cavalcante-Arraias domains, and marked in surface by the Rio Maranhão Thrust, can be explained by a Neoproterozoic lower crust delamination affecting both Brasiliano orogens and the terrane they were accreted against, the Campinorte Domain. Second, Paleoproterozoic Campinorte Arc rocks crop out along the Rio Maranhão Thrust and no Neoproterozoic collisional rocks have been

reported along this important geological limit. Third, Tocantins Suprovince Mesoproterozoic granites intruded both sides of the Rio Maranhão Thrust and, therefore, indicate the two domains were amalgamated prior to the Mesoproterozoic. Coeval Goiás Massif and São Francisco Craton rifting events around 1.76 Ga and 1.58 Ga suggest they were actually part of the same paleoplate. The occurrence of 2.2 to 2.0 Ga orogens with metamorphic peak from 2.12 to 2.05 Ga in both the Goiás Massif and São Francisco Craton might suggest that not only they were part of the same plate but they also were assembled in the same tectonic cycle. This thesis proposes this amalgamation event to be responsible for the formation of the São Francisco Paleoplate itself from 2.2 to 2.0 Ga and henceforth named Franciscano Event. The plate eventually became part of the Atlantica Landmass as a stable block during the Columbia Supercontinent amalgamation from 1.9 to 1.8 Ga.

Key words: Paleoproterozoic tectonics, Goiás Massif, São Francisco Craton, magmatic arc, granulites

Conteúdo

Conteúdo.....	10
CAPÍTULO 1 – INTRODUÇÃO	12
1.1 Apresentação e objetivos.....	13
1.2 Geologia Regional	15
1.2.1 Nomenclatura e posicionamento tectônico do Maciço de Goiás.....	19
1.2.2 Compartimentação tectônica do Maciço de Goiás.....	25
CAPÍTULO 2 – O ARCO PALEOPROTEROZOICO CAMPINORTE: EVOLUÇÃO TECTÔNICA DE UM ORÓGENO PRÉ-COLUMBIA NO BRASIL CENTRAL	29
1. Introduction	31
2. Geological setting.....	33
2.1 Campinorte Sequence, Pau de Mel Suite and granulites.....	37
3. Analytical Procedures	42
4. Samples and results	44
5. Whole-rock geochemistry and petrogenetic implications.....	47
6. Discussion.....	51
6.1 Granulite Formation.....	51
6.2. Correlation with Crixás-Goiás metasedimentary rocks	53
7. Campinorte Arc evolution	56
8. Conclusions	60
Acknowledgements.....	60
References	62
CAPÍTULO 3 – ARCABOUÇO TECTÔNICO DO MACIÇO DE GOIÁS NO BRASIL CENTRAL: CONSEQUÊNCIAS PARA O CICLO DE AMALGAMAMENTO CONTINENTAL DE 2.2-2.0 Ga.....	79
1. Introduction	81
2. Geological overview	82
2.1. Northern Brasília Belt Basement - Goiás Massif	84
2.2. Campinorte Arc	89
3. Analytical Procedures	91
3.1. Samples and Results.....	93
4. Discussion.....	98

4.1. Campinorte Arc U-Pb and Hf isotopes data	98
4.2 Campinorte Arc data	100
4.3. The formation of the Goiás Massif and its links with the São Francisco Craton	101
5. Conclusions	111
References	113
CAPÍTULO 4 – DISCUSSÃO, CONCLUSÕES E RECOMENDAÇÕES DE TRABALHOS FUTUROS	130
4.1 – Discussão.....	131
4.1.1 – Definição do Arco Campinorte e formação de granulitos (Capítulo 2).....	131
4.1.2 – Correlação da Sequência Campinorte com rochas metassedimentares dos Greenstone Belts de Guarinos e Crixás.....	132
4.1.3 – A formação do Maciço de Goiás (Capítulo 3).....	133
4.1.4 O Evento Franciscano de 2.2-2.0 Ga	137
4.2 - Conclusões	140
4.3 - Recomendações de trabalhos posteriores	145
Referências.....	146

CAPÍTULO 1 – INTRODUÇÃO

1.1 Apresentação e objetivos

A presente tese de doutoramento tem como objetivo apresentar dados geoquímicos, geocronológicos e isotópicos de rochas coletadas na região compreendida entre as cidades de Campinorte, Niquelândia e Goianésia (Figura 1). Adicionalmente ela tem como objetivo apresentar os dados obtidos em conjunto com estudo aprofundado da literatura regional de modo a propor o quadro tectônico de formação e evolução geológica dos terrenos envolvidos.

Os terrenos do embasamento da Faixa Brasília norte têm recebido grande atenção nos últimos vinte anos com estudos localizados de mineralogia, geoquímica, geologia estrutural e econômica. No entanto, apesar do volume de dados obtidos, ainda não houve trabalho regional que compilasse toda essa informação e propusesse um modelo tectônico de formação e evolução desses terrenos. Parte da dificuldade na formação de um modelo é a grande diversidade geológica das rochas do embasamento e a interpretação de sua compartimentação. Outro fator complicador é a escassez de afloramentos em regiões de contato entre blocos de características geológicas distintas. Para poder fundamentar o modelo tectônico do embasamento da Faixa Brasília norte, esta tese inclui revisão bibliográfica de rochas da região e novos dados geocronológicos e geoquímicos de porções do embasamento, cujo conhecimento é escasso e que são chave para uma proposta inicial de compartimentação tectônica regional.

De forma individualizada, cada terreno que forma o embasamento da Faixa Brasília (que nesta tese é sinônimo para Maciço de Goiás) é bem compreendido, muito embora a nomenclatura desses terrenos, blocos ou maciços seja confusa, interpretativa e não uniforme. Com o objetivo de facilitar o entendimento da geologia, esta tese também propõe reavaliação da nomenclatura dos domínios que fazem parte do embasamento da Faixa Brasília em conjunto com a proposta do seu significado tectônico.

O terreno de maior destaque nesta tese será o Domínio Campinorte. Este domínio é parte do Maciço de Goiás, que segundo a nomenclatura proposta refere-se

ao conjunto de terrenos Arqueanos a Paleoproterozoicos do embasamento norte da Faixa Brasília. O Domínio Campinorte é situado entre o Arco Magmático de Goiás e os domínios Crixás-Goiás e Cavalcante-Arraias e até os trabalhos de Kuyumijian et al. (2004) e Giustina et al. (2009) era um dos terrenos menos compreendidos do Maciço de Goiás e, portanto, desconsiderado nos poucos modelos tectônicos regionais existentes. Os dados adicionais fornecidos nesta tese permitirão contextualizar essas rochas e preencher um vazio até então existente na compartimentação do Maciço de Goiás.

Esta tese é dividida em quatro capítulos. Capítulo 1 contém a introdução ao trabalho desenvolvido, os objetivos específicos do estudo e uma revisão da geologia e geofísica regional. Os capítulos 2 e 3 são constituidos pelos artigos “*The Paleoproterozoic Campinorte Arc: Tectonic evolution of a central Brazil pre-Columbia orogen*” e “*Central Brazil Goiás-Massif tectonic framework: implications for a 2.2-2.0 Ga continent wide amalgamation cycle*” a serem publicados em periódicos internacionais. O Capítulo 4 contém a síntese, integração da discussão dos artigos e a conclusão final da tese.

1.2 Geologia Regional

- a) A área de estudo encontra-se na Faixa Brasília da Província Tocantins (Almeida, 1967) um conjunto de rochas metassedimentares dobradas, arcos magmáticos e rochas associadas a rifte que foram geradas no Brasiliano durante a colisão de protocontinentes pré-neoproterozoicos. A Faixa Brasília norte é dividida com base em um zoneamento tectônico sugerido por Fuck et al. (1994), Pimentel et al. (2000), Dardenne (2000) e Valeriano et al. (2008): **Zona de Antepaís** que inclui sequências sedimentares autóctones ou parautóctones neoproterozoicas (grupos São João Del Rei, Carandaí e Bambuí).
- b) **Zona Externa** que inclui terrenos granito-greenstone Paleoproterozoicos (Terreno granito-greenstone de Almas-Dianópolis), sequências de rifte-marinhais paleo-mesoproterozoicas (grupos Araí e Paranoá), sequências metassedimentares neo-mesoproterozoicas de margem passiva ou de ambiente indeterminado (Andrelândia, Canastra, Vazante, Ibiá).
- c) **Zona Interna** abarca o Grupo Araxá, a porção oeste do Grupo Andrelândia e as rochas máficas toleíticas associadas, complexos ofiolíticos, fragmentos de embasamento, leucogranitos sin-colisionais e complexos neoproterozoicos de alto grau metamórfico (Anápolis-Itauçu, Uruaçu, Socorro-Guaxupé).
- d) **Maciço de Goiás** inclui complexos granito-gnaissicos Arqueanos, sequências meta-vulcanossedimentares e greenstone belts paleoproterozoicos, sequências meta-vulcanosedimentares mesoproterozoicas (Juscelândia, Palmeirópolis, Indaiánópolis), complexos mafico-ultramafico acamadados meso a neoproterozoicos.
- e) **Arco Magmático de Goiás** contém rochas metassedimentares, metavulcânicas, granitos e ortognaisses neoproterozoicos.

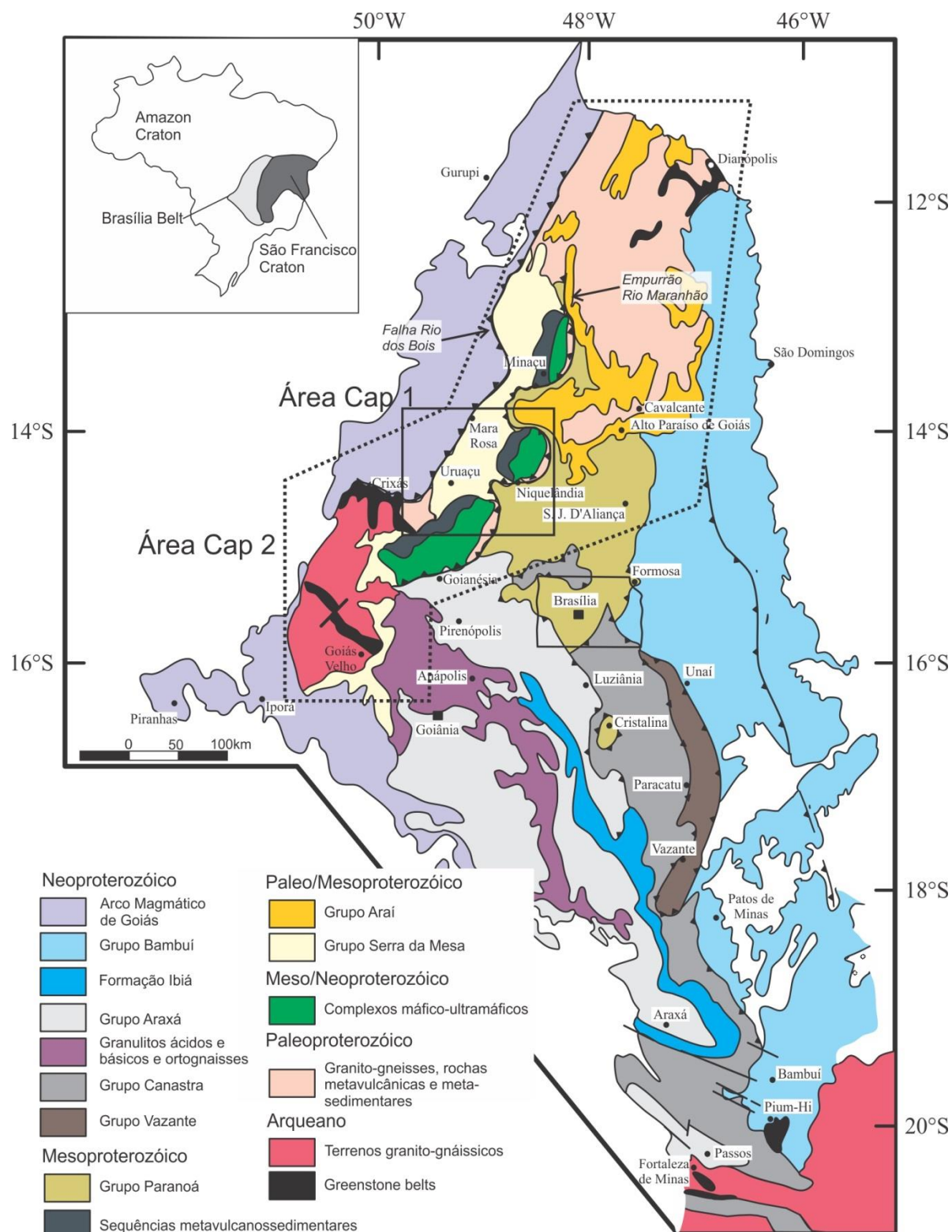


Figura 1 – Arcabouço Geológico da Faixa Brasília mostrando as áreas de enfoque dos artigos nesta tese (atualizado de Dardenne, 2000).

Segundo esse zoneamento a área de estudo do Capítulo 1 enfoca o conjunto de rochas agrupado por Kuyumijian et al. (2004) e Giustina et al. (2009) como a Sequência Campinorte e tonalitos-granodioritos associados da Suite Pau de Mel, enquanto a área do Capítulo 2 abarca todo o Maciço de Goiás. Adicionalmente, rochas granulíticas para- e ortoderivadas aflorantes na borda da represa Serra da Mesa são consideradas neste trabalho como formadas sob o mesmo evento tectônico. Com base nos dados geológicos, geocronológicos e geoquímicos desta tese, deu-se o nome de Arco Campinorte ao terreno formado pela Sequência Campinorte, Suite Pau de Mel e granulitos associados.

O Arco Campinorte na área tipo descrita por Kuyumijian et al. (2004), Oliveira et al. (2006) e Giustina et al. (2009) é composto predominantemente por quartzo-muscovita xisto com quantidades variáveis de rochas carbonáticas, quartzito, chert e lentes de gondito da Sequência Campinorte. Metatufo e metalapilli tufo subordinados afloram como corpos pequenos por entre rochas metassedimentares com raras rochas metavulcânicas felsicas. Idades U-Pb em zircão forneceram idades deposicionais máximas de ~2.2 Ga para a unidade metassedimentar e idade de cristalização de 2179 ± 4 Ma em grãos de zircão de um metatufo felsico (Giustina et al., 2009). Pelo menos dois eventos de deformação estão registrados nessas rochas de fácies xisto-verde. Acamadamento primário pode ser reconhecido em alguns afloramentos mas é mais provável que a estratigrafia original foi desfeita por deformação paleo-neoproterozoica (Oliveira et al., 2006). Xistos ultramáficos com talco, anfibólio e clorita, intensamente intemperizados, são interpretados como lascas tectônicas do assoalho oceânico obductadas durante a inversão da bacia.

Corpos elongados de até 12 km predominantemente metagranodioríticos, com metatalitolitos e metagranitos subordinados, da Suíte Pau de Mel ocorrem dentre rochas metassedimentares da Sequência Campinorte. Essa suite possui variados graus de deformação e relações de contato indeterminadas, apesar de serem interpretadas como intrusivas na Sequência Campinorte. Idades de cristalização de zircão por volta de 2.15 Ga para a Suite Pau de Mel e idades modelo de Hf entre 2.1 e 2.4 Ga fornecidas nesta tese confirmam idades Paleoproterozoicas dessas rochas

conforme inicialmente proposto por Pimentel et al. (1997) e detalhado por Giustina et al. (2009). O curto espaço de tempo entre idade modelo e de cristalização de zircão da Suite Pau de Mel e sua assinatura meta peraluminosa sugerem caráter juvenil para essas rochas e que sua formação envolveu grande volume de fusão parcial de rochas metasedimentares.

Paragranulitos e granulitos maficos afloram como janelas em rochas metassedimentares do Grupo Serra da Mesa nas cercanias de Uruaçu. Gnaisses granulíticos paraderivados contém sillimanita, hercynita, cordierita e granada, sugerindo paragênese de alta temperatura e apresentam idades por volta de 2.08 Ga (apresentados nesta tese). Com base nestes dados geocronológicos, a formação desses granulitos paleoproterozoicos se relaciona com o Arco Campinorte e indica a idade do pico do metamorfismo. Além disso, esses granulitos em conjunto com rochas de assinatura de arco vulcânico demonstram a existência de complexo ambiente de arco de ilhas oceânicas onde formação de bacia, inversão, formação de orógeno, metamorfismo de alto grau e pico do metamorfismo ocorreram em um intervalo de tempo menor que 100 Ma.

1.2.1 Nomenclatura e posicionamento tectônico do Maciço de Goiás

Nomenclatura foi uma das principais dificuldades encontradas nesta tese para a proposta de compartimentação tectônica do embasamento da Faixa Brasília Norte. Por exemplo, os poucos estudos focados nessas rochas predominantemente paleoproterozoicas colocaram-nas como parte do Complexo Basal (Almeida, 1967), Complexo Basal Goiano (Hasui e Almeida, 1970), Complexo Granito-Gnáissico (Cordani & Hasui 1975), Maciço Mediano de Goiás (Almeida, 1976) e Maciço de Goiás (Almeida 1984). O termo Maciço de Goiás tornou-se mais comum e as demais nomenclaturas foram praticamente descontinuadas. O significado deste maciço e as características dos terrenos que o compunham, no entanto, permaneceram vagos.

A partir de sua determinação os limites do Maciço de Goiás evoluíram conforme o avanço dos conhecimentos da geologia da Faixa Brasília para: a) abratar todas as rochas cristalinas da Faixa Brasília Norte (Pimentel e Fuck 1992), b) representar todas as rochas do embasamento da Faixa Brasília menos o Arco Magmático de Goiás (Pimentel et al., 1996), c) o grupo de terrenos anterior, com a exceção das rochas de alto grau do Complexo Anápolis-Itauçu (Dardenne, 2000); d) um microcontinente arqueano-paleoproterozoico alóctone durante o evento colisional Brasiliano no Neoproterozoico (Jost et al., 2013).

Nesta tese o termo Maciço de Goiás assemelha-se à definição de Dardenne (2000) e não possui qualquer conotação interpretativa. Maciço de Goiás, portanto, refere-se às rochas arqueanas e paleoproterozoicas que formam o substrato da zona interna e externa da Faixa Brasília e o anteparo contra o qual o arco de ilhas que forma parte do Arco Magmático de Goiás colidiu no Neoproterozoico. O termo Maciço de Goiás também é utilizado como sinônimo para “embasamento da Faixa Brasília Norte” e pode ser usado como generalização para o substrato não aflorante sob as sequências metassedimentares da Faixa Brasília.

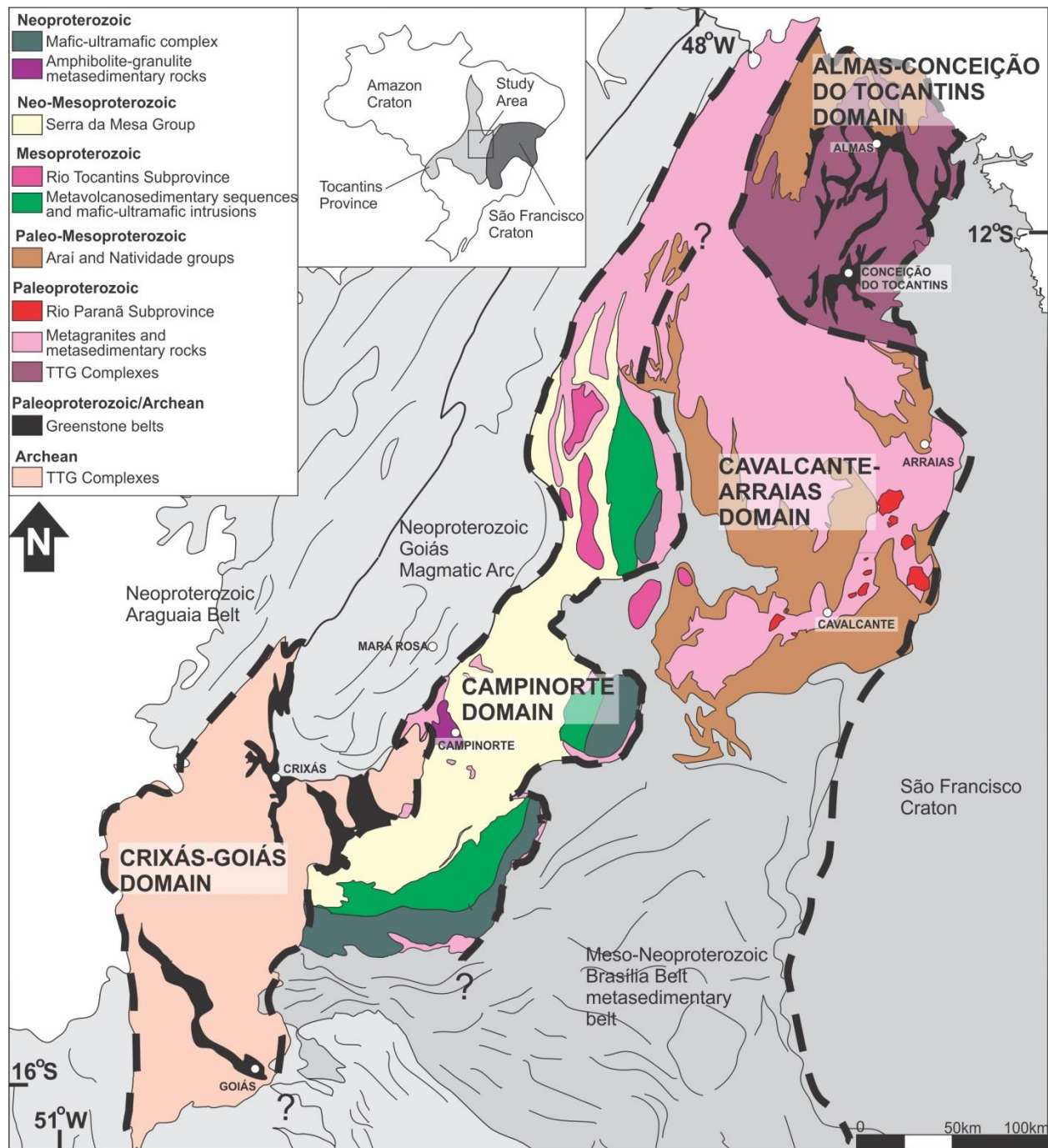


Figura 2 – Mapa de domínios do Maciço de Goiás conforme sugerido nesta tese (adaptado de Fuck et al., 2014).

Duas hipóteses conflitantes foram sugeridas para o significado tectônico do Maciço de Goiás. A primeira delas é a de que o Maciço de Goiás representa a borda oeste do Paleocontinente São Francisco que foi fortemente afetado por eventos neoproterozoicos. Os quase 400 km de sistema Neoproterozoico de foreland cobrindo a região de contato entre o Cráton São Francisco e o Maçico de Goiás dificultam a confirmação desta hipótese por meios de mapeamento. Dados sísmicos e estratigráficos (Martins-Neto 2009), estruturais (D'el-Rey Silva et al., 2008) e gravimétricos (Pereira e Fuck, 2005) argumentam a favor da ocorrência de rochas da Paleocontinente São Francisco sob a cobertura metassedimentar externa da Faixa Brasília.

A segunda e mais amplamente aceita hipótese é a de que o Maciço de Goiás é um microcontinente amalgamado à porção oeste do Paleocontinente São Francisco no evento neoproterozoico Brasiliano. Este cenário foi inicialmente sugerido por Brito Neves e Cordani (1991) em um desenho esquemático altamente especulativo, mas que explicava a presença de rochas arqueanas isoladas de terrenos contemporâneos. Trabalhos posteriores assumiram esta hipótese como bem estabelecida e forneceram parte de suas conclusões tendo-a como base (Pimentel et al., 2000; Blum et al., 2003; Pimentel et al., 2004; Queiroz et al., 2008; Valeriano et al., 2008; Ferreira Filho et al., 2010). Variações comumente citadas desta hipótese são: a) O microcontinente incluía os terrenos Arqueanos da região de Crixás-Goiás e terrenos Paleoproterozoicos pobemente expostos a leste-nordeste, sendo a sutura colisional supostamente marcada em superfície pelo Empurrão Rio Maranhão (Marangoni et al., 1995; Pimentel et al., 1999; Moraes et al., 2006; Jost et al., 2013); b) O microcontinente era restrito aos terrenos arqueanos da região de Crixás-Goiás (Pimentel et al., 2000; Valeriano et al., 2008). Dados sísmicos e gravimétricos foram apresentados posteriormente como evidência para comprovar a hipótese (Assumpção et al., 2004; Soares et al., 2006).

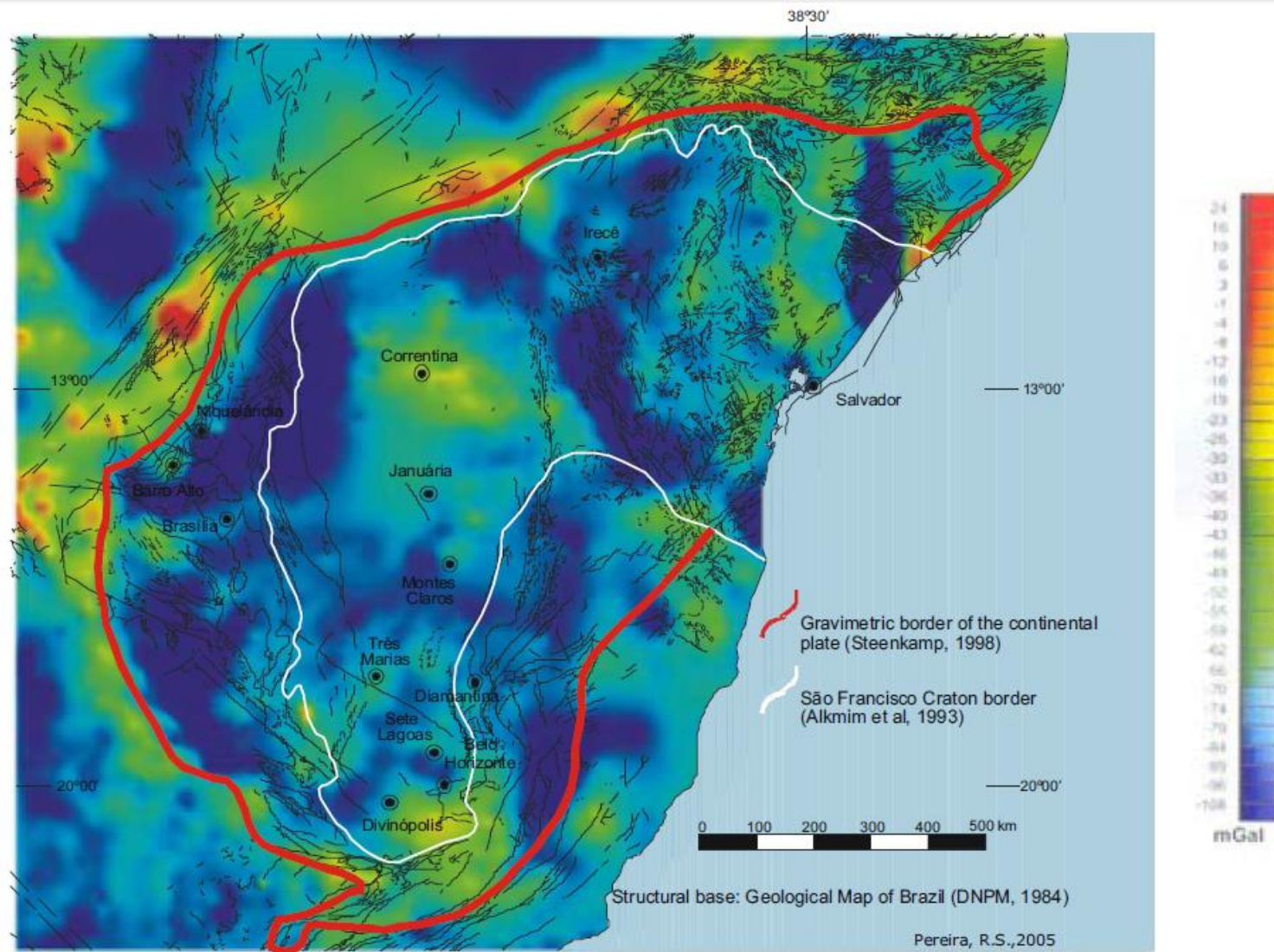


Figura 3 – Limite gravimétrico inferido do Paleocontinente São Francisco (Pereira e Fuck, 2005 e Pereira, 2007).

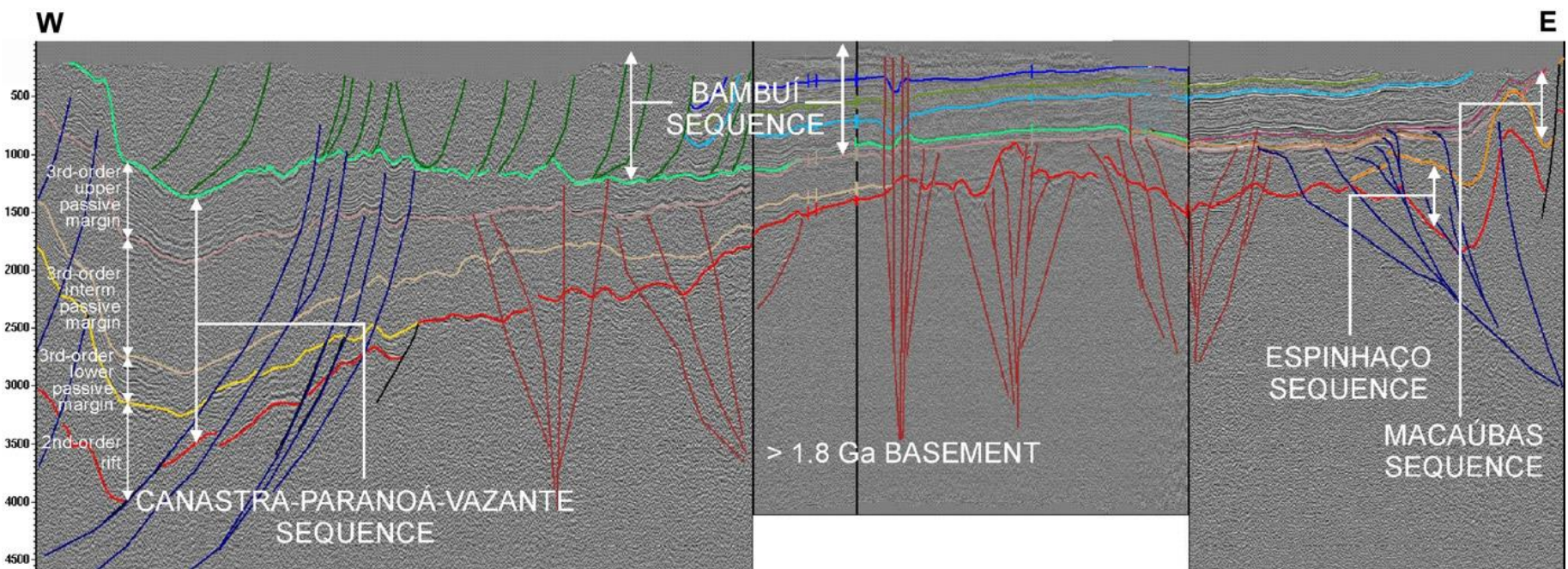


Figura 4 – Perfil interpretado de reflexão sísmica através do Cráton São Francisco mostrando o empilhamento de sequências metassedimentares meso-neoproterozoicas após um evento de rifteamento crustal (extraído de Martins-Neto, 2009). Escala vertical em TWTT (*two way travel time*).

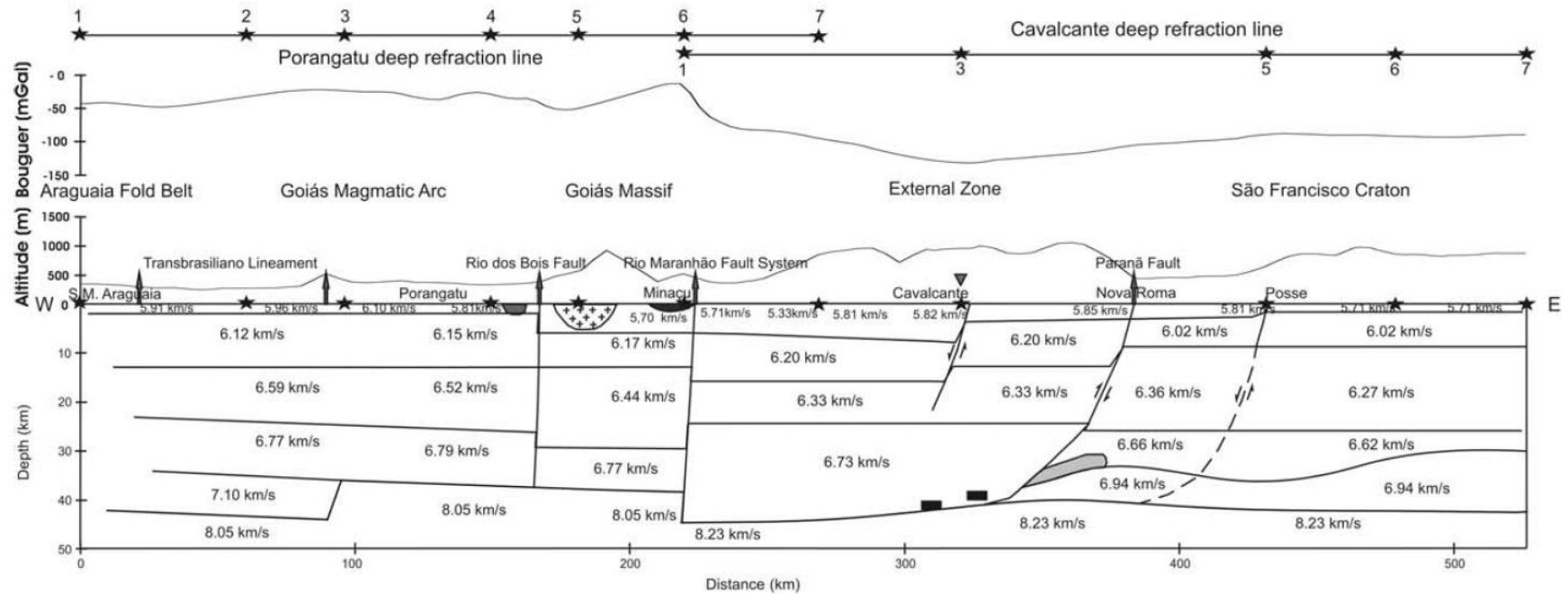


Figura 5 – Modelo bi-dimensional da crosta e manto superior das linhas de refração profunda sob Porangatu e Cavalcante (Soares et al., 2006). A variação de espessura crustal do Domínio Campinorte comparado com terrenos a leste tem sido argumentado como evidência para a hipótese de um microcontinente arqueano-paleoproterozoico.

1.2.2 Compartimentação tectônica do Maciço de Goiás

A proposta de compartimentação tectônica do Maciço de Goiás nesta tese o divide de sudoeste para nordeste em quatro domínios: Crixás-Goiás, Campinorte, Cavalcante-Arraias e Almas-Conceição do Tocantins. Os limites entre esses domínios são interpretados com base em falhas de caráter regional e/ou variações nos litotipos e ainda não estão plenamente estabelecidos. Assim como o termo Maciço de Goiás, esses domínios são descritivos e quaisquer terrenos ou cinturões com características interpretativas como arcos magmáticos, terrenos granito-greenstone, eventos de rifte, etc, podem ser utilizados.

Domínio Crixás Goiás

Granitos, tonalitos, trondjemitos e charnockitos arqueanos ocorrem na porção oeste do Maciço de Goiás envolvidos por greenstone belts com sequências komatiíticas provavelmente arqueanas e metassedimentares paleoproterozoicas explotadas para ouro (Jost et al., 2010). Conquanto bem estudado em trabalhos anteriores, a combinação desses complexos TTG e *greenstone belts* foi nomeado ‘Terreno Granito-Greenstone de Crixás’ (Queiroz et al., 2000), ‘Terrenos Arqueanos de Crixás-Goiás’ (Pimentel et al., 2000), ‘Núcleo Arqueano de Goiás’ (Jost et al., 2001), ‘Bloco Arqueano Crixás-Goiás’ (Pimentel et al., 2003), ‘Bloco Crixás-Goiás’ (Delgado et al., 2003), ‘Terreno Arqueano do Brasil Central’ (Jost et al., 2010), ‘Bloco Arqueano de Goiás’ (Jost et al., 2012) e o mais recente ‘Terreno Arqueano-Paleoproterozoico do Brazil Central’ (Jost et al., 2013).

Seguindo a abordagem de nomenclaturas descritivas, esta tese se referirá ao terreno no Brasil central composto por complexos arqueanos TTG e envoltos por unidades do tipo greenstone belt como ‘Domínio Crixás-Goiás’. Adjetivos apropriados ao objeto de estudo serão adicionados conforme a necessidade: ‘Rochas Arqueanas do Domínio Crixás Goiás’, ‘Terrenos granito-greenstone do Domínio Crixás Goiás’, etc.

Domínio Campinorte

A ocorrência de um domínio de pouca exposição entre terrenos dominadamente arqueanos do Domínio Crixás-Goiás e rochas Paleoproterozoicas a leste certamente contribuiu para a ausência de um modelo tectônico regional. Portanto, a

definição do Domínio Campinorte ainda é uma contribuição em andamento para geologia do Brasil central desde a descrição da Sequência Campinorte composta por rochas meta-vulcanossedimentares paleoproterozoicas (Kuyumijian et al., 2004; Oliveira et al., 2006; Giustina et al., 2009) e da datação de um granito paleoproterozoico, nomeado de Granito Pau de Mel por Pimentel et al. (1997) e definido nesta tese como parte de uma unidade magmática formada em ambiente de arco de ilhas. Este domínio é limitado a oeste pela Falha Rio dos Bois e a leste pelo Empurrão Rio Maranhão e aberto a norte e a sul.

Domínio Cavalcante-Arraias

Este domínio também foi nomeado como parte do Complexo Almas-Cavalcante (Delgado et al., 2003) e do Bloco Araí (Alvarenga et al., 2007). O Domínio Cavalcante-Arraias é limitado a oeste pela Empurrão Rio Maranhão e coberto por rochas metassedimentares meso-neoproterozoicas a oeste e sul. O contato norte é inferido conforme apresentado na Figura 2. Este domínio é predominantemente composto por metagranitos peraluminosos paleoproterozoicos, 2,17-2,12 Ga (Botelho et al., 2006), da Suite Aurumina que cortam gnaisses, migmatitos e xistos portadores de grafita da Formação Ticunzal. Essas unidades são cobertas por rochas vulcânicas do Rifte Araí e sequência metassedimentar associada e também intrudida por magmatismo intraplaca contemporâneo da Suprovíncia Paraná (Alvarenga et al., 2007). Sobre o Grupo Araí e parte do embasamento depositaram-se sedimentos de margem passiva do Grupo Paranoá e a sequência de antepaís neoproterozoica do Grupo Bambuí.

Muscovita-biotita granitos da Suíte Aurumina são peraluminosos e registram uma assinatura geoquímica sin-tectônica incompatível com os granitos de arco vulcânico da Suite Pau de Mel no Domínio Campinorte. A formação da Suíte Aurumina mais provavelmente envolveu fusão parcial de rochas da Formação Ticunzal em um ambiente sin-colisional (Botelho et al., 2006).

Domínio Almas-Conceição do Tocantins

Este domínio também foi chamado por Terreno granito-greenstone de Almas-Dianópolis (Saboia, 2009), Terreno granito-greenstone do Tocantins (Cruz and Kuyumijian, 1999; Kuyumijian et al., 2012) e proposto por Cruz e Kuyumijian (1993)

como parte da margem do Cráton São Francisco retrabalhada por eventos neoproterozoicos. O Domínio Almas-Conceição do Tocantins é composto por complexos TTG paleoproterozoicos envoltos por sequências *greenstone* de idade sugerida contemporânea (Cruz e Kuyumijian, 1999). Este domínio é coberto ao norte pela Bacia do Parnaíba e ao leste pelos grupos Bambuí e Urucuia. Seu contato a oeste é inferido com o Domínio Campinorte (Figura 2).

Três suites graníticas ocorrem neste domínio: a) Suíte TTG do Complexo Ribeirão das Areias de idade ~2,4 Ga, b) Tonalitos e granitos portadores de anfibólio da Suite 1 de idade 2,2 Ga, c) TTG portadores de biotita com idade de 2,2 Ga (Cruz et al., 2003). Sequências greenstone são da base para o topo formadas por derrames basálticos com volume subordinado de rochas ultramáficas e filitos com formações ferríferas intercaladas, quartzito, conglomerado e vulcânicas félsicas (Cruz e Kuyumijian, 1998).

**CAPÍTULO 2 – O ARCO PALEOPROTEROZOICO
CAMPINORTE: EVOLUÇÃO TECTÔNICA DE UM ORÓGENO
PRÉ-COLUMBIA NO BRASIL CENTRAL**

The Paleoproterozoic Campinorte Arc: tectonic evolution of a central Brazil pre-Columbia orogen

Abstract

The Campinorte Arc is a poorly exposed 2.19 to 2.07 Ga Paleoproterozoic island arc in contact with the Goiás Magmatic Arc by the Rio dos Bois Fault in the northern Brasília Belt, Central Brazil. The Campinorte Arc is divided into Pau de Mel Suite, which includes metatonalites to metamonzogranites, and the Campinorte Volcano-sedimentary Sequence. Pau de Mel Suite whole rock geochemistry indicates at least three separate coeval parental magmas compatible with arc signatures and interpreted as formed as an island arc. In this paper we also provide U-Pb geochronology data of paragranulites and mafic granulites exposed in the region as part of the Campinorte Arc Paleoproterozoic evolution. We propose as a mechanism able to preserve these granulites that the back arc basin underwent tectonic switching and consequent lithospheric thinning from 2.14 to 2.09 Ga with metamorphic peak from 2.11 to 2.08 Ga. A Pau de Mel Suite granodiorite sample dated at c.a. 2.08 Ga marks the post-peak magmatism. The arc was thereafter rapidly contracted preserving Paleoproterozoic high metamorphic grade mineral assemblages. Geographic proximity, coeval maximum sedimentation and the occurrence of similar rock types including felsic volcanism indicate that the Campinorte Arc and the neighbouring Crixás/Guarinos greenstone belts may have shared the same source of sediments. Gravimetric and seismic data also support our common Campinorte-Crixás-Guarinos basin hypothesis. The formation of the Campinorte Arc is contemporaneous to other northern Brasília Belt basement terranes and, along with similar arcs within and at the São Francisco Craton edges, indicate a continental crust formation event that eventually led to the assemblage of Columbia.

Keywords: Paleoproterozoic, accretionary orogeny, São Francisco Craton; Tocantins Province, Campinorte Arc, granulites

1. Introduction

The link between orogenic events and granulites, including ultra-high temperature metamorphic assemblages, has been well documented in belts formed during four main periods in Earth's history (Brown, 2007): Archean-Paleoproterozoic (2.7-2.45 Ga), mid-Paleoproterozoic (2.0-1.8 Ga), Late Mesoproterozoic to early Neoproterozoic (1.4-1.0 Ga) and Late Proterozoic-Cambrian (630-510 Ga). These periods coincide with continental agglutination and formation of supercontinents (Kenorland, Nuna/Columbia, Rodinia and Gondwana, respectively) and suggest a link between high-temperature granulite metamorphism and supercontinent amalgamation events.

The Central Brazil northern Brasília Belt basement encompasses evidence of arc-related granulite formation that still lacks correlation with supercontinent assemblage/breakup events. Geochronological evidence of a Paleoproterozoic accretionary event is preserved in the Goiás Massif Campinorte Sequence containing ~2.17-2.05 Ga volcanic arc rocks and correlated sedimentary sequences (Kuyumjian et al., 2004; Giustina et al., 2009a), in spite of pervasive regional Neoproterozoic metamorphic and structural overprint.

The occurrence of high temperature granulites within the northern Brasília Belt basement is in tandem with coeval arcs in neighbouring São Francisco and Amazonian cratons (Rosa-Costa et al., 2006; Oliveira et al., 2011). In both cratons the metamorphic ages fall within the 2.1 to 2.0 Ga range. Contemporaneous metamorphism is also described in the Mantiqueira and Juiz de Fora arcs (Heilbron et al., 2010), Araguaia Belt basement (Gorayeb et al., 2000) and São Luis Craton (Klein and Moura, 2008), in Brazil; the Dahomeyide Belt in Africa (Agbossoumoundé et al., 2007); and the Dabie orogeny in China (Wu et al., 2008). These São Francisco plate coeval orogens point to a widespread arc formation and amalgamation cycle that has been formerly described in central Brazil as the Trans-Amazonian Cycle (Hurley et al., 1968, Brito Neves, 2011). As the timing of these metamorphic events coincides with the amalgamation stage of Columbia, a better understanding of the

Campinorte Sequence and related rocks would contribute to a better understanding of its crustal evolution.

In this paper we present whole-rock geochemistry results of several Pau de Mel Suite rocks, including tonalite, granodiorite and monzogranite, in addition to new *in situ* zircon U-Pb LA-ICP-MS geochronology of a granodiorite and a monzogranite, in order to refine the studied area tectonic and geological setting. We also provide U-Pb LA-ICP-MS ages for Campinorte Domain para- and orthogranulites to better constrain the timing of Paleoproterozoic metamorphism in the Goiás Massif and infer its links with neighbouring terranes. Our main goal is to propose a model of Paleoproterozoic evolution in the northern Brasilia Belt that can be used as backbone for a more detailed regional tectonic framework.

2. Geological setting

The Northern Brasília Belt basement forms a 600 km long and 150 km wide NE trending area. The belt is in contact to the west with the Neoproterozoic Goiás Magmatic Arc by the Rio dos Bois Thrust. To the east, toward the São Francisco Craton, the Goiás Massif is covered by the Bambuí Group; to the south by Paranoá Group metasedimentary rocks and to the north by the Paleozoic Parnaíba basin. Northern Brasília Belt basement terranes have been grouped under several different names in the past, such as Median Goiás Massif (Almeida, 1976), Granite-gneiss Complex (Cordani & Hasui 1975), Goiano Basal Complex (Marini et al., 1978) and Goiás Massif (Pimentel et al., 2000) and in this paper we favour this latter term.

The Goiás Massif is interpreted as a microplate accreted to the São Francisco Craton in the Neoproterozoic Brasiliano Orogeny (Pimentel et al., 2000; Valeriano et al., 2008; Jost et al., 2013) or as the western tip of the São Francisco Plate (Pimentel et al., 1996, 1999). An alternative non-descriptive nomenclature has been proposed by Cordeiro (2014) dividing these three Goiás Massif terranes into the Crixás-Goiás, Campinorte and Cavalcante-Arraias and also supporting the hypothesis that they represented the São Francisco plate western edge during the Brasiliano Orogeny. However, the most common division of the Goiás Massif from southwest to northeast in the studied area is as follows:

- a) 2.8 to 2.6 Ga **Archean TTG complexes wrapped by greenstone belts** (Queiroz et al., 2008) with Archean komatiite sequences covered by gold-bearing ~2.17 Ga Paleoproterozoic metasedimentary rocks (Jost et al., 2010, 2012).
- b) 2.19 to 2.07 Ga **Campinorte Sequence metavolcano-sedimentary rocks and Pau de Mel Suite metagranites** depicted in Figure 1 and detailed by Kuyumjian et al. (2004), Oliveira et al. (2006) and Giustina et al. (2009a). These rocks are well exposed at the contact with the Rio dos Bois Thrust whereas restricted structural windows also occur within the Neo-Mesoproterozoic Serra da Mesa Group to the east. Paleoproterozoic granite-gneiss, felsic milonites and ultramylonites southeast of the Barro Alto mafic-

ultramafic Complex (Fuck et al., 1981; Correia et al., 1997) are grouped under this domain.

- c) ~2.17-2.12 Ga syn- to post-collisional **Aurumina Suite** peraluminous metagranites intrusive in Ticunzal Formation metasedimentary graphite-bearing schists to paragneisses (Botelho et al., 2006; Alvarenga et al., 2007). Para-derived gneisses and graphite-rich nodules (restites) are common at the Aurumina Suite intrusive contacts. Other evidence of the Ticunzal Formation as an important source for this voluminous Paleoproterozoic syn-collisional peraluminous magmatism include compatible Sm-Nd TDM ages, U-Pb ages and migmatite features (Botelho et al., 2006).

Even though Paleoproterozoic rocks are predominant in the Goiás Massif, the Brasília Belt was affected by earlier events that are far better understood and discussed (Pimentel et al., 2011). The Goiás Massif was rifted in the Late Paleoproterozoic (~1.77 Ma, Pimentel et al., 1991) with consequent bimodal magmatism marking the beginning of the Araí Group sedimentation. The Nd T_{DM} model ages of the Araí Group sedimentary rocks range from 2.0 to 2.5 Ga and zircon U-Pb maximum sedimentation age is at c.a. 2.0 Ga. These ages suggest contribution of Paleoproterozoic and Archean sources (Marques, 2010) in agreement with Goiás Massif exposed rocks.

In the Mesoproterozoic these terranes underwent reactivations along the Araí Rift or new rift events. The first Mesoproterozoic rift around 1.56 Ga generated Tocantins and Paraná suprvinces A-type granites that intruded Paleoproterozoic basement as 5-50 km long intrusions west of the Rio Maranhão Thrust and also as smaller, few km wide intrusions east of it, within the Cavalcante-Arraias Domain (Pimentel et al., 1999; Pimentel and Botelho 2001; Lenharo et al., 2002). The second Mesoproterozoic rift occurred at c.a. 1.3 Ga and generated the Palmeirópolis, Indaianópolis and Juscelândia metavolcano-sedimentary sequences, presenting MORB-like signature mafic rocks. The coeval Serra dos Borges and Serra da Malacacheta layered mafic-ultramafic complexes are interpreted as formed in the same event (Ferreira Filho et al., 2010).

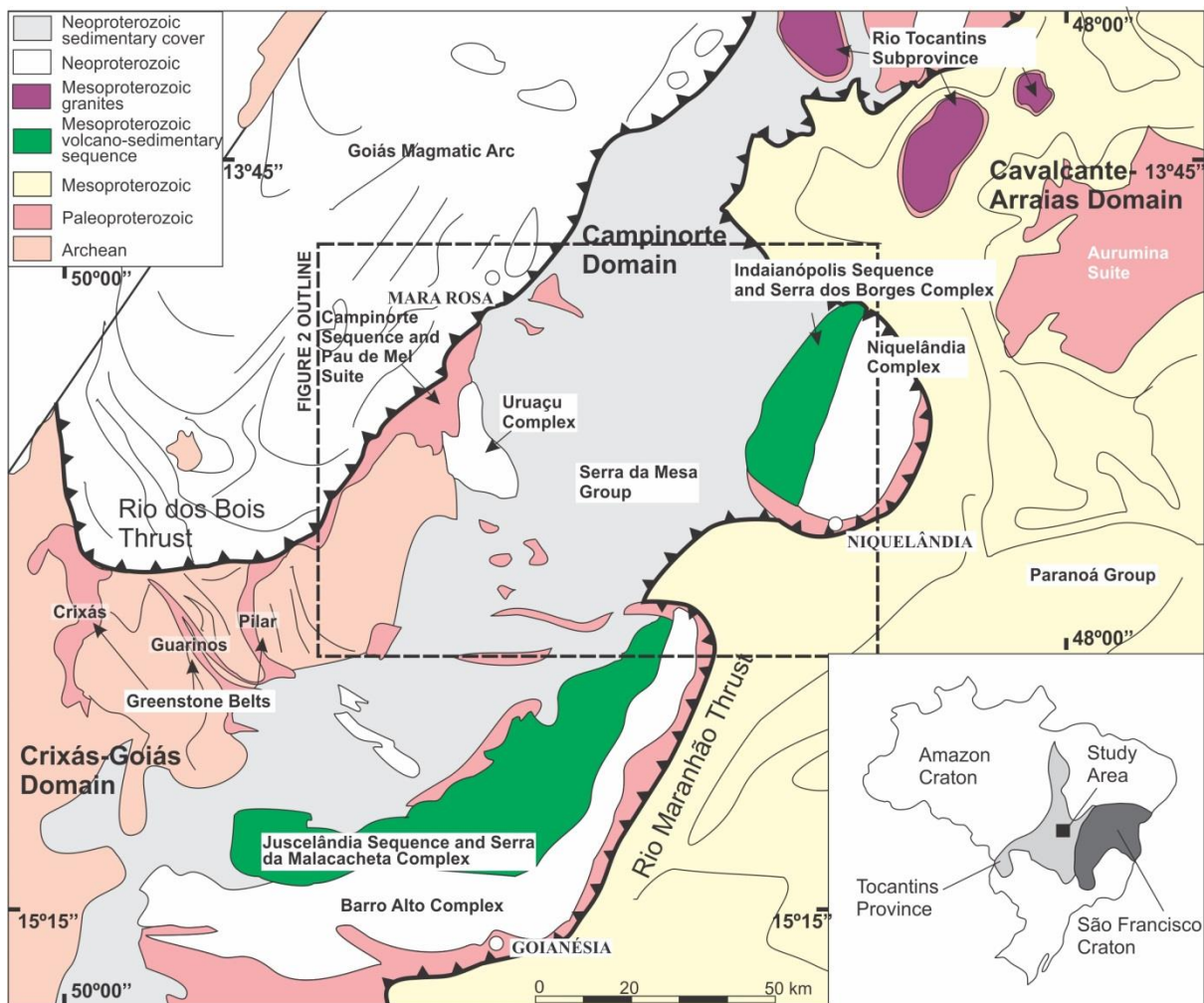


Figure 1 – Geological sketch of the terrane between the Crixás-Goiás Block and the Barro Alto and Niquelândia complexes (Fuck, 1994; Delgado et al. 2003; Giustina et al., 2009a; Ferreira Filho et al., 2010; Jost et al., 2010a).

The Brasiliano Orogeny was the utmost responsible for the Brasília Belt present tectonic architecture, generating continent wide structures as the Transbrasiliano lineament (Brito Neves and Fuck, 2013). A Neoproterozoic island arc formed around 900 Ma was amalgamated to the Goiás Massif western margin and its sediments, probably the Serra da Mesa Group, formed a foreland/back arc basin over dominantly Paleoproterozoic basement. The ~650 Ma Urucu Complex high grade metamorphic rocks has formed at a metamorphic peak during of a Neoproterozoic event (Giustina et al., 2009b) and probably underwent diapiric ascention as a metamorphic core complex within Campinorte Arc rocks (Oliveira & Della Giustina, personal communication). Around 630-620 Ma the Rio Maranhão Thrust was propagated upwards tilting Meso-Neoproterozoic mafic-ultramafic complexes and the Paleoproterozoic basement to their present position (D'el-Rey Silva et al., 2008). Felsic Neoproterozoic magmatism is also observed in the Crixás-Goiás and Campinorte domains.

2.1 Campinorte Sequence, Pau de Mel Suite and granulites

The Paleoproterozoic terrane comprising the Campinorte Sequence and Pau de Mel Suite is limited by the Rio dos Bois Thrust to the west, by the Rio Maranhão Thrust to the east, but its limits are unexposed to north and south (Figure 2). Meso-Neoproterozoic Serra da Mesa metasedimentary rocks cover most of this terrane, making the determination of underlying units possible only within structural windows and at the footwall of the Barro Alto, Niquelândia and Cana Brava layered mafic-ultramafic complexes. To the north, west of the Palmeirópolis Sequence, Paleoproterozoic rocks are better exposed though still correlated with the Aurumina Suite instead of with the Pau de Mel Suite (Marques, 2010).

The Campinorte Sequence is dominated by quartz-muscovite schist with variable amount of carbonaceous material (Figure 3A), quartzite, chert and gondite lenses. Subordinate metatuffs and metalapilli tuffs crop out as small elongated bodies within various metasedimentary rocks with rare felsic metavolcanics (Figure 3B). U-Pb in zircon provided a maximum depositional age of ~2.2 Ga for the metasedimentary unit and a direct age of 2179 ± 4 Ma for a felsic metatuff (Giustina et al., 2009a). At least two deformational events are recorded in these greenschist facies rocks. Primary bedding can be recognized in some outcrops but original stratigraphy was disrupted by Paleoproterozoic and Neoproterozoic deformation (Oliveira et al., 2006). Intensely weathered ultramafic talc-, amphibole- and chlorite-bearing schists are interpreted as tectonic slices of ocean floor imbricated during the basin inversion (Giustina et al., 2009a).

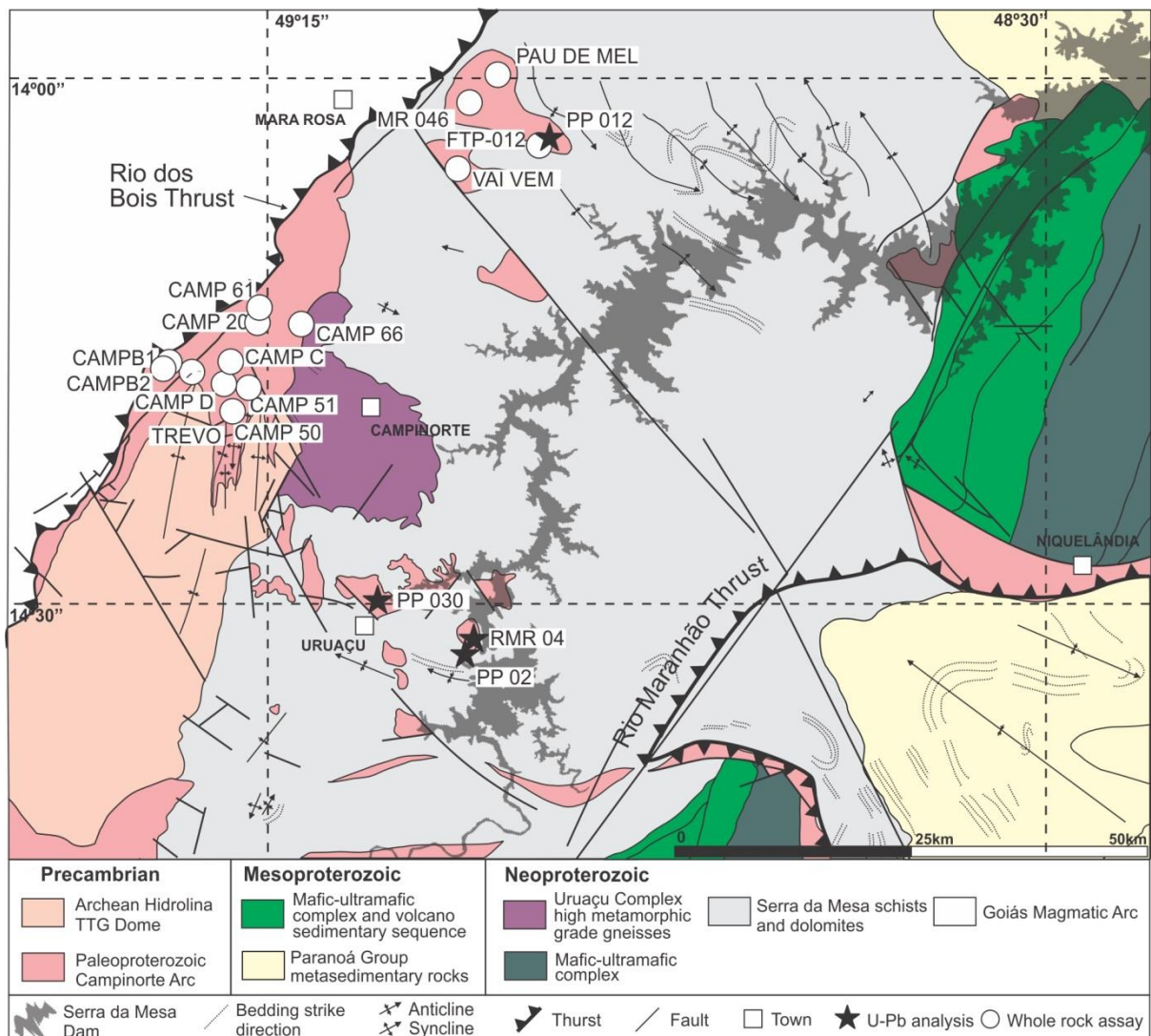


Figure 2 – Geological map of the Campinorte Arc granitoids and volcano-sedimentary rocks
(modified after Baeta Júnior et al. 1972, Baeta Júnior, 1987 and Oliveira et al., 2006)

Up to 12 km long and 2 km wide Pau de Mel Suite NNE-trending metatonalites, metagranodiorites and metamonzogranites occur within the Campinorte sequence metasedimentary rocks (Fig. 3C and 3D). These metagranites have variable degrees of deformation and unclear contact relations, although interpreted as intrusive within the Campinorte Sequence. Zircon crystallization ages from 2.17 to 2.07 Ga for the Pau de Mel Suite confirmed Paleoproterozoic ages (Giustina et al., 2009a). The time gap between igneous crystallization and Sm-Nd T_{DM} model ages of 2.1 to 2.4 Ga suggest a juvenile character.

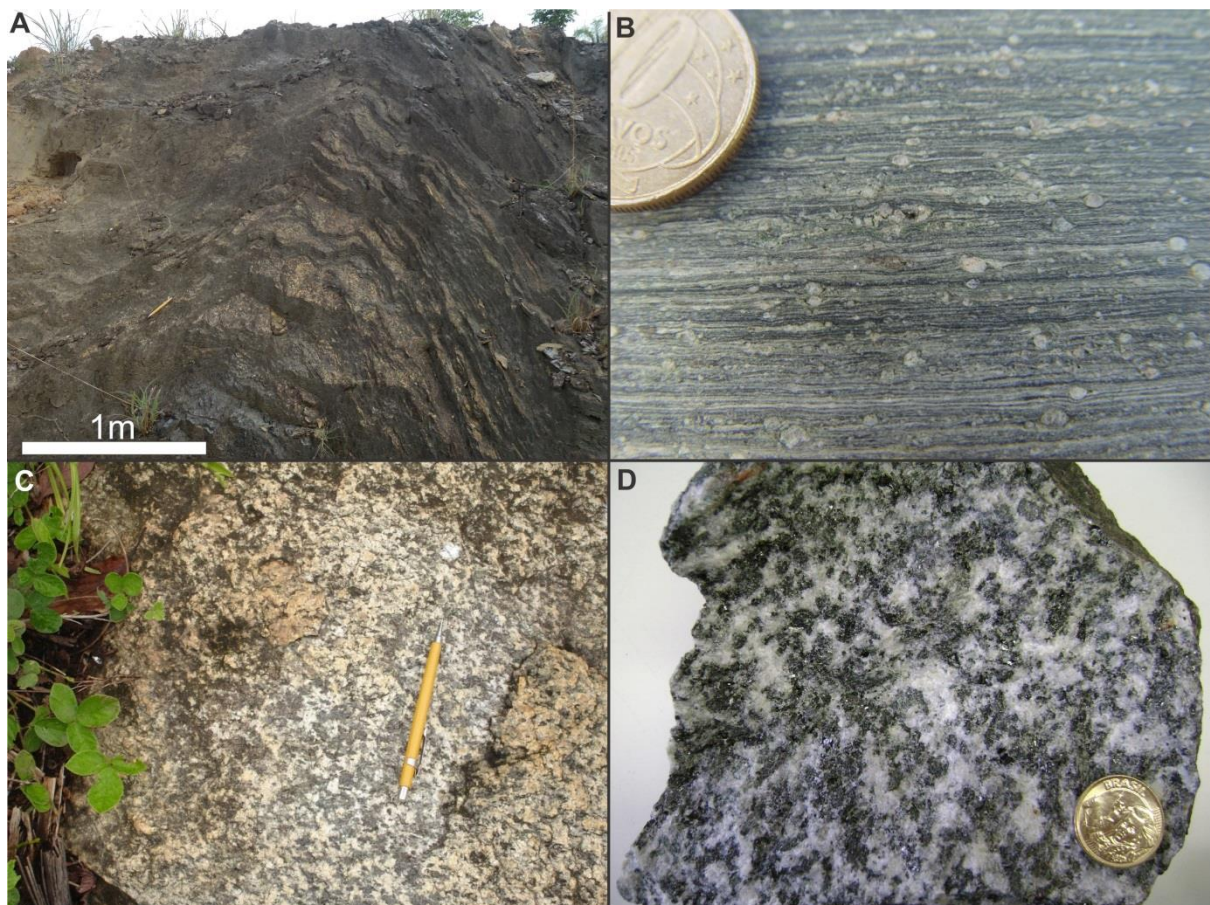


Figure 3 – Campinorte Sequence and Pau de Mel Suite A) Folded and bedded carbonaceous schist outcrop; B) Undeformed felsic volcaniclastic rock with potasssic feldspar phenocrysts; C) biotite-amphibole metagranodiorite outcrop; D) Metatonalite CAMP-B1

Paragranulites (Figure 4A, B, C and D) and mafic granulites (Figure 4E and F) crop out as structural windows within the Meso-Neoproterozoic Serra da Mesa Group around the town of Urucuá. These rocks are part of a regional magnetic anomaly identified by Barreto Filho (1992) and interpreted as the alleged missing piece of mafic-ultramafic complex between the Barro Alto and Niquelândia complexes, named Água Branca Complex. Winge (1995) first describes a sillimanite-garnet-cordierite kinzigitic gneiss and interpret its origins as derived from metapelites. Field relations with Pau de Mel Suite granites and other rocks of the Campinorte Sequence are still unknown but U-Pb ages presented in this work led us to consider them as part of the Campinorte Sequence.

These paragranulites are in general medium-grained and show a green to pink color due to intercalation of cordierite-bearing and garnet-feldspar-bearing (andesine and perthitic orthoclase) bands (Figure 4B). The rock preserves a granoblastic texture with banding parallel prismatic sillimanite. Small green spinel occurs isolated from the matrix by sillimanite and garnet coronas, thus suggesting a reaction with quartz. Poikiloblastic cordierite shows a typical alteration to pinite and well developed pleochroic halos around monazite inclusions. Later hypidioblastic biotite occurrence is restricted. This assemblage is almost entirely transformed to a fine-grained hydrated rock in nearby outcrops, with abundant muscovite and chlorite as alteration products of granulite minerals.

The spinel+quartz assemblage has traditionally been described as indicative of ultra-high temperature metamorphic conditions (Harley 1998). However, preliminary microprobe investigations reveal an elevated Zn content in this spinel (Moraes, R., personal communication) which thus extends the spinel+quartz stability field to granulite facies conditions (Waters 1991). Since cordierite is restricted to lower P values, its occurrence suggests a nearly ITD (isothermal decompression) path for these paragranulites.

Mafic granulites occur as meter to tenths of meter-sized bodies within the paragranulites domain. These rocks vary from medium to fine-grained and show a massive to banded structure. Relict ortho- and clinopyroxene grains with exsolution textures are transformed into a granoblastic assemblage and occur in equilibrium with large, poikiloblastic brown hornblende and granoblastic andesine (4E and F).

Retrometamorphism to greenschist facies conditions is marked by actinolite, chlorite and albite.

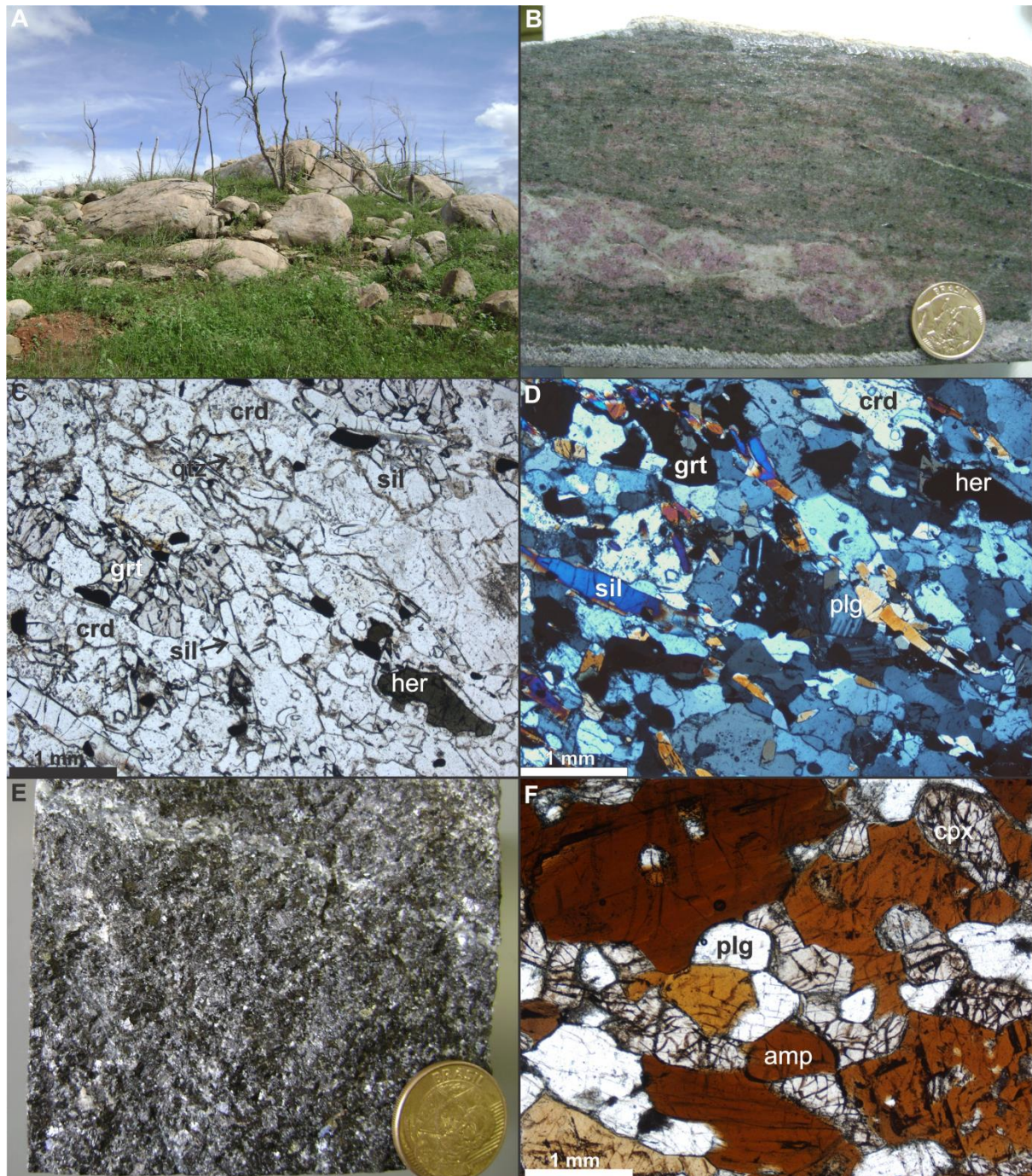


Figure 4 – Campinorte Sequence paragranulites. A) Typical paragranulite cropping out as rounded boulders; B) Paragranulite PP02 hand sample; C) Parallel nicols granulite assemblage photomicrograph of PP02; D) Crossed nicols granulite assemblage photomicrograph of PP02; E) Mafic granulite RMR04 hand sample; F) Nicol parallel mafic granulite RMR04 photomicrograph (qtz-quartz; crd-cordierite; sil-silimanite; grt-garnet; cpx-clinopyroxene; amp-amphibole, plg-plagioclase)

3. Analytical Procedures

Four samples were selected for U-Pb LA-ICPMS investigation in the Geochronology Laboratory of the University of Brasília: a) PP012 metagranodiorite, b) PP030 granodiorite, c) RMR04 mafic granulite and d) PP02 paragranulite. Fourteen samples of fresh metatonalites, metagranodiorites and metamonzogranites were selected for whole rock assay ICP-ES for major elements and ICP-MS for trace-elements at the Acme Labs Vancouver (Table 1).

U-Pb isotopic analyses followed the analytical procedure described by Bühn et al. (2009). Zircon concentrates were extracted from ca. 10 kg rock samples using conventional gravimetric and magnetic techniques at the Geochronology Laboratory of the University of Brasília. Mineral fractions were handpicked under a binocular microscope to obtain fractions of similar size, shape and color.

For in situ ICP-MS analyses, handpicked zircon grains were mounted in epoxy blocks and polished to obtain a smooth surface. Backscattering electron (BSE) images were obtained using a scanning electron microscope in the Geochronology Laboratory of the University of Brasília in order to investigate the internal structures of the zircon crystals prior to analysis.

Before LA-ICP-MS analyses, mounts were cleaned with dilute (ca. 2%) HNO₃. The samples were mounted in an especially adapted laser cell and loaded into a New Wave UP213 Nd:YAG laser ($\lambda = 213$ nm), linked to a Thermo Finnigan Neptune Multi-collector ICPMS. Helium was used as the carrier gas and mixed with argon before entering the ICP. The laser was run at a frequency of 10 Hz and energy of 50% and a spot size of 30 μm .

Two international zircon standards were analyzed throughout the U-Pb analyses. Zircon standard GJ-1 (Jackson et al., 2004) was used as the primary standard in a standard-sample bracketing method, accounting for mass bias and drift correction. The resulting correction factor for each sample analysis considers the relative position of each analysis within the sequence of four samples bracketed by two standard and two blank analyses each (Albarède et al., 2004). An internal standard (PAD-1) was run at the start and the end of each analytical session, yielding an accuracy around 2% and a precision in the range of 1%. The errors of

sample analyses were propagated by quadratic addition of the external uncertainty observed for the standards to the reproducibility and within-run precision of each unknown analysis. The instrumental set-up and further details of the analytical method applied are given by Buhn et al. (2009). Plotting of U–Pb data was performed by ISOPLOT v.3 (Ludwig, 2003) and errors for isotopic ratios are presented at the 1s level. The U-Pb results are listed in tables 2, 3, 4 and 5 (Appendix A).

4. Samples and results

4.1 - PP02

Sample PP-02 corresponds to a sillimanite-garnet-cordierite paragranulite cropping out at the margin of the Serra da Mesa dam. The sample was investigated by LA-ICPMS to determine the provenance pattern of the high grade metasedimentary sequence and metamorphic ages. The zircon grains contain a single population of clear pinkish zircon crystals with no internal structure under microscope and BSE images. Thirty nine spots were performed in zircon grains cores and rims with thirty six concordant analyses. Results from crystals cores and rims showed same results within the error margin. The sample yielded only Paleoproterozoic ages with strong concentration around 2.1 Ga and subordinate groups at ~2.15 Ga and ~2.18 Ga (Figure 5A). The single zircon population contains two groups identified based on the Th/U ratio. The first group shows $\text{Th}/\text{U} > 0.1$ and ages with the range of 2.19-2.10 Ga, interpreted as detrital zircons that give maximum depositional ages of ~2.11 Ga (Figure 5 A inset). The second group shows $\text{Th}/\text{U} < 0.1$ ranging from 2.15 to 2.03 Ga, interpreted as metamorphic zircons formed at a proposed metamorphic peak from 2.11 to 2.09 Ga.

4.2 - RMR04

Sample RMR04 is a two pyroxene mafic granulite that occurs within the more widespread paragranulite represented by sample PP02. The zircon grains are composed of a single population of clear pinkish zircon crystals with no internal structure under microscope and BSE images. Thirty three concordant analyses yielded an upper intercept age of 2098 ± 8 Ma (Figure 5B) interpreted as the age of crystallization of the original magma. As in the paragranulite PP02, two groups of zircon analysis can be identified based on the Th/U ratio. The first group ($\text{Th}/\text{U} > 0.1$) contains ages from 2140 Ga to 2080 Ga, interpreted as related to igneous zircon crystallization. The second group of grains ($\text{Th}/\text{U} < 0.1$) shows ages from 2125 to 2060 Ga that could indicate metamorphic ages in agreement with those of the paragranulite PP02.

4.3 - PP012

A Pau de Mel Suite metagranodiorite (PP012) cropping out within a window in the Serra da Mesa Group, east of the town of Mara Rosa, was investigated by LA-ICPMS to determine its crystallization age. Two zircon populations are identified: i) small zircon grains ($100\text{ }\mu\text{m}$) are prismatic, rounded, fractured and with inclusions; whereas ii) larger zircon grains ($>200\text{ }\mu\text{m}$) are well formed and lack mineral inclusions. However, there is no correlation among zircon population and the data obtained. Thirty five spot analyses with fifteen concordant results yielded an upper intercept age of 2169 ± 8 Ma (Figure 5), which is interpreted as representative of the igneous crystallization of the protolith. The lower intercept indicates a well-constrained age of 751 ± 28 Ma, compatible with the Barro Alto and Niquelânia complexes granulitization age of 750-760 Ma (Ferreira Filho et al., 2010; Giustina et al., 2011).

4.4 – PP030

The PP030 sample is an amphibole-garnet-biotite granodiorite with well-preserved igneous texture, collected in the vicinities of the town of Uruaçu. The single zircon population was investigated and seventeen concordant analyses yielded an upper intercept age of 2080 ± 24 Ga (Figure 5). As with the other samples, zircon grains showed no zonation under BSE. The Concordia age is roughly coeval with interpreted metamorphic peak ages in this paper (Figure 5) and suggest felsic magmatism associated with granulite formation.

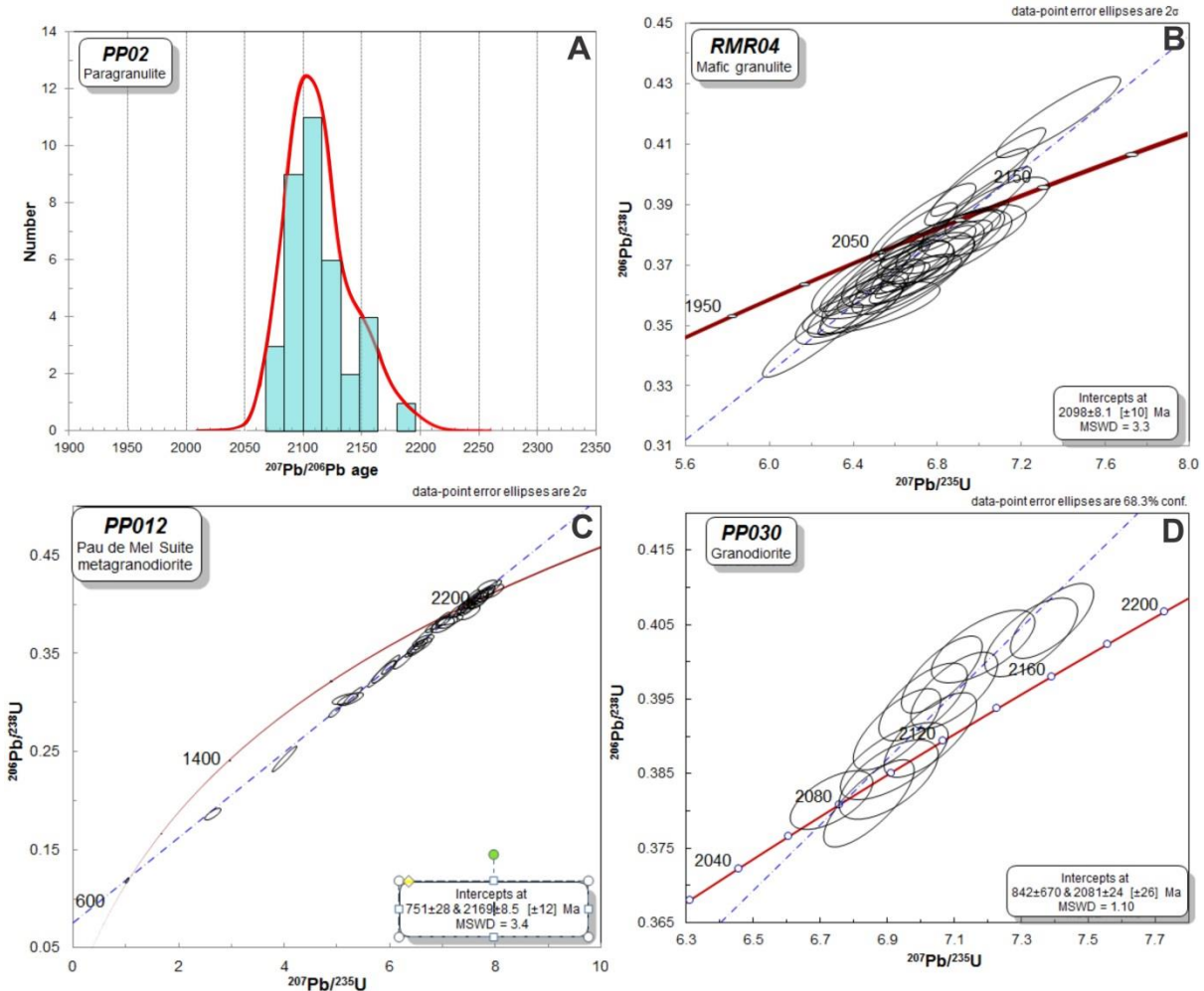


Figure 5 – A) Probability density plot of $^{207}\text{Pb}/^{206}\text{Pb}$ ages obtained from detrital zircon grains for sample PP02; and concordia diagrams for LA-ICP-MS analyses of zircon grains from B) the mafic granulite RMR04, C) the metagranodiorite PP012 and D) the granodiorite PP030.

5. Whole-rock geochemistry and petrogenetic implications

Whole-rock geochemistry study of Pau de Mel Suite metatonalites, metagranodiorites and metamonzogranites throughout the Campinorte Suite type-area (Figure 2) provided insights on the original Paleoproterozoic tectonic setting. This assessment allowed us to propose three *latu-sensu* metagranite groups, types 1, 2 and 3, based on major oxides and trace elements variations.

Major oxides compositions are in tandem with plagioclase predominance over potassic-feldspar as expected of dominant tonalitic-granodioritic compositions. **Type 1** is composed of metagranodiorites with major oxides varying around 70% SiO₂, 4.5% Na₂O, 3% CaO and 2% K₂O, **Type 2** are metagranodiorites to metamonzogranites with SiO₂ contents varying between 67 and 74 %, K₂O from 2.5% to 3.5%, Na₂O from 3% to 4.5% and CaO 1% to 3.5% whereas **Type 3** varies from metatonalites to metagranodiorites with major oxides from 59 to 69 % SiO₂, 4 to 5 % Na₂O, 2 to 6 % CaO and 1 to 2.5 % K₂O.

Normalized rare earth elements add further information on the origin and evolution of the Pau de Mel Suite. The three metagranite types vary from a [La/Lu]_N ratio around 55 (Type 1), 20 (Type 3) and 6 (Type 2) pointing to strong to weak LREE fractionation compared to HREE. Whereas LREE patterns are fairly parallel, the HREE vary widely among types 1, 2 and 3. Decoupled HREE patterns suggest the three studied metagranite types derived from distinct parental magmas even though contemporaneous and spatially related. Type 2 granites display pronounced Eu anomaly and negative Sr anomaly in the multi-element diagram (Figure 6) coupled with general higher REE enrichment indicating plagioclase fractionation in later magmatic stages.

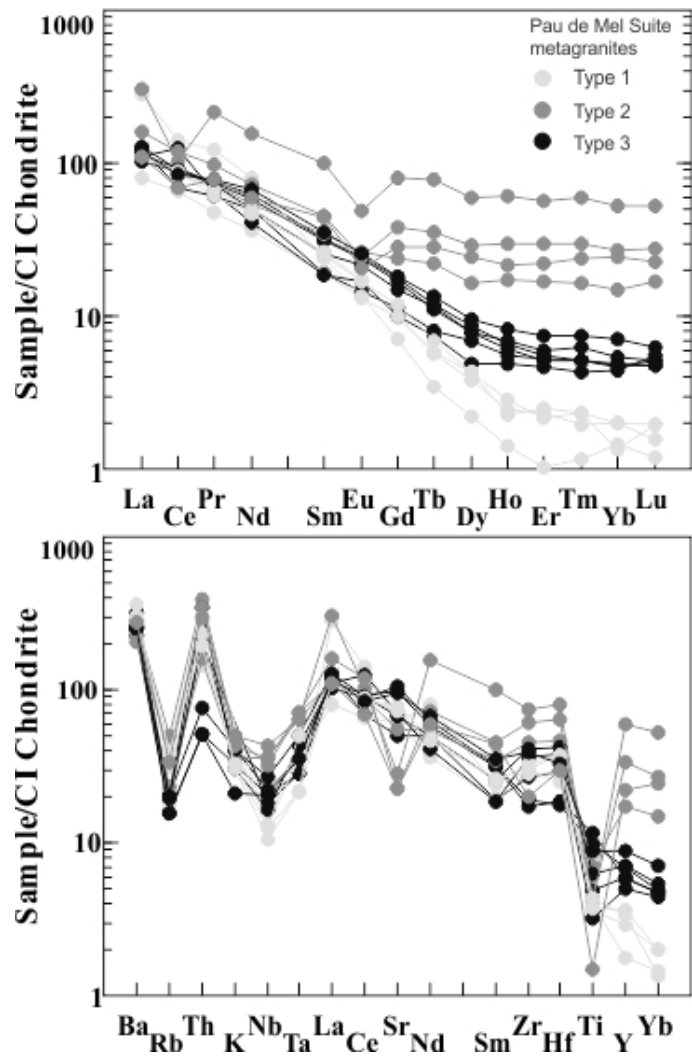


Figure 6 - REE elements plot of Pau de Mel Suite granitoids and multi-element diagram showing comparative trace elements variation between rock types.

The Pau de Mel Suite shows calcic-alkalic and calcic signature (Figure 7A) and low-K enrichment. AN/K versus A/CNK plot indicates a metaluminous to peraluminous nature for these metagranites. In a Rb versus Y+Nb diagram (Figure 7B), most samples compositions fall within the volcanic arc granite field (VAG) whereas a couple of Type 2 metamonzogranoites have compositions similar to post-collisional signatures. A R1xR2 plot shows a spread of samples from Type 3 pre-plate collision metatonalites towards types 1, 2 and 3 metagranodiorites to metamonzogranoites with VAG to slightly post-orogenic signatures (Figure 7C).

These granite and tectonic classification schemes suggest a complex evolution in a volcanic arc setting. This evolution most likely involved sediment melting in order to produce weakly peraluminous magmas (Figure 7D). We interpret that while metagranite types 1 and 3 were related to initial stages of the arc evolution, the more evolved Type 2 metagranodiorites to metamonzogranoites weak with within-plate granites signature that are interpreted as late stage (Figure 7B).

Based on our geochemical, geological and geochronological observations and those of Kuyumjian et al. (2004), Oliveira et al. (2006) and Giustina et al. (2009a) we propose that the terrane comprised of Paleoproterozoic metavolcano-sedimentary rocks and related metagranites east of the Rio dos Bois Thrust represent a Paleoproterozoic arc setting and should henceforth be referred to as Campinorte Arc. The Campinorte Arc is likely to have formed as an island arc due to juvenile ε Nd from -2.14 to +3.36 and lack of pre-Campinorte Arc zircon inheritance (Giustina et al., 2009 a). It represents a very dynamic tectonic setting where mountain range formation, erosion, basin deposition, granulite facies metamorphism and closure occurred within a time span of less than 100 Ma.

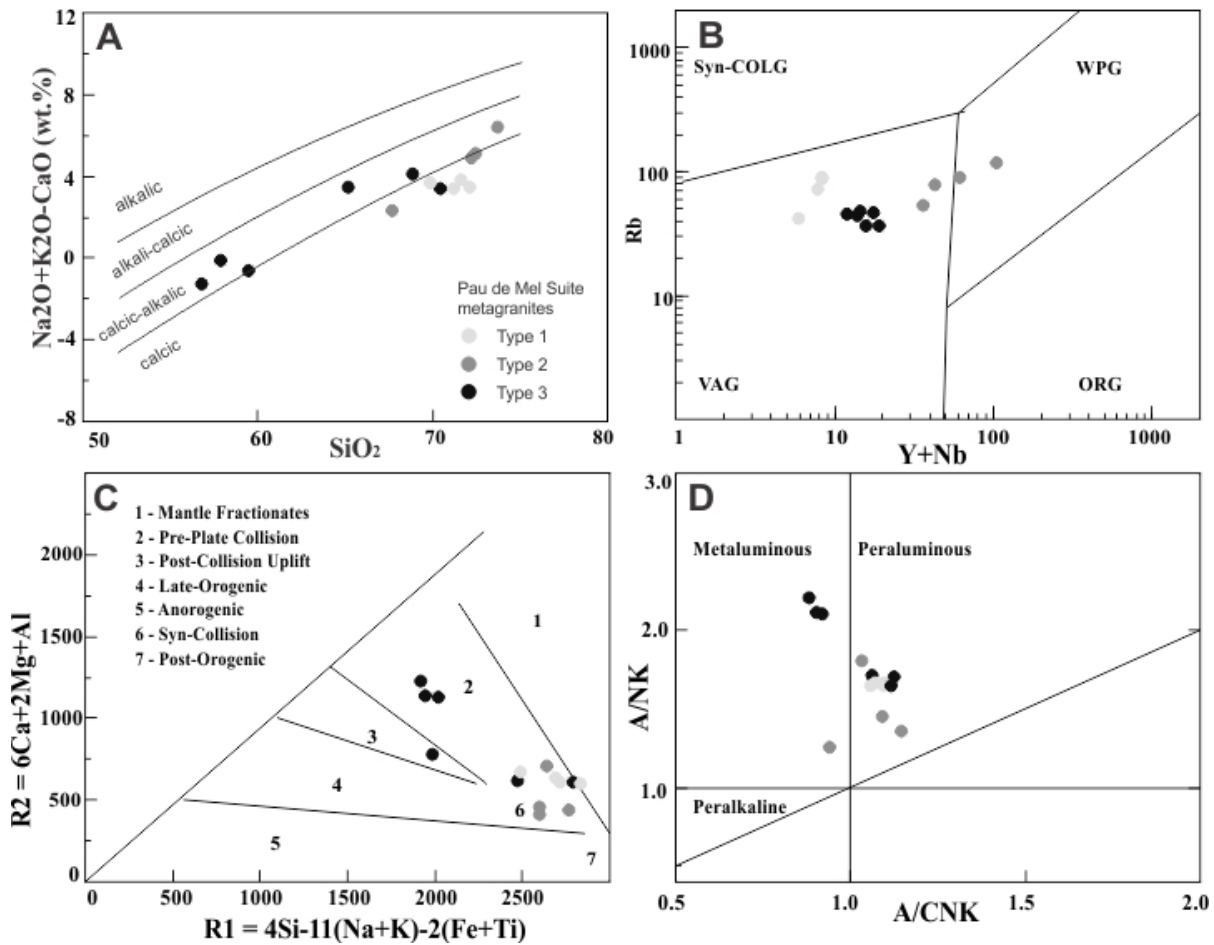


Figure 7 – A) SiO_2 versus $\text{K}_2\text{O} + \text{Na}_2\text{O} - \text{CaO}$ plot from Frost et al. (2001); B) Rb versus $\text{Y} + \text{Nb}$ plot of Pearce et al. (1984); C) R1-R2 cationic plot of Batchelor and Bowden (1985); D) A/NK versus A/CNK (Shand diagram) plot.

6. Discussion

6.1 Granulite Formation

Granulites can be generated either through crustal thickening during subduction or through crustal extention that produces ultrahigh to high-temperature granulites (Gibson and Ireland, 1995; Brown, 2007; Touret and Huizenga, 2012). In order to assess the formation mechanism of the Campinorte Arc granulites it is important to understand the implications of their peculiar mineral assemblage.

According to Waters (1991) the assemblage hercynite + quartz with cordierite, garnet and/or sillimanite indicates high-temperature granulite-facies metamorphism at mid-crustal depths. Terranes with this assemblage show probable peak temperatures at ~800 °C and pressures from 4-7 kbar implicating in magmatic advection and lithospheric thinning rather than thermal relaxation and uplift after a continental collision. Any geodynamic model for the Campinorte Arc has to account for the juxtaposition of greenschist facies Campinorte Sequence metasedimentary rocks and these younger high-temperature granulites.

Granulites are widely described in the Barro Alto Complex and Uruaçu Complex (Moraes and Fuck 2000; Giustina et al., 2009b; Ferreira Filho et al., 2011) and any granulite in the poorly mapped vicinities would naturally be considered part of these younger units. However, our Paleoproterozoic granulite ages (Figure 5A and 5B) lack evidence of later events and show concordant zircon grains rims/cores analyses with ages around 2.1 Ga. We conclude the mafic granulite and paragranulite cropping out at the margins of the Serra da Mesa dam indicate a Paleoproterozoic high-temperature, low-pressure, metamorphic event peaking at 2.1 Ga, approximately 60 Ma after the main Campinorte Arc formation event.

A tectonic model able to explain high temperature granulite formation in accretionary arcs should also reconcile structural evidence for crustal thickening at the metamorphic peak and lithospheric extention (Collins, 2002; Brown, 2007; Touret and Huizenga, 2012). Crust thinning due to Moho upwelling or large volumes of magmatism could provide heat source for granulite metamorphism. Thickening immediately followed by thinning while the crust is still hot could account for both (Gibson and Ireland, 1995; Thompson et al., 2001) and generate granulites and

coeval volcanism slightly younger than the main arc formation event. Our Campinorte Arc paragranulite sample (PP02) shows zircon grains with ages between 2.18 to 2.08 Ga that overlap ages provided for the Campinorte Sequence type area (Giustina et al., 2009a). Younger ages from 2.14 Ga to 2.08 Ga could represent both metamorphic zircon grains and magmatic activity concomitant with basin formation in mafic granulite lenses within paragranulites (RMR 04). Post 2.08 Ga felsic intrusives, as in the granodiorite PP030, suggest post-collisional magmatism of unknown extention.

Late-stage granulite formation in the Campinorte Arc is in tandem with global data compilation showing that high temperature metamorphism tends to occur at the final stage of a supercontinent amalgamation (Brown, 2007; Touret and Huizenga 2012). We propose that lithospheric thinning of the 2.19-2.07 Ga Campinorte Arc generated a back-arc basin that within a time span of 60 Ma was inverted and granulitized followed by crustal thickening that preserved metamorphic-peak granulitic mineral assemblages. Unlike the Pau de Mel Suite metagranite (PP012) data, zircon grains from these granulites somehow lack overprint by later metamorphic events of the Neoproterozoic Brasiliano Cycle.

6.2. Correlation with Crixás-Goiás metasedimentary rocks

In order to understand the Campinorte Arc evolution we reviewed the available published data on neighbouring terranes, particularly within Archean-Paleoproterozoic rocks southwest of the studied area. These rocks are part of a block that has been largely interpreted as an isolated allochthonous microplate amalgamated to the western part of the São Francisco-Congo paleocontinent during the Neoproterozoic Brasiliano orogeny (Pimentel et al., 2000; Valeriano et al., 2008). Hence, a revision of evidence favoring the microcontinent hypothesis or alternatives would help to establish details on the Crixás-Goiás Block and Campinorte Arc amalgamation.

The Crixás-Goiás Domain (Figure 1) is composed of Archean TTG complexes wrapped by Paleoproterozoic metavolcano-sedimentary belts originally deposited as a back arc basin over basalts and komatiites of probable Archean age (Fortes et al., 2003; Jost et al., 2010, 2012). From bottom to top the greenstone belts sequence can be summarized as a) basal metakomatiite; b) metabasalts with local pillow structures and; c) metasedimentary sequence with carbonaceous phyllite, metagraywacke, schist, metachert and gondites. Magmatism coeval with Paleoproterozoic basin formation is evidenced by 2.17 Ga mafic dikes cutting Crixás metagraywacke (Jost and Scandolara, 2010), ~2.14 Ga metafelsic rock in the Pillar greenstone belt (Queiroz et al., 1999) and the ~2.16 Ga Posselândia diorite east of the Caiamar Complex (Jost et al., 1993). A provenance study of the Crixás and Guarinos greenstone belts upper metasedimentary rocks by Jost et al. (2010a, 2012) provided a Paleoproterozoic sedimentation age of ~2.15 Ga. Mixed mafic and felsic source contributions with Eu anomalies were determined by whole-rock geochemistry (Jost et al., 1996). The authors considered that the lack of rocks with negative Eu anomalies within the Crixás-Goiás Block demanded an external source for the basin sediments.

A tectonic evolution review of the Crixás-Goiás Block and the Campinorte Arc could help explain their common geological and geochemical characteristics. The drifting microcontinent hypothesis was first suggested by Brito Neves and Cordani (1991) in a South American tectonic review paper that contained a speculative sketch of central Brazil paleoplates interaction. From then on, despite referring to

very little evidence to support the hypothesis, following regional studies assumed the Crixás-Goiás Block as a microcontinent (Pimentel et al., 2000; Blum et al., 2003; Pimentel et al., 2004; Queiroz et al., 2008; Valeriano et al., 2008; Ferreira Filho et al., 2010). A common argument to favour the microcontinent hypothesis is the sharp gravimetric contrast between terranes separated by the Rio Maranhão Thrust (Marangoni et al., 1995; Pimentel et al., 2004). No geochemical or petrological evidence detailing such interaction has been proposed.

An alternative less commonly mentioned hypothesis suggests that the block was actually part of the São Francisco-Congo paleocontinent westernmost tip before the Neoproterozoic collision (Pimentel et al., 1996; D'el-Rey Silva et al., 2011). D'el-Rey Silva et al. (2008) published the only detailed geological-structural study on the structure, the Rio Maranhão Thrust, arguing against the suture hypothesis. Aside from their own structural data the authors mention the Araí-Serra da Mesa lateral correlation and the occurrence of Paranoá Group rocks within the Brasília Belt internal zone as evidence for the Rio Maranhão Thrust being an intraplate fault development rather than a collisional suture.

The present work is limited in scope to test the validity of the microcontinent hypothesis but there are several common traits between the Crixás-Goiás and Campinorte terranes to suggest they were already amalgamated prior to the Neoproterozoic. Campinorte Arc felsic volcanism evidenced by felsic metavolcanoclastics (Figure 3B), rhyolitic crystal metatuffs and metalapilli tuffs (Giustina et al., 2009a) could share a common source with felsic pumice within Crixás schists. Arc magmatism responsible for the Pau de Mel suite could also have generated Paleoproterozoic diorite (Jost et al., 1993) and felsic bodies (Queiroz et al., 1999) within and in contact with the Crixás-Goiás Block. Absence of europium anomalies in most Pau de Mel Suite types 1 and 3 metagranites (Figure 6) is in tandem with the arc as a viable sediments source for the upper Crixás-Goiás metasedimentary sequences. Proximity to TTG domes would allow Crixás and Guarinos metasedimentary rocks to receive more Archean contribution than the Campinorte Sequence, as shown by Crixás metasedimentary rocks zircon ages (Jost et al., 2010a, 2012).

Gravimetric and seismic data argued to support the microcontinent hypothesis is not able to distinguish the Crixás-Goiás Block and Campinorte Arc. Gravimetric data reinterpretation coupled with newly acquired deep seismic refraction information (Assumpção et al., 2004; Berrocal et al., 2004; Soares et al., 2006; Perosi, 2006; Ventura et al., 2011) indicated an upwelling Moho boundary under the Goiás Magmatic Arc, the Crixás-Goiás Block and the Campinorte Arc. Additionally, CPRM (Brazil Geological Survey) magnetic surveys show the continuity of Hidrolina Dome low magnetic anomalies and Guarinos greenstone belt high magnetic anomalies into the Campinorte Arc terrane, underneath the Serra da Mesa Group, which most likely represent covered lithologies/structures trending out of the Crixás-Goiás Block. Based on magnetic anomalies continuity, lack of gravimetric contrast and similar coeval rock types covering both terranes we suggest that the Crixás-Goiás Block and the Campinorte Arc were accreted in the Paleoproterozoic and affected by the Brasiliano Cycle as a single crustal block.

Our hypothesis is incompatible with the widely accepted theory that the Crixás-Goiás Block was part of a drifting microcontinent (Pimentel et al., 2000; Valeriano et al., 2008). Either the block was adrift along with the Campinorte Arc or was part of the western margin of the São Francisco paleocontinent prior to the Neoproterozoic. We believe that the microcontinent hypothesis deserves further discussion in order to better refine the tectonic evolution of Central Brazil Archean-Paleoproterozoic rocks (Goiás Massif).

7. Campinorte Arc evolution

The compilation shown on figures 8A and 8B summarizes Campinorte Arc U-Pb and Nd_{TDM} data in comparison with published Goiás Massif ages. The present Campinorte Arc data compilation points to the occurrence of 2.18–2.15 Ma juvenile (Nd_{TDM} from 2.5 to 2.2 Ga), calc-alkaline, island arc metagranites within a metasedimentary basin with maximum depositional age of ~2.19 Ga (Kuyumjian et al., 2004; Giustina et al., 2009a). U-Pb ages provided in this work of long recognized granulites in the region showed zircon grains ages from 2.17 to 2.08 Ga whereas mafic lenses within them have interpreted crystallization ages of ~ 2.10 Ga.

Campinorte Arc petrographic, geochronologic, geochemical and isotopic data recorded three Paleoproterozoic stages, over an Archean one. These stages are summarized on Figure 9 and detailed as follows:

(1) ~ 2.19 to 2.15 Ga – Oceanic subduction event generating a dominantly granodioritic island arc (Pau de Mel Suite) and coeval forearc and back-arc basins. Erosion of the arc provided clay and silt deposition interbedded with manganese-silica-rich chemical sediments, sand and volcaniclastics of both Campinorte Sequence and Crixás-Goiás Block metasedimentary rocks. Major Paleoproterozoic contribution suggests that Campinorte Arc erosion as the main source of sediments whereas Archean TTG contribution was stronger in distal basin zones (Crixás and Guarinos sedimentary sequences). Basin closure was marked by intrusion of Crixás greenstone belt mafic dikes and younger Pau de Mel Suite granites.

(2) ~ 2.14-2.09 Ga – Tectonic switching, lithospheric thinning in the back-arc. The back-arc was composed of sediments (paragranulite PP02) and coeval mafic magmatism (mafic granulite RMR04). Upwelling Moho metamorphosed these rocks under granulite facies with peak at around 2.10 Ga.

(3) ~2.08 Ga – Contraction-led crustal thickening preserved peak-metamorphic mineral assemblages in Campinorte Arc granulites. Post-peak granitic magmatism (granodiorite PP030).

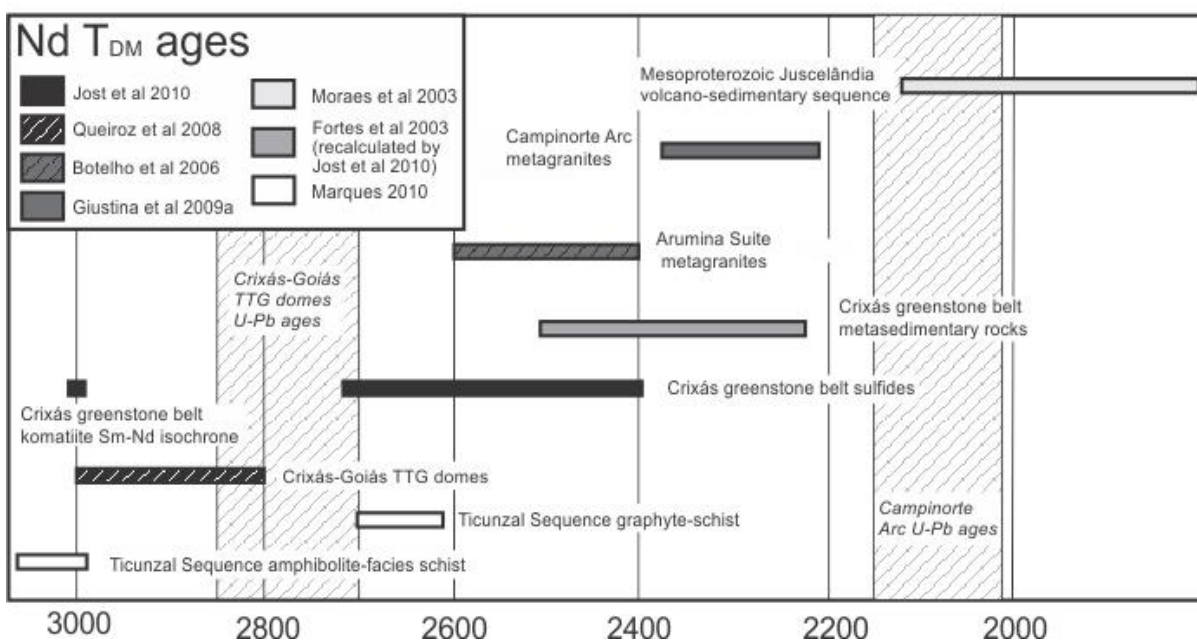
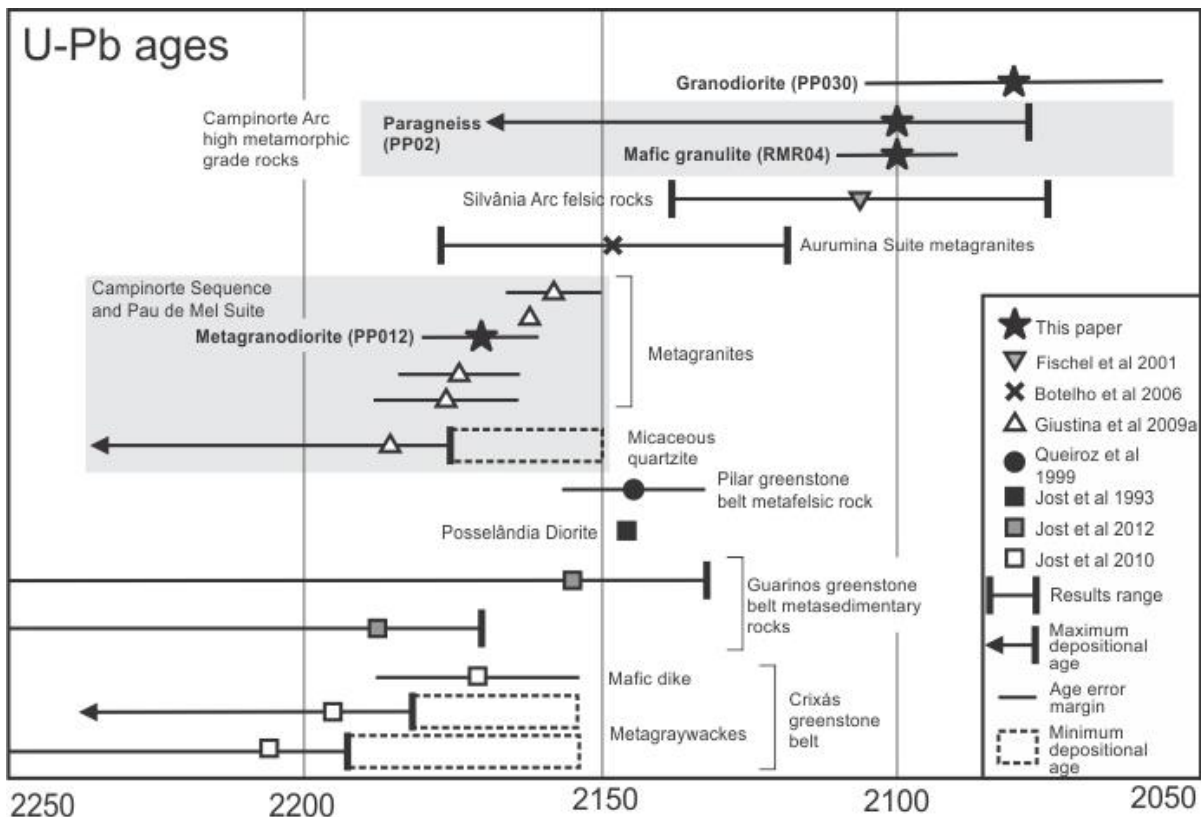
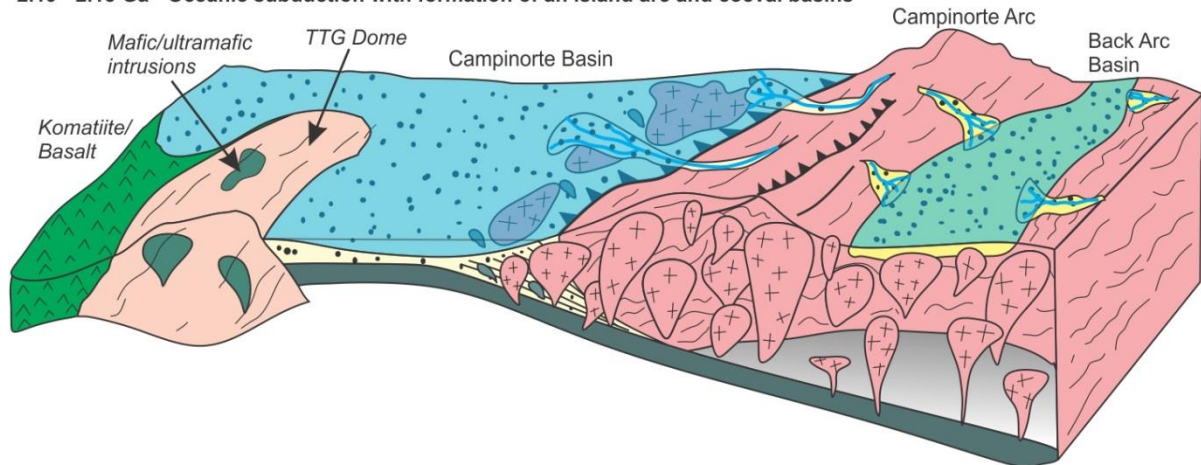


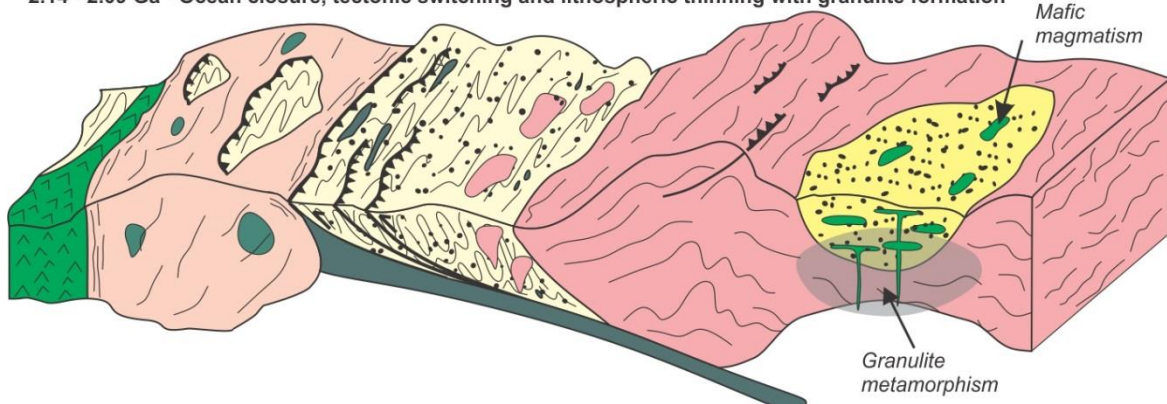
Figure 8 – A) Paleoproterozoic U-Pb ages and B) Archean-Paleoproterozoic Nd T_{DM} ages of the Campinorte Sequence and neighbor or coeval terranes (Jost et al., 1993; Fischel et al., 2001; Fortes et al., 2003; Moraes et al., 2003; Botelho et al., 2006; Queiroz et al., 2008; Giustina et al., 2009a; Jost et al., 2010; Marques 2010). Minimum sedimentation ages are inferred from U-Pb ages of rocks intrusive in the sequence.

The Campinorte Arc is not the sole example of Paleoproterozoic metagranites and related metavolcano-sedimentary rocks in a seemly arc setting. Contemporaneous northern Brasília Belt basement rocks as the Aurumina Suite (Botelho et al., 2006; Alvarenga et al., 2007) and the Silvânia Arc (Fischel et al., 2001) could be somehow related to the Campinorte Arc evolution. Unlike the Pau de Mel Suite, however, the biotite-muscovite-bearing Aurumina Suite is characterized by extensive peraluminous syn-collisional magmatism (Alvarenga et al., 2007). Such magmatism probably has been produced in a tectonic setting other than an island arc. Silvânia sequence metagranites and felsic metavolcanics, further south, show ages comparable to the Campinorte back arc granulites and are loosely interpreted as part of a magmatic arc (Fischel et al., 2001). Its genetic relationship with the Campinorte Arc deserves further study. Erosion of these Paleoproterozoic terranes would concur with data from Pimentel et al. (2011) and Matteini et al. (2012) showing major juvenile Paleoproterozoic sediments sources for the Mesoproterozoic Paranoá Group and Juscelândia Sequence (Figure 8).

~2.19 - 2.15 Ga - Oceanic subduction with formation of an island arc and coeval basins



~2.14 - 2.09 Ga - Ocean closure, tectonic switching and lithospheric thinning with granulite formation



After 2.08 Ga - Crustal thickening, granite magmatism and later exposure of granulites

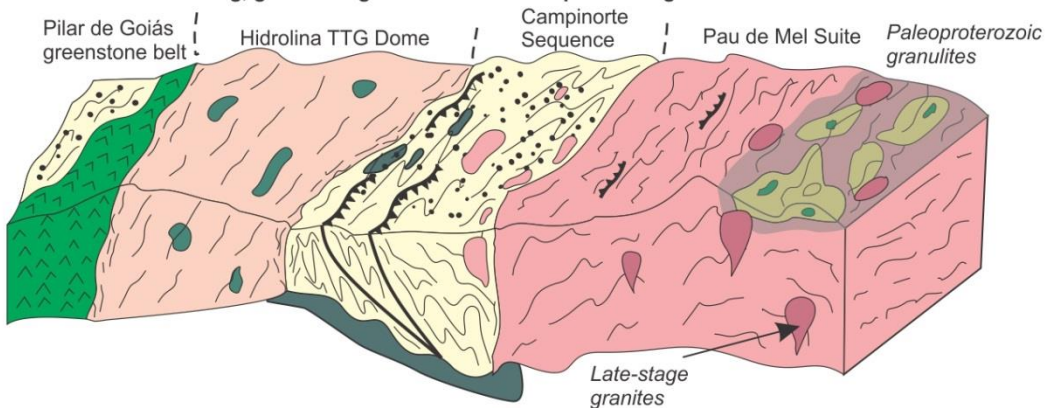


Figure 9 – Campinorte Arc tectonic evolution model.

8. Conclusions

Based on data made available in this paper and previously published information we conclude that:

Geochemical data, compatible tectonic settings and coeval crystallization ages argue in favour of a Paleoproterozoic arc of undefined extent, henceforth named Campinorte Arc. This arc is in contact to the west with the Neoproterozoic Goiás Magmatic Arc by the Rio dos Bois Thrust and to the east with the terrane composed of the Aurumina Suite and Ticunzal Formation by the Rio Maranhão Thrust. The Campinorte Arc tectonic relationship with the Aurumina Suite is unknown but they are likely to represent coeval orogens with no consanguinity. The Campinorte Arc is likely to have formed as an island arc due to juvenile ϵ Nd from -2.14 to +3.36 and lack of pre-Campinorte Arc zircon inheritance as observed by Giustina et al. 2009a.

Textural evidence of felsic volcanism influence, geographic proximity, similar rock types, coeval maximum sedimentation and model ages indicate that the Campinorte and Crixás/Guarinos greenstone belts metasedimentary sequences shared the same source of sediments and were probably part of the same basin. Gravimetric and seismic data support our common Campinorte-Crixás-Guarinos basin hypothesis. Alas, Hidrolina Dome low and Guarinos greenstone belt high magnetic analytical signal trending underneath the Serra da Mesa Group could imply blind TTG domes and greenstone belts within the region presently mapped as part of the Campinorte Arc. Given the predominance of Archean TTG rocks in the Crixás-Goiás Block against Paleoproterozoic metagranites and metasedimentary rocks in the Campinorte Sequence, they should remain separate terranes.

Granulites formed in a back arc basin from 2.14 to 2.09 Ga due to tectonic switching and consequent lithospheric thinning with metamorphic peak from 2.11-2.08 Ga. The arc was thereafter rapidly contracted preserving Paleoproterozoic metamorphic-peak mineral assemblages while allowing for an unknown volume of granitic magmatism (Sample PP030).

Acknowledgements

This work was supported by the Brazilian Council for Research and Technological Development (CNPQ), which granted a PhD scholarship to the first author and by research grants to CGO, MESDG, RVS and ELD. The University of Brasília is gratefully acknowledged for fieldwork support and access to laboratory facilities. B. Lima and E.N.P. Zacchi are thanked for helping with geochronology data acquisition and R.A. Fuck and N.F. Botelho for revising an earlier manuscript.

References

- Agbossoumoundé, Y., Ménot, R.-P., Paquette, J.L., Guillot, S., Yéssoufu, S., Perrache, C., 2007. Petrological and geochronological constraints on the origin of the Palimé–Amlamé granitoids (South Togo, West Africa): A segment of the West African Craton Paleoproterozoic margin reactivated during the Pan-African collision. *Gondwana Research* 12, 476-488.
- Albarède, F., Telouk, P., Blichert-Toft, J., Boyet, M., Agranier, A., Nelson, B., 2004. Precise and accurate isotopic measurements using multiple collector ICPMS. *Geochimica et Cosmochimica Acta* 68, 2725–2744
- Almeida, F.F.M., 1976. Evolução tectônica do Centro-Oeste brasileiro no Proterozóico Superior. *Anais da Academia Brasileira de Ciências* 40, 285-295.
- Alvarenga, C.J.S., Dardenne, M.A., Botelho, N.F., Lima, O.N.B., Machado, M.A., Almeida, T., 2007. Nota Explicativa das folhas SD.23-V-C-III (Monte alegre de Goiás), SD.23-V-C-V (Cavalcante) , SD.23-V-C-VI (Nova Roma). CPRM, 2007. 65 pp.
- Assumpção, M., An, M., Bianchi, M., França, G.S.L., Rocha, M., Barbosa, J.R., Berrocal, J., 2004. Seismic studies of the Brasília fold belt at the western border of the São Francisco Craton, Central Brazil, using receiver function, surface-wave dispersion and teleseismic tomography. *Tectonophysics* 388, 173-185.
- Baeta Jr., J.D.A., Figueiredo, A.N., Souza, E.P., Mello, J.C.R., 1972. Projeto Goianésia Barro Alto, Relatório Final. CPRM internal report, 123 pp with annexes.
- Baeta Jr., J.D.A., 1987. Uruaçu Folha SD.22-Z-B – Região Centro Oeste. Carta Metalogenética e de previsão de recursos minerais, Escala 1:250.000. CPRM/DNPM report, 9 pp with annexes.
- Barreto Filho, J.A., 1992. O maciço básico-ultrabásico de Água Branca: continuidade física dos maciços de Niquelândia e Goianésia-Barro Alto. *Boletim da Sociedade Brasileira de Geologia* 15, 23-29.
- Batchelor, R.A., Bowden, P., 1985. Petrogenetic interpretation of granitoid rock series using multicationic parameters. *Chemical Geology* 48, 43-55.

- Berrocal, J., Marangoni, Y., Sá, N.C., Fuck, R., Soares, J.E.P., Dantas, E., Perosi, F., Fernandes, C., 2004. Deep seismic refraction and gravity crustal model and tectonic deformation in Tocantins Province, Central Brazil. *Tectonophysics* 388, 187-199.
- Blum, M.L.B., Jost, H., Moraes, R.A.V., Pires, A.C.B., 2003. Caracterização dos complexos ortognáissicos arqueanos de goiás por gamaespectrometria aérea. *Revista Brasileira de Geociências* 33, 147-152.
- Botelho, N.F., Fuck, R.A., Dantas, E.L., Laux, J.L., Junges, S.L., 2006. The Paleoproterozoic Aurumina granite Suite, Goiás and Tocantins, whole rock geochemistry and U-Pb and Sm-Nd isotopic constraints. *The Paleoproterozoic Record of the São Francisco Craton. Brazil, IGCP 509*, 9-21.
- Brito Neves, B.B., Cordani, U.G., 1991. Tectonic evolution of South America during the Late Proterozoic. *Precambrian Research* 53, 23–40.
- Brito Neves, B.B., 2011. The Paleoproterozoic in the South American continent: Diversity in the geologic time. *Journal of South American Earth Sciences* 32, 270-286.
- Brito Neves, B.B., Fuck, R.A., 2013. Neoproterozoic evolution of the basement of the South American platform. *Journal of South American Earth Sciences* 47, 72-89.
- Brown, M., 2007. Metamorphism, plate tectonics, and the supercontinent cycle. *Earth Science Frontiers* 14, 1-18.
- Bühn, B., Pimentel, M.M., Matteini, M., Dantas, E.L., 2009. High spatial resolution analysis of Pb and U isotopes for geochronology by laser ablation multi-collector inductively coupled plasma mass spectrometry (LA-MC-ICP-MS). *Anais da Academia Brasileira de Ciências* 81, 1–16.
- Collins, W.J., 2002. Hot orogens, tectonic switching, and creation of continental crust. *Geology*, 30, 535-538.
- Cordeiro, P.F.O., 2014. Compartimentação Tectônica do Maciço de Goiás e o Arco de Campinorte. Unpublished PhD Thesis.
- Cordani, U.G., Hasui, Y., 1975. Comentários sobre os dados geocronológicos da Folha Goiás. In: Schobbenhaus, C. *Carta Geológica do Brasil ao Milionésimo – SD-22 – Folha Goiás*, Brasília, DNPM.

- Correia, C.T., Tassinari, C.C.G., Lambert, D.D., Kinny, P.D. and Girardi, V.A.V., 1997. U-Pb (SHRIMP), Sm-Nd and Re-Os systematics of the Cana Brava, Niquelândia and Barro Alto layered intrusions in central Brazil and constraints on the tectonic evolution. In: South American Symposium on Isotope Geology, 1, Campos do Jordão. 1997, p. 88-89.
- Cruz, E.L.C.C., Kuyumjian, R.M., Boaventura, G.R., 2003. Low-K calc-alkaline granitic series of southeastern Tocantins state: chemical evidence for two sources for the granite-gneissic complex in the Paleoproterozoic Almas-Dianópolis terrane. Revista Brasileira de Geociências 33, 125-136.
- Delgado, I.M., Souza, J.D., Silva, L.C., Silveira Filho, N.C., Santos, R.A., Pedreira, A.J., Guimarães, J.T., Angelim, L.A., Vasconcelos, A.M., Gomes, I.P., Lacerda Filho, J.V., Valente, C.R., Perrota, M.M., Heinick, C.A., 2003. Província Tocantins, in: Bizzi, L.A., Schobbenhaus, C., Vidotti, R.M., Gonçalves, J.H. (Eds.), Geologia, Tectônica e Recursos Minerais do Brasil. CPRM, Rio de Janeiro, pp. 281-292.
- Ferreira Filho, C.F., Pimentel, M.M., Araújo, S.M., Laux, J.H., 2010 Layered intrusions and volcanics sequences in Central Brazil: geological and geochronological constraints for Mesoproterozoic (1.25 Ga) and Neoproterozoic (0.79 Ga) igneous associations. Precambrian Research 183, 617-634.
- Fischel, D.P., Pimentel, M.M., Fuck, R.A., Armstrong, R., 2001. U-Pb SHRIMP and Sm-Nd geochronology of the Silvânia Volcanics and Jurubatuba Granite: juvenile Paleoproterozoic crust in the basement of the Neoproterozoic Brasília Belt, Goiás, central Brazil. Anais Academia Brasileira de Ciências 73, 445-460.
- Fortes, P.T.F.O., Pimentel, M.M., Santos, R.V., Junges, S.L., 2003. Sm–Nd studies at Mina III gold deposit, Crixás greenstone belt, Central Brazil: implications for the depositional age of the upper metasedimentary rocks and associated Au mineralization. Journal of South American Earth Sciences 16, 503–512.
- Frost, B.R., Barnes, C.G., Collins, W.J., Arculus, R.J., Ellis, D.J., Frost, C.D., 2001. A Geochemical classification for granitic rocks. Journal of Petrology 42, 2033-2048.

- Fuck, R.A., 1994. A Faixa Brasília e a compartimentacão tectônica na Província Tocantins. In: SBG, Simpósio de Geologia do Centro-Oeste, 4, Anais, 184–187.
- Fuck, R.A., Danni, J.C.M., Winge, M., Andrade, G.F., Barreira, C.F., Leonards, O.H., Kuyumjian, R.M., 1981. Geologia da Região de Goianésia. Simpósio de Geologia do Centro-Oeste, Goiânia, p.447-469.
- Gibson, G.M., Ireland, T.R., 1995. Granulite formation during continental extention in Fiordland, New Zealand. *Nature* 375, 479-482.
- Giustina, M.E.S.D., Oliveira, C.G., Pimentel, M.M., Melo, L.V., Fuck, R.A., Dantas, E.L., Buhn, B., 2009a. U–Pb and Sm–Nd constraints on the nature of the Campinorte Sequence and related Paleoproterozoic juvenile orthogneisses, Tocantins Province, Central Brazil. *Geological Society of London Special Publication* 323, 255-269.
- Giustina, M.E.S.D., Oliveira, C.G., Pimentel, M.M., Buhn, B., 2009b. Neoproterozoic magmatism and high-grade metamorphism in the Goiás Massif: New LA-MC-ICPMS U–Pb and Sm–Nd data and implications for collisional history of the Brasília Belt. *Precambrian Research* 172, 67-79.
- Giustina, M.E.S.D., Pimentel, M.M., Ferreira Filho, C.F., Fuck, R.A., Andrade, S., 2011. U–Pb–Hf-trace element systematics and geochronology of zircon from a granulite-facies metamorphosed mafic–ultramafic layered complex in Central Brazil. *Precambrian Research* 189, 176-192.
- Gorayeb, P.S.S., Moura, C.A.V., Barros, G.R., 2000. Pb-Pb zircon ages of the Porto Nacional high-grade metamorphic terrain, northern portion of the Goiás Massif, Central Brazil. *Revista Brasileira de Geociências* 30, 190-194.
- Harley, S.L., 1998. On the occurrence and characterization of ultrahigh-temperature crustal metamorphism. *Geological Society of London. Special Publication* 138, 81–107.
- Heilbron, M., Duarte, B.P., Valeriano, C.M., Simonetti, A., Machado, N., Nogueira, J.R., 2010. Evolution of reworked Paleoproterozoic basement rocks within the Ribeira belt (Neoproterozoic), SE-Brazil, based on U–Pb geochronology: Implications for paleogeographic reconstructions of the São Francisco-Congo paleocontinent. *Precambrian Research* 178, 136-148.

- Jackson, S.E., Pearson, N.J., Griffin,W.L., Belousova, E.A., 2004. The application of laser ablation-inductively coupled plasma-mass spectrometry to in situ U-Pb zircon geochronology. *Chemical Geology* 211, 47–69.
- Jost, H., Pimentel, M.M., Fuck, R.A., Danni, J.C.M., Heaman, L., 1993. Idade U-Pb do diorito Posselândia, Hidrolina, Goiás. *Revista Brasileira de Geociências* 23, 352-355.
- Jost, H., Theodoro, S.M.C., Figueiredo, A.M.G., Boaventura, G.R., 1996. Propriedades geoquímicas e proveniência de rochas metassedimentares detritícias arqueanas dos greenstone belts de Crixás e Guarinos, Goiás. *Revista Brasileira de Geociências* 26, 151-166.
- Jost, H., Chemale, F., Dussin, I.A., Tassinari, C.C.G., Martins, R., 2010. A U-Pb zircon Paleoproterozoic age for the metasedimentary host rocks and gold mineralization of the Crixás greenstone belt, Goiás, central Brazil. *Ore Geology Reviews*, 37:127-139.
- Jost, H. and Scandolara, J.E., 2010. Características estruturais, petrográficas e geoquímicas de enxames de diques maficos intrusivo em rochas metassedimentares do Greenstone Belt de Crixás, Goiás. *Geologia USP Série Científica* 10, 119-134.
- Jost, H., Rodrigues, V.G., Carvalho, M.J., Chemale, F., Marques, J.C., 2012. Estratigrafia e geocronologia do greenstone belt de Guarinos, Goiás. *Geologia USP Série Científica* 12, 31-48.
- Klein, E.L., Moura, A.V., 2008. São Luís Craton and Gurupi Belt (Brazil): possible links with the West African Craton and surrounding Pan-African belts. *Geological Society, London, Special Publications* 294, 137-151.
- Kuyumjian, R.M., Oliveira, C.G., Campos, J.E.G., Queiroz, C.L., 2004. Geologia do limite entre os terrenos Arqueanos e o Arco Magmático de Goiás na região de Chapada-Campinorte, Goiás. *Revista Brasileira de Geociências* 34, 329-334.
- Lenharo, S.L.R., Moura, M.A., Botelho, N.F., 2002. Petrogenetic and mineralization processes in Paleo- to Mesoproterozoic rapakivi granites: examples from Pitinga and Goiás, Brazil. *Precambrian Research* 119, 277-299.
- Ludwig, K.R., 1993. PBDAT. A computer program for processing Pb-U-Th isotope data. USGS Open File Report, 88-542, pp. 34.

- Ludwig, K.R., 2003, User's Manual for Isoplot/Ex v. 3.00. A Geochronological Toolkit for Microsoft Excel. BGC Special Publication 4, Berkeley, 71 pp.
- Marangoni, Y., Assumpção, M., Fernandes, E.P., 1995. Gravimetria em Goiás, Brasil. Revista Brasileira de Geofísica 13, 205–219.
- Marini, O.J., Liberal, C.S., Reis, L.T., Trindade, C.A.H., Souza, S.L., 1978 Nova unidade litoestratigráfica do Pré-Cambriano do estado de Goiás, In: SBG, Congresso Brasileiro de Geologia, 30, Recife, 126-127.
- Marques, G.C., 2010. Geologia dos grupos Araí e Serra da Mesa e seu embasamento no sul do Tocantins. Unpublished MSc thesis, Universidade de Brasília, 122 pp.
- Matteini, M., Dantas, E.L., Pimentel, M.M., Alvarenga, C.J.S., Dardenne, M.A., 2012. U-Pb and Hf isotope study on detrital zircons from the Paranoá Group, Brasilia Belt, Brazil: Constraints on depositional age at Mesoproterozoic – Neoproterozoic transition and tectono-magmatic events in the São Francisco craton. Precambrian Research 206-207, 168-181.
- Moraes, R., Fuck, R.A., 2000. Ultra-high-temperature metamorphism in Central Brazil: the Barro Alto Complex. Journal of Metamorphic Geology 18, 345-358.
- Moraes, R., Fuck, R.A., Pimentel, M.M., Gioia, S.M.C.L., Figueiredo, A.M.G., 2003. Geochemistry and Sm-Nd isotopic characteristics of bimodal volcanic rocks of Juscelândia, Goiás, Brazil: Mesoproterozoic transition from continental rift to ocean basin. Precambrian Research 125, 317-336.
- Moraes, R., Fuck, A.R., Pimentel, M.M., Gioia, S.M.C.L., Hollanda, M.H.B.M., Armstrong, R., 2006. The bimodal rift-related volcanosedimentary sequence in Central Brazil: Mesoproterozoic extention and Neoproterozoic metamorphism. Journal of South American Earth Sciences 20, 287–301
- Oliveira, C.G., Oliveira, F.B., Dantas, E.L., Fuck, R.A., 2006. Programa Geologia do Brasil – Folha Campinorte. FUB/CPRM, Brasília, 124.
- Oliveira, E.P., Souza, Z.S., McNaughton, N.J., Lafon, N.J., Costa, F.G., Figueiredo, A.M., 2011. The Rio Capim volcanic-plutonic-sedimentary belt, São Francisco Craton, Brazil: Geological, geochemical and isotopic evidence for oceanic arc accretion during Palaeoproterozoic continental collision. Gondwana Research 19, 735-750.

- Pearce, J.A., Harris, N.B.W., and Tindle, A.G., 1984. Trace element discrimination diagrams for the tectonic interpretation of granitic rocks. *Journal of Petrology* 25, 956-983.
- Perosi, F.A., 2006. Estrutura crustal do setor central da Província Tocantins utilizando ondas P, S e fases refletidas com dados de refração de sísmica profunda. Unpublished PhD thesis, Universidade de São Paulo, 162 pp.
- Pimentel, M.M., Heaman, L., Fuck, R.A., Marini, O.J., 1991. U-Pb zircon geochronology of Precambrian tin-bearing continental-type acid magmatism in central Brazil. *Precambrian Research* 52, 321-335.
- Pimentel, M.M., Fuck, R.A., Silva, J.L.H., 1996. Dados Rb-Sr e Sm-Nd da região de Jussara- Goiás-Mossâmedes (GO), e o limite entre terrenos antigos do Maciço de Goiás e o Arco Magmático de Goiás. *Revista Brasileira de Geociências* 26, 61–70.
- Pimentel, M.M., Fuck, R.A., Botelho, N.F., 1999. Granites and the geodynamic history of the Neoproterozoic Brasília belt, Central Brazil: a review. *Lithos* 46, 463-483.
- Pimentel, M.M., Fuck, R.A., Jost, H., Ferreira Filho, C.F., Araújo, S.M., 2000. The basement of the Brasília Belt and the Goiás Magmatic Arc. In: Cordani, U.G., Milani, E.J., Thomaz Filho, A., Campos, D.A. (eds) *Tectonic Evolution of South America. 31st International Geological Congress, Rio de Janeiro*, 195–229.
- Pimentel, M.M., Botelho, N.F., 2001. Sr and Nd isotopic characteristics of 1.77-1.58 Ga rift-related granites and volcanics of the Goiás tin province, Central Brazil. *Anais da Academia Brasileira de Ciências* 73, 263-276.
- Pimentel, M.M., Ferreira Filho, C.F., Armstrong, R.A., 2004. SHRIMP U-Pb and Sm-Nd ages of the Niquelândia layered complex: Meso- (1.25 Ga) and Neoproterozoic (0.79 Ga) extentional events in central Brazil. *Precambrian Research* 132, 133-153.
- Pimentel, M.M., Rodrigues, J.B., Giustina, M. E. S., Junges, S., Matteini, M., Armstrong, R., 2011. The tectonic evolution of the Neoproterozoic Brasília Belt, central Brazil, based on SHRIMP and LA-ICPMS U-Pb sedimentary provenance data: A review. *Journal of South American Earth Sciences* 31, 345-357.

- Queiroz C.L., Jost H., McNaughton N.J., 1999. U/Pb - SHRIMP ages of Crixás granite-greenstone belt terranes: from Archaean to Neoproterozoic. Extended abstract, Simpósio Nacional de Estudos Tectônicos, Lençóis, Anais, p. 35-37.
- Queiroz, C.L., Jost, H., Silva, L.C., McNaughton, N.J., 2008. U-Pb SHRIMP and Sm-Nd geochronology of granite-gneiss complexes and implications for the evolution of the Central Brazil Archean Terrain. *Journal of South American Earth Sciences* 26, 100-124.
- Rosa-Costa, L.T., Lafon, J.M., Delor, C., 2006. Zircon geochronology and Sm-Nd isotopic study: Further constraints for the Archean and Paleoproterozoic geodynamical evolution of the southeastern Guiana Shield, north of Amazonian Craton, Brazil. *Gondwana Research* 10, 277-300.
- D'el-Rey Silva, J.H., Vasconcelos, M.A.R., Silva, D.V.G., 2008. Timing and role of the Maranhão River Thrust in the evolution of the Neoproterozoic Brasília Belt and Tocantins Province, central Brazil. *Gondwana Research* 13, 352-374.
- D'el-Rey Silva, J.H., Oliveira, I.L., Pohren, C.B., Tanizaki, M.L.N., Carneiro, R.C., Fernandes, G.L.F., Aragão, P.E., 2011. Coeval perpendicular shortenings in the Brasília Belt: collision of irregular plate margins leading to orocinal bending in the Neoproterozoic of central Brazil. *Journal of South American Earth Sciences* 32, 1-13.
- Soares, J.E., Berrocal, J., Fuck, R.A., Mooney, W.D., Ventura, D.B.R., 2006. Seismic characteristics of central Brazil crust and upper mantle: A deep seismic refraction study. *Journal of Geophysical Research* 111, 1-31.
- Stacey, J.S., Kramers, J.D., 1975. Approximation of terrestrial lead isotope evolution by a two-stage model. *Earth and Planetary Science Letters* 26, 207–221.
- Thompson, A.B., Schulmann, K., Jeezek, J., Tolar, V., 2001. Thermally softened continental zones (arcs and rifts) as precursors to thickened orogeny belts: *Tectonophysics* 332, 115-141.
- Touret, J.L.R., Huizenga, J.M., 2012. Fluid-assisted granulite metamorphism: a continental journey. *Gondwana Research* 21, 224-235.
- Valeriano, C.M., Pimentel, M.M., Heilbron, M., Almeida, J.C.H., Trouw, R.A.J., 2008. Tectonic evolution of the Brasília Belt, Central Brazil, and early assembly of Gondwana. *Geological Society, London, Special Publication* 294, 197-210.

Ventura, D.B.R., Soares, J.E.P., Fuck, R.A., Caridade, L.C.C., 2011. Caracterização sísmica e gravimétrica da litosfera sob a linha de refração sísmica profunda de Porangatu, Província Tocantins, Brasil Central. Revista Brasileira de Geociências 41, 130-140.

Waters, D.J., 1991. Hercynite-quartz granulites: phase relations, and implications for crustal processes. European Journal of Mineralogy 3, 367-386.

Winge, M., 1995. Evolução dos terrenos granulíticos da Província Estrutural Tocantins, Brasil Central. Unpublished PhD Thesis, 149 pp with annexes.

Wu, Y.-B., Zhen, Y.-F., Gao, S., Jiao, W.-F., Liu, Y.-S., 2008. Zircon U-Pb age and trace element evidence for Paleoproterozoic granulite-facies metamorphism and Archean crustal rocks in the Dabie Orogen. Lithos 101, 308-322.

Table 1 – Pau de Mel Suite representative whole-rock geochemistry data

Sample	CAMPB2	TREVO	CAMP 61B	MR-046	PAU DE MEL	CAMP20	CAMP66	CAMP50	VAI-VEM
Type	3 Meta tonalite	3 Meta tonalite	3 Grano diorite	1 Grano diorite	1 Grano diorite	2 Grano diorite	2 Grano diorite	2 Grano diorite	2 Monzo granite
Rock									
<i>Major elements (wt%)</i>									
SiO ₂	56.75	59.47	68.87	71.21	69.86	72.24	72.45	67.68	73.74
Al ₂ O ₃	17.15	17.38	15.41	15.14	16.23	12.92	12.31	14.49	14.28
TiO ₂	0.73	0.66	0.46	0.28	0.32	0.32	0.32	0.52	0.11
Fe ₂ O ₃ t	6.56	5.95	3.31	2.29	2.05	4.83	4.15	4.90	1.44
MnO	0.10	0.08	0.03	0.04	0.04	0.07	0.06	0.08	0.03
MgO	4.02	2.84	1.10	0.74	0.79	0.29	0.42	1.48	0.30
CaO	6.44	6.06	2.45	2.84	2.98	1.65	1.83	3.32	1.08
Na ₂ O	3.79	4.09	3.96	4.25	4.51	3.21	4.08	3.34	4.24
K ₂ O	1.42	1.38	2.61	2.02	2.14	3.31	2.84	2.33	3.27
P ₂ O ₅	0.30	0.26	0.13	0.12	0.10	0.04	0.06	0.19	0.01
LOI	2.40	1.70	1.50	0.80	0.90	0.90	1.30	1.50	1.40
Total	99.65	99.88	99.80	99.73	99.93	99.76	99.82	99.79	99.89
V	110.0	90.0	34.0	25.0	25.0	18.0	19.0	62.0	8.0
Ni	34.7		2.2	5.3		1.8	1.8	3.1	
Zn	59.0		25.0	68.0		89.0	72.0	38.0	
Ga	20.0	19.7	19.0	19.5	21.0	21.3	17.3	14.9	18.5
Rb	36.4	36.4	46.8	89.7	87.9	116.8	90.1	53.9	77.5
Sr	757.5	694.3	487.5	573.7	525.6	205.9	164.9	399.8	164.3
Y	10.9	14.0	11.0	5.7	5.3	93.4	53.0	27.2	34.6
Zr	73.7	150.8	158.7	128.0	119.0	288.9	235.7	176.0	77.4
Nb	5.0	5.1	6.7	2.6	3.1	10.6	8.6	9.0	7.8
Ba	543.0	622.3	606.0	669.0	740.4	685.0	497.0	550.0	664.4
Ta	0.4	0.5	0.7	0.3	0.7	0.9	1.0	0.9	1.0
Pb	0.9	1.0	2.5	2.5	1.9	5.1	8.6	0.7	2.9
Th	1.5	1.5	6.3	6.8	5.7	11.3	8.6	4.6	10.0
Hf	1.9	3.5	4.5	4.0	4.0	8.5	6.8	4.9	3.2
U	0.8	0.7	1.1	1.2	1.2	2.8	2.4	1.2	4.1
<i>Rare earth elements (ppm)</i>									
La	24.30	28.10	30.10	25.90	27.00	72.70	38.00	26.00	26.20
Ce	54.40	51.40	55.90	52.70	53.60	62.90	72.50	54.40	42.60
Pr	7.22	7.34	6.94	6.33	5.73	20.45	9.24	6.97	7.34
Nd	29.40	31.40	23.50	23.50	21.90	72.90	33.60	25.40	27.90
Sm	4.89	5.40	3.97	3.80	4.00	15.42	6.97	5.28	6.80
Eu	1.42	1.49	1.26	0.97	1.00	2.84	1.41	1.54	1.18
Gd	3.60	3.75	3.06	2.46	2.08	16.38	7.90	4.86	5.84
Tb	0.45	0.51	0.44	0.26	0.22	2.91	1.32	0.82	1.07
Dy	2.21	2.41	1.97	1.10	1.11	15.02	7.41	4.20	6.23
Ho	0.37	0.47	0.39	0.16	0.13	3.42	1.69	0.97	1.22
Er	0.92	1.22	0.99	0.36	0.42	9.42	4.96	2.77	3.65
Tm	0.13	0.19	0.16	0.06	0.06	1.53	0.76	0.42	0.61
Yb	0.83	1.22	0.92	0.34	0.23	8.95	4.53	2.55	4.12
Lu	0.12	0.16	0.13	0.05	0.05	1.33	0.70	0.43	0.57

Table 2 – LA-ICPMS data for sample PP012

Sample	Isotopic ratios								Apparent ages								
	f(206) %	Th/U	$^{206}\text{Pb}/^{204}\text{Pb}$	$^{207}\text{Pb}/^{206}\text{Pb}$	1s (%)	$^{207}\text{Pb}/^{235}\text{U}$	1s (%)	$^{206}\text{Pb}/^{238}\text{U}$	1s (%)	$^{207}\text{Pb}/^{206}\text{Pb}$	2σ	$^{207}\text{Pb}/^{235}\text{U}$	2σ	$^{206}\text{Pb}/^{238}\text{U}$	2σ	Rho	Conc (%)
Metagranite PP012																	
PP012-Z1	0.17	0.46	8591	0.13072	0.4	6.7868	0.6	0.3766	0.5 0	2107.6	7	2084.0	5	2060.2	8	0.69	98
PP012-Z2	0.02	0.23	63355	0.13438	0.4	7.5915	0.7	0.4097	0.6 0	2155.9	7	2183.9	6	2213.7	10	0.76	103
PP012-Z3	0.25	0.13	6077	0.12922	1.5	6.6840	2.7	0.3752	2.2 0	2087.4	27	2070.5	24	2053.6	39	0.94	98
PP012-Z4	0.14	0.24	10694	0.12875	0.4	5.9824	0.9	0.3370	0.8 0	2081.0	7	1973.3	8	1872.2	14	0.89	90
PP012-Z5	0.01	0.30	185981	0.13539	0.5	7.4915	1.4	0.4013	1.3 0	2169.1	9	2172.0	13	2175.0	24	0.93	100
PP012-Z6	0.02	0.12	97411	0.13174	0.4	6.9761	1.0	0.3841	0.9 0	2121.3	7	2108.4	9	2095.2	16	0.89	99
PP012-Z7	0.04	0.30	41663	0.12517	1.6	5.2519	1.9	0.3043	0.9 0	2031.3	28	1861.1	16	1712.6	14	0.71	84
PP012-Z8	0.04	0.23	35252	0.13259	0.4	6.5882	0.8	0.3604	0.6 0	2132.6	8	2057.8	7	1983.9	11	0.78	93
PP012-Z9	0.10	0.27	17387	0.07283	1.4	1.6943	2.0	0.1687	1.4 0	1009.2	29	1006.4	13	1005.1	13	0.68	100
PP012-Z10	0.18	0.04	8736	0.12327	0.5	4.9480	0.9	0.2911	0.7 0	2004.1	9	1810.5	7	1647.1	10	0.80	82
PP012-Z11	0.03	0.35	59127	0.13292	1.1	6.5746	1.4	0.3587	0.9 0	2136.9	20	2056.0	13	1976.2	15	0.80	92
PP012-Z12	0.13	0.36	12171	0.12491	0.5	5.2914	1.4	0.3072	1.3 0	2027.5	9	1867.5	12	1727.1	20	0.93	85
PP012-Z13	0.01	0.32	125489	0.13794	0.7	7.7918	0.9	0.4097	0.6 0	2201.6	12	2207.3	9	2213.4	12	0.62	101
PP012-Z14	0.01	0.21	295833	0.07151	0.5	1.7392	0.7	0.1764	0.5 0	972.1	11	1023.2	5	1047.2	5	0.62	108
PP012-Z15	0.17	0.28	9112	0.13215	1.0	6.6345	1.3	0.3641	0.7 0	2126.7	18	2064.0	11	2001.7	12	0.71	94
PP012-Z16	0.01	0.23	147826	0.13726	0.8	7.7589	1.1	0.4100	0.8 0	2193.0	13	2203.5	10	2214.8	15	0.70	101
PP012-Z17	0.01	0.26	124391	0.13757	0.7	7.6758	1.1	0.4047	0.8 0	2196.8	13	2193.8	10	2190.5	15	0.71	100
PP012-Z18	0.30	0.38	5430	0.11950	0.6	4.0120	2.3	0.2435	2.2 0	1948.8	10	1636.6	19	1404.8	28	0.97	72
PP012-Z19	0.01	0.29	265359	0.13552	0.8	7.8536	1.0	0.4203	0.6 0	2170.8	14	2214.4	9	2261.8	11	0.68	104
PP012-Z20	0.01	0.43	235152	0.13573	0.4	7.6099	0.7	0.4066	0.5 0	2173.5	7	2186.0	6	2199.4	10	0.71	101
PP012-Z21	0.01	0.41	257792	0.13654	0.4	7.4825	0.7	0.3975	0.6 0	2183.7	8	2170.9	7	2157.3	11	0.74	99
PP012-Z22	0.09	0.32	16204	0.14072	0.9	7.2790	1.4	0.3752	1.1 0	2236.0	15	2146.2	12	2053.7	19	0.78	92
PP012-Z23	0.01	0.12	131026	0.13416	1.3	7.1316	1.4	0.3855	0.6 0	2153.1	23	2128.0	13	2102.1	10	0.54	98
PP012-Z24	0.02	0.44	78162	0.13186	0.4	6.4641	1.1	0.3555	1.0 0	2122.9	7	2041.0	10	1961.0	17	0.92	92
PP012-Z25	0.00	0.21	354594	0.13804	0.4	7.9440	0.9	0.4174	0.8 0	2202.8	7	2224.7	8	2248.6	16	0.87	102
PP012-Z26	0.42	0.47	3656	0.12826	0.6	5.8937	2.1	0.3333	2.0 0	2074.3	10	1960.3	18	1854.2	32	0.96	89
PP012-Z27	0.57	0.45	2747	0.12294	1.7	5.1601	1.9	0.3044	0.8 0	1999.3	31	1846.1	16	1713.1	12	0.62	86
PP012-Z28	0.00	0.24	663919	0.13282	0.4	7.0226	0.7	0.3835	0.5 0	2135.5	7	2114.3	6	2092.5	10	0.73	98
PP012-Z30	0.02	0.33	72072	0.13381	1.0	7.0118	1.3	0.3801	0.8 0	2148.5	17	2112.9	11	2076.6	15	0.61	97
PP012-Z31	0.01	0.18	159768	0.12995	1.1	6.8369	3.8	0.3816	3.6 0	2097.3	20	2090.5	33	2083.7	64	0.95	99
PP012-Z32	0.01	0.44	246289	0.13438	1.0	7.0850	1.2	0.3824	0.7 0	2156.0	17	2122.2	11	2087.4	12	0.53	97
PP012-Z35	0.13	0.45	11422	0.13785	0.7	6.8093	1.1	0.3583	0.9 0	2200.4	12	2086.9	10	1973.9	15	0.76	90

Sample	Isotopic ratios								Apparent ages									
	f(206) %	Th/U	$^{206}\text{Pb}/^{204}\text{Pb}$	$^{207}\text{Pb}/^{206}\text{Pb}$	1s (%)	$^{207}\text{Pb}/^{235}\text{U}$	1s (%)	$^{206}\text{Pb}/^{238}\text{U}$	1s (%)	$^{207}\text{Pb}/^{206}\text{Pb}$	2σ	$^{207}\text{Pb}/^{235}\text{U}$	2σ	$^{206}\text{Pb}/^{238}\text{U}$	2σ	Rho	Conc (%)	
PP012-Z36	0.02	0.26	75823	0.13641	0.6	7.4600	0.9	0.3966	0.7	0	2182.1	11	2168.2	8	2153.6	12	0.70	99
PP012-Z37	0.03	0.28	50194	0.13837	0.9	7.4960	1.2	0.3929	0.8	0	2206.9	15	2172.5	11	2136.3	14	0.63	97
PP012-Z38	0.36	0.29	4531	0.12430	1.1	4.1625	2.0	0.2429	1.7	0	2018.8	18	1666.7	17	1401.7	22	0.94	69
PP012-Z39	0.24	0.42	6370	0.13183	0.5	6.2443	1.2	0.3435	1.1	0	2122.5	9	2010.7	10	1903.7	18	0.89	90
PP012-Z40	0.00	0.64	306353	0.13994	0.6	8.0006	0.9	0.4146	0.6	0	2226.5	10	2231.1	8	2236.1	12	0.70	100
PP012-Z41	11.12	0.02	140	0.11957	2.5	4.6900	3.2	0.2845	1.7	0	1949.8	45	1765.5	26	1613.9	27	0.54	83
PP012-Z42	0.02	0.40	66649	0.13334	1.4	7.2543	2.6	0.3946	2.2	0	2142.4	24	2143.2	23	2144.1	39	0.94	100
PP012-Z43	0.01	0.36	151924	0.06145	0.6	1.0219	1.1	0.1206	0.9	0	654.9	13	714.9	5	734.1	6	0.80	112
PP012-Z44	0.01	0.46	149575	0.07332	0.7	1.7918	0.9	0.1772	0.6	0	1022.8	13	1042.5	6	1051.9	5	0.57	103
PP012-Z45	0.57	0.29	2856	0.13111	0.5	4.2356	1.5	0.2343	1.5	0	2112.9	8	1680.9	13	1357.0	18	0.95	64
PP012-Z46	0.01	0.25	165452	0.13309	0.7	6.5143	1.1	0.3550	0.8	0	2139.1	12	2047.8	9	1958.4	14	0.86	92
PP012-Z47	0.02	0.25	64242	0.13100	0.5	6.6536	1.0	0.3684	0.9	0	2111.4	9	2066.5	9	2021.8	15	0.85	96
PP012-Z48	0.01	0.32	221505	0.13735	0.6	7.8272	0.9	0.4133	0.7	0	2194.0	10	2211.3	8	2230.1	13	0.73	102
PP012-Z50	0.60	0.18	2796	0.10249	2.0	2.6516	2.4	0.1876	1.3	0	1669.8	36	1315.1	17	1108.5	14	0.78	66
PP012-Z51	0.13	0.17	11701	0.12862	0.7	5.9005	1.6	0.3327	1.4	0	2079.2	12	1961.3	14	1851.6	23	0.89	89
PP012-Z53	0.01	0.22	253768	0.13556	0.5	7.5326	0.7	0.4030	0.6	0	2171.2	9	2176.9	7	2182.9	10	0.68	101
PP012-Z54	0.01	0.33	108472	0.13422	0.8	7.3054	1.1	0.3948	0.7	0	2153.9	14	2149.5	9	2144.9	13	0.76	100
PP012-Z56	0.18	0.34	8062	0.13738	0.5	7.7123	0.9	0.4072	0.7	0	2194.4	9	2198.0	8	2202.0	13	0.79	100
PP012-Z57	0.01	0.22	177111	0.13464	0.5	7.4365	0.7	0.4006	0.5	0	2159.4	8	2165.4	6	2171.7	10	0.68	101
PP012-Z59	0.01	0.25	183697	0.13498	0.5	7.4156	0.9	0.3984	0.7	0	2163.8	9	2162.9	8	2161.9	13	0.77	100
PP012-Z61	0.01	0.35	133194	0.13771	0.6	7.6527	0.9	0.4030	0.7	0	2198.6	11	2191.1	8	2183.0	13	0.70	99

Table 3 – LA-ICPMS data for sample RMR04

Sample	Isotopic ratios								Apparent ages								
	f(206) %	Th/U	$^{206}\text{Pb}/^{204}\text{Pb}$	$^{207}\text{Pb}/^{206}\text{Pb}$	1s (%)	$^{207}\text{Pb}/^{235}\text{U}$	1s (%)	$^{206}\text{Pb}/^{238}\text{U}$	1s (%)	$^{207}\text{Pb}/^{206}\text{Pb}$	2σ	$^{207}\text{Pb}/^{235}\text{U}$	2σ	$^{206}\text{Pb}/^{238}\text{U}$	2σ	Rho	Con%
RMR04_Z1a	0.09	0.09	17844	0.13057	0.5	6.4612	1.4	0.3589	1.3	2105.6	9.3	2040.6	12.6	1977.0	22.8	0.93	97
RMR04_Z1b	0.02	0.15	90377	0.13227	0.6	6.7168	0.8	0.3683	0.6	2128.4	9.9	2074.8	7.3	2021.3	10.3	0.77	97
RMR04_Z1c	0.13	0.09	11380	0.12797	0.6	6.4896	1.6	0.3678	1.4	2070.3	11.4	2044.5	13.8	2019.0	24.7	0.91	99
RMR04_Z1d	0.03	0.10	72117	0.13171	0.5	6.6200	0.9	0.3645	0.8	2120.9	7.9	2062.0	7.8	2003.7	13.1	0.84	97
RMR04_Z1e	0.14	0.09	10834	0.13034	0.6	6.2060	1.6	0.3453	1.4	2102.6	10.9	2005.3	13.8	1912.2	24.0	0.92	95
RMR04_Z1f	0.11	0.08	12636	0.12793	0.6	6.9889	1.4	0.3962	1.3	2069.7	10.8	2110.0	12.8	2151.7	23.9	0.90	102
RMR04_Z1g	0.09	0.08	15748	0.12742	0.5	7.0441	1.6	0.4010	1.5	2062.7	9.6	2117.0	14.0	2173.4	27.4	0.94	103
RMR04_Z1h	0.06	0.08	23871	0.12765	1.0	7.3792	1.6	0.4193	1.3	2065.9	17.2	2158.4	14.6	2257.1	24.8	0.91	105
RMR04_Z1i	0.08	0.11	17757	0.12752	0.6	6.7102	1.1	0.3817	1.0	2064.0	10.0	2074.0	10.1	2084.0	17.7	0.86	100
RMR04_Z1j	0.09	0.10	15849	0.13091	0.6	6.6697	1.2	0.3695	1.0	2110.2	10.6	2068.6	10.2	2027.1	17.2	0.84	98
RMR04_Z1k	0.10	0.08	14423	0.12704	0.7	6.7333	1.5	0.3844	1.4	2057.4	12.3	2077.0	13.6	2096.8	24.5	0.89	101
RMR04_Z1l	0.03	0.12	45106	0.13181	0.7	6.8221	1.9	0.3754	1.8	2122.3	12.9	2088.6	16.8	2054.6	30.9	0.97	98
RMR04_Z1m	0.06	0.07	23860	0.13020	0.6	6.9805	1.6	0.3889	1.5	2100.6	10.5	2109.0	14.0	2117.5	26.4	0.92	100
RMR04_Z1n	0.02	0.20	86721	0.12973	0.4	6.5900	1.1	0.3684	1.0	2094.3	7.0	2058.0	9.6	2021.9	17.6	0.93	98
RMR04_Z1o	0.03	0.08	46154	0.12889	0.5	6.4686	1.3	0.3640	1.2	2082.9	8.4	2041.6	11.3	2001.1	20.4	0.92	98
RMR04_Z1p	0.23	0.27	6428	0.13039	1.0	6.6434	1.4	0.3695	1.0	2103.3	18.2	2065.1	12.6	2027.1	17.2	0.67	98
RMR04_Z5	0.74	0.24	2027	0.13178	1.4	6.8359	1.9	0.3762	1.3	2121.8	24.0	2090.4	17.0	2058.7	23.6	0.69	98
RMR04_Z6	1.18	0.26	1260	0.13207	0.9	7.0874	1.4	0.3892	1.1	2125.7	16.3	2122.5	12.7	2119.1	19.5	0.74	100
RMR04_Z7	0.58	0.21	2630	0.12974	1.5	6.5416	2.1	0.3657	1.5	2094.5	27.2	2051.5	18.7	2009.0	25.2	0.68	98
RMR04_Z8	1.10	0.17	1366	0.13064	1.4	6.8177	1.7	0.3785	1.0	2106.6	24.0	2088.0	15.2	2069.3	18.2	0.79	99
RMR04_Z9	1.24	0.19	1209	0.13162	1.0	6.8631	1.5	0.3782	1.1	2119.6	18.2	2093.9	13.7	2067.8	20.3	0.73	99
RMR04_Z10	1.43	0.20	1059	0.13214	1.1	6.6859	1.8	0.3670	1.5	2126.5	18.4	2070.8	15.9	2015.2	25.3	0.81	97
RMR04_Z11	0.95	0.17	1584	0.13264	1.1	6.9777	1.5	0.3815	0.9	2133.2	19.7	2108.6	13.0	2083.4	16.6	0.62	99
RMR04_Z12	0.18	0.25	8511	0.13197	1.4	6.6492	1.6	0.3654	0.9	2124.3	23.7	2065.9	14.5	2007.8	16.1	0.77	97
RMR04_Z13	1.23	0.20	1229	0.13166	0.7	6.7589	1.4	0.3723	1.2	2120.2	12.1	2080.4	12.2	2040.4	20.9	0.86	98
RMR04_Z15	0.84	0.32	1814	0.13047	0.8	6.5322	1.3	0.3631	1.0	2104.3	14.1	2050.2	11.4	1996.9	17.4	0.77	97
RMR04_Z17	1.50	0.18	1007	0.13084	1.3	6.6841	2.1	0.3705	1.6	2109.3	23.3	2070.5	18.3	2031.8	27.6	0.76	98
RMR04_Z20	1.04	0.19	1469	0.13216	1.8	6.4879	2.1	0.3560	1.0	2126.9	31.6	2044.3	18.2	1963.4	17.1	0.70	96
RMR04_Z22	0.58	0.17	2629	0.13129	1.4	6.6121	2.2	0.3653	1.8	2115.3	24.4	2061.0	19.8	2007.0	30.3	0.78	97
RMR04_Z23	0.88	0.20	1730	0.13027	1.0	6.3850	1.7	0.3555	1.3	2101.6	18.1	2030.2	14.7	1960.7	22.2	0.78	97
RMR04_Z24	0.18	0.20	8267	0.13148	1.1	6.7992	1.6	0.3750	1.1	2117.9	20.1	2085.6	14.1	2053.1	19.5	0.84	98
RMR04_Z29	0.42	0.23	3619	0.13041	0.9	6.4232	1.5	0.3572	1.2	2103.5	15.4	2035.4	13.3	1969.0	21.1	0.81	97

Table 4 – LA-ICPMS data for sample PP02

Sample	Isotopic ratios								Apparent ages								
	f(206) %	Th/U	$^{206}\text{Pb}/^{204}\text{Pb}$	$^{207}\text{Pb}/^{206}\text{Pb}$	1s (%)	$^{207}\text{Pb}/^{235}\text{U}$	1s (%)	$^{206}\text{Pb}/^{238}\text{U}$	1s (%)	$^{207}\text{Pb}/^{206}\text{Pb}$	2σ	$^{207}\text{Pb}/^{235}\text{U}$	2σ	$^{206}\text{Pb}/^{238}\text{U}$	2σ	Rho	Conc%
Paragranulite PP02																	
PP02_Z2	0.13	0.11	11977	0.13151	0.4	6.6242	0.9	0.3653	0.8	2118.2	6.8	2062.6	7.8	2007.3	13.8	0.88	97
PP02_Z11	0.10	0.02	15678	0.12978	0.4	6.4222	0.8	0.3589	0.6	2094.9	7.5	2035.3	6.8	1977.0	10.9	0.80	97
PP02_Z9	0.09	0.10	17621	0.13070	0.5	6.6889	0.9	0.3712	0.8	2107.3	8.9	2071.2	8.3	2035.0	13.8	0.82	98
PP02_Z26	0.10	0.03	15460	0.12917	0.5	6.3033	1.0	0.3539	0.9	2086.7	9.1	2018.9	8.9	1953.3	14.7	0.84	97
PP02_Z37	0.01	0.03	141271	0.12799	0.6	6.4620	1.1	0.3662	1.0	2070.5	9.9	2040.7	9.8	2011.4	16.7	0.85	99
PP02_Z21	0.51	0.05	2960	0.12886	0.6	6.3642	1.5	0.3582	1.4	2082.5	9.9	2027.3	13.5	1973.6	24.4	0.93	97
PP02_Z30	0.18	0.03	8516	0.12622	0.6	6.2299	1.4	0.3580	1.3	2046.0	10.2	2008.7	12.5	1972.6	22.1	0.91	98
PP02_Z25	0.07	0.02	22993	0.13114	0.6	6.9233	1.1	0.3829	0.9	2113.3	10.4	2101.7	9.5	2089.8	15.9	0.81	99
PP02_Z35	0.13	0.15	11480	0.13005	0.6	7.2112	1.4	0.4021	1.3	2098.7	10.5	2137.9	12.6	2178.9	23.6	0.90	102
PP02_Z29	0.07	0.03	20331	0.12994	0.6	6.5817	1.4	0.3674	1.3	2097.1	10.5	2056.9	12.3	2017.0	21.9	0.90	98
PP02_Z42	0.02	0.43	81029	0.13390	0.6	7.0021	1.1	0.3793	0.9	2149.8	11.0	2111.7	9.6	2072.8	15.5	0.79	98
PP02_Z33	0.16	0.23	9488	0.13475	0.6	7.2345	1.8	0.3894	1.7	2160.7	11.2	2140.8	16.1	2120.0	30.5	0.93	99
PP02_Z41	0.09	0.02	17462	0.13047	0.6	6.7239	1.2	0.3738	1.0	2104.3	11.4	2075.8	10.6	2047.2	17.7	0.83	99
PP02_Z14	0.30	0.22	5121	0.13149	0.7	6.2666	2.8	0.3457	2.7	2117.9	11.5	2013.8	24.4	1913.9	44.8	0.97	95
PP02_Z3	0.01	0.00	101933	0.13272	0.7	7.2118	1.4	0.3941	1.2	2134.2	11.9	2138.0	12.5	2141.9	22.3	0.87	100
PP02_Z7	0.01	0.00	188335	0.12271	0.7	5.5847	2.9	0.3301	2.8	1996.1	12.3	1913.7	24.9	1838.7	44.9	0.97	96
PP02_Z2	0.01	0.00	105962	0.12944	0.7	6.7354	2.5	0.3774	2.4	2090.3	12.3	2077.3	22.3	2064.1	42.8	0.96	99
PP02_Z45	0.05	0.06	30070	0.12853	0.7	6.4598	1.2	0.3645	1.0	2078.0	12.4	2040.4	10.4	2003.5	16.4	0.79	98
PP02_Z38	0.16	0.05	9438	0.13100	0.7	7.0331	1.3	0.3894	1.1	2111.4	13.0	2115.6	11.5	2120.0	19.0	0.80	100
PP02_Z19	0.10	0.43	15700	0.13365	0.8	7.0750	1.9	0.3839	1.8	2146.5	13.5	2120.9	17.2	2094.6	31.7	0.91	99
PP02_Z5	0.01	0.00	191716	0.13013	0.8	6.6949	3.1	0.3731	3.0	2099.8	13.6	2072.0	27.0	2044.1	51.8	0.97	99
PP02_Z43	0.07	0.02	21437	0.12937	0.8	6.1830	1.3	0.3466	1.0	2089.5	13.7	2002.1	11.1	1918.4	16.6	0.78	96
PP02_Z17	0.18	0.06	8282	0.13079	0.8	6.8627	1.9	0.3806	1.7	2108.6	14.5	2093.8	16.8	2078.9	30.4	0.90	99
PP02_Z6	0.09	0.04	16615	0.13061	0.8	6.9868	2.1	0.3880	1.9	2106.1	14.7	2109.7	18.6	2113.5	34.6	0.92	100
PP02_Z47	0.01	0.11	158454	0.13195	0.8	7.1636	1.3	0.3938	1.0	2124.0	14.8	2132.0	11.7	2140.2	18.3	0.75	100
PP02_Z48	0.08	0.05	18770	0.13034	0.9	6.7502	1.4	0.3756	1.1	2102.5	15.7	2079.2	12.4	2055.8	19.1	0.84	99
PP02_Z12	0.17	0.39	9026	0.13641	0.9	7.2673	1.9	0.3864	1.7	2182.1	16.3	2144.8	17.4	2106.1	30.6	0.95	98
PP02_Z46	0.11	0.02	13720	0.12940	1.0	6.1342	1.6	0.3438	1.3	2089.8	17.0	1995.1	14.2	1905.0	21.6	0.80	95
PP02_Z15	0.43	0.08	3464	0.12615	1.0	7.0170	1.6	0.4034	1.2	2045.0	17.3	2113.6	13.7	2184.8	22.1	0.76	103
PP02_Z39	0.05	0.03	30434	0.13101	1.0	7.2177	1.4	0.3996	1.0	2111.5	18.0	2138.7	12.5	2167.1	17.6	0.66	101
PP02_Z23	0.16	0.03	9669	0.13123	1.0	6.3626	1.7	0.3516	1.4	2114.5	18.0	2027.1	15.1	1942.4	23.1	0.79	96
PP02_Z44	0.02	0.05	63648	0.13087	1.1	6.7042	1.7	0.3715	1.4	2109.7	18.8	2073.2	15.4	2036.6	24.1	0.88	98
PP02_Z34	0.08	0.05	18874	0.13153	1.1	6.7945	1.6	0.3747	1.2	2118.4	18.9	2085.0	14.5	2051.3	21.6	0.74	98
PP02_Z13	0.12	0.02	12574	0.13173	1.2	7.1592	2.0	0.3942	1.6	2121.2	21.0	2131.4	17.8	2142.1	29.2	0.80	100
PP02_Z10	0.21	0.35	7003	0.13476	1.3	7.3273	1.9	0.3943	1.4	2161.0	22.6	2152.1	16.7	2142.9	24.7	0.71	100
PP02_Z7	0.13	0.07	11672	0.13238	1.3	6.6355	1.7	0.3635	1.1	2129.7	23.2	2064.1	15.3	1999.0	19.1	0.63	97

Table 4 – LA-ICPMS data for sample PP02 (continuation)

Sample	Isotopic ratios								Apparent ages								
	f(206) %	Th/U	$^{206}\text{Pb}/^{204}\text{Pb}$	$^{207}\text{Pb}/^{206}\text{Pb}$	1s (%)	$^{207}\text{Pb}/^{235}\text{U}$	1s (%)	$^{206}\text{Pb}/^{238}\text{U}$	1s (%)	$^{207}\text{Pb}/^{206}\text{Pb}$	2σ	$^{207}\text{Pb}/^{235}\text{U}$	2σ	$^{206}\text{Pb}/^{238}\text{U}$	2σ	Rho	Conc%
Paragranulite PP02																	
PP02_Z28	0.10	0.06	15287	0.12925	1.3	6.6604	1.8	0.3737	1.3	2087.9	23.3	2067.4	16.2	2046.9	22.3	0.85	99
PP02_Z40	0.02	0.13	97895	0.13113	1.6	7.0467	2.0	0.3897	1.2	2113.2	27.7	2117.3	17.8	2121.6	22.3	0.80	100
PP02_Z5	0.27	0.03	5661	0.13422	1.8	6.8915	2.5	0.3724	1.8	2154.0	30.9	2097.6	22.2	2040.6	31.0	0.70	97

Table 5 – LA-ICPMS data for sample PP030

Sample	Isotopic ratios								Apparent ages								
	f(206) %	Th/U	$^{206}\text{Pb}/^{204}\text{Pb}$	$^{207}\text{Pb}/^{206}\text{Pb}$	1s (%)	$^{207}\text{Pb}/^{235}\text{U}$	1s (%)	$^{206}\text{Pb}/^{238}\text{U}$	1s (%)	$^{207}\text{Pb}/^{206}\text{Pb}$	2σ	$^{207}\text{Pb}/^{235}\text{U}$	2σ	$^{206}\text{Pb}/^{238}\text{U}$	2σ	Rho	Conc%
Metagranodiorite PP030																	
PP030_Z2	0.22	0.04	6814	0.13221	0.7	7.3918	1.1	0.4055	0.8	2127.5	13.0	2160.0	9.9	2194.3	15.3	0.71	103
PP030_Z4	0.00	0.80	308871	0.12962	1.2	7.1859	1.4	0.4021	0.8	2092.8	20.6	2134.8	12.7	2178.6	14.8	0.67	104
PP030_Z3	0.22	0.04	6814	0.13181	0.9	7.3294	1.3	0.4033	0.9	2122.2	15.7	2152.4	11.1	2184.2	16.1	0.67	103
PP030_Z5	0.05	0.45	32649	0.13687	0.8	7.6946	1.5	0.4077	1.2	2187.9	14.6	2196.0	13.3	2204.6	22.7	0.81	101
PP030_Z9	0.02	0.68	71023	0.13030	0.8	6.8449	1.3	0.3810	1.0	2102.0	14.3	2091.5	11.5	2081.0	18.1	0.76	99
PP030_Z10	0.01	0.82	109282	0.13290	0.9	6.8217	1.2	0.3723	0.7	2136.6	15.7	2088.5	10.3	2040.2	12.8	0.60	95
PP030_Z11	0.01	0.62	160764	0.13557	1.3	7.9633	1.6	0.4260	1.0	2171.4	22.0	2226.9	14.4	2287.7	18.6	0.71	105
PP030_Z12	0.01	0.94	155995	0.13032	1.1	6.9036	1.4	0.3842	0.9	2102.3	19.0	2099.1	12.6	2095.9	16.4	0.62	100
PP030_Z13	0.01	0.81	164127	0.13064	0.9	7.0282	1.3	0.3902	1.0	2106.5	15.3	2115.0	11.5	2123.7	17.4	0.72	101
PP030_Z14	0.02	0.55	88057	0.12997	0.8	7.0996	1.2	0.3962	0.9	2097.6	14.9	2124.0	10.7	2151.4	15.7	0.69	103
PP030_Z15	0.01	0.80	135829	0.12981	1.3	6.9206	1.5	0.3867	0.9	2095.4	22.0	2101.3	13.6	2107.4	15.9	0.67	101
PP030_Z17	0.01	0.40	196181	0.12877	0.9	7.0066	1.2	0.3946	0.9	2081.3	15.6	2112.3	11.0	2144.2	16.0	0.68	103
PP030_Z21	0.01	0.33	119944	0.13485	1.0	7.5461	1.3	0.4058	0.8	2162.1	16.8	2178.5	11.3	2195.9	15.1	0.61	102
PP030_Z22	0.00	0.04	452178	0.12861	0.7	7.0626	1.1	0.3983	0.9	2079.0	12.9	2119.3	10.0	2161.2	15.8	0.74	104
PP030_Z23	0.01	0.47	247705	0.12803	1.0	6.7331	1.2	0.3814	0.7	2071.0	17.6	2077.0	10.7	2083.0	12.1	0.61	101
PP030_Z25	0.00	0.08	431094	0.12854	0.8	6.9288	1.2	0.3909	0.9	2078.1	14.7	2102.3	11.1	2127.2	16.7	0.72	102
PP030_Z28	0.02	0.79	93748	0.13292	0.9	6.8168	1.3	0.3720	0.9	2136.9	15.8	2087.9	11.3	2038.6	15.6	0.68	95

CAPÍTULO 3 – AR CABOUÇO TECTÔNICO DO MACIÇO DE GOIÁS NO BRASIL CENTRAL: CONSEQUÊNCIAS PARA O CICLO DE AMALGAMAMENTO CONTINENTAL DE 2.2-2.0 Ga

Central Brazil Goiás Massif tectonic framework: implications for a 2.2-2.0 Ga continent wide amalgamation cycle

Abstract

The Goiás Massif is composed of Archean-Paleoproterozoic terranes that represent the Brasília Belt basement. The massif is divided from southwest to northeast into the Crixás-Goiás, Campinorte, Cavalcante-Arraias and Almas-Conceição do Tocantins domains based on petrographical and geochronological criteria. Even though widely studied, the Goiás Massif tectonic setting and evolution is still poorly understood. The commonly cited hypothesis that the Campinorte and Crixás-Goiás domains represented an allochthonous block during the Neoproterozoic Brasiliano Orogeny is questioned in this paper based on our geochronology and reinterpretation of published data. First, seismic and gravimetric studies that suggest a sharp crustal thickness contrast between the Campinorte and Cavalcante-Arraias domains, and marked in surface by the Rio Maranhão Thrust, can be explained by a Neoproterozoic lower crust delamination affecting both Brasiliano orogens and the terrane they were accreted against, the Campinorte Domain. Second, Paleoproterozoic Campinorte Arc rocks crop out along the Rio Maranhão Thrust and no Neoproterozoic collisional rocks have been reported along this important geological limit. Third, Tocantins Supravince Mesoproterozoic granites intruded both sides of the Rio Maranhão Thrust and, therefore, indicate the two domains were amalgamated prior to the Mesoproterozoic. Coeval Goiás Massif and São Francisco Craton rifting events around 1.76 Ga and 1.58 Ga suggest they were actually part of the same paleoplate. The occurrence of 2.2 to 2.0 Ga orogens with metamorphic peak from 2.12 to 2.05 Ga in both the Goiás Massif and São Francisco Craton might suggest that not only they were part of the same plate but they also were assembled in the same tectonic cycle. The plate eventually became part of the Atlantica landmass as a stable block during the Columbia Supercontinent amalgamation from 1.9 to 1.8 Ga.

Keywords: Paleoproterozoic; São Francisco Craton; Tocantins Province, Campinorte Arc; Supercontinent

1. Introduction

Supercontinents reconstructions play an important role in understanding global plate tectonics dynamics as well as variations in temperature, oxidation state, weathering and paleoclimate throughout Earth's history. A drastic change in a single of these interdependent parameters could induce a chain reaction that would modify all other parameters (Reddy and Evans, 2009). A better understanding of the continuous history of assembly and breakup of supercontinents occurring in at least four major events at an estimated interval of ~750 Ma (Meert, 2012) has great implications on understanding the planet's tectonic dynamics.

Large exposures of Paleoproterozoic rocks, for example, can provide information to study terranes that precluded Columbia, a large paleocontinent formed from 1.9-1.85 Ga. In this sense, vast tracts of rocks older than 2.0 Ga cropping out in central Brazil and grouped as the Goiás Massif could provide additional information on the global Paleoproterozoic tectonic framework. The region shares many features with São Francisco-Congo paleoplate belts but has been largely ignored in supercontinent reconstructions due to restricted geochronology and tectonic studies. A detailed geological study of the Goiás Massif could provide additional information on its positioning relative to the São Francisco Craton and its role in supercontinent assembly/break up events.

In this paper we provide new LA-ICPMS zircon ages and Hf isotopes of Goiás Massif metagranites. We also review the vast available literature produced in the region on events prior to the Brasiliano orogeny (Neoproterozoic) to determine how our data fit in the regional context. Additionally, we propose a standardized nomenclature for the terranes involved to avoid confusion and misinterpretation in future research. Our main goal is to suggest a regional tectonic model able to explain the present Goiás Massif tectonic framework.

2. Geological overview

The Brasília Belt is an assemblage of NW-NE trending Meso-Neoproterozoic metasedimentary, magmatic and metamorphic rocks that converged to the east against the São Francisco-Congo platform (Pimentel et al., 2000). From west to east the Brasília belt is divided into the Goiás Magmatic Arc, the high grade metamorphic core, thrust-fold alloctonous metasedimentary rocks and the foreland system mostly over the São Francisco craton (Valeriano et al., 2008; Pimentel et al., 2011). Deformation and metamorphism imprinted in Brasília Belt rocks is a result of Neoproterozoic accretion of juvenile arcs and the São Francisco-Congo and Amazonian plates.

Whereas Neoproterozoic rocks have been the focus of Brasília Belt studies in the last twenty years, few regional studies have focused on its basement. These variably deformed and generally poorly exposed rocks have been named Basal Complex (Almeida, 1967), Goiano Basal Complex (Marini et al., 1984), Granite-gneiss Complex (Cordani & Hasui 1975), Median Goiás Massif (Almeida, 1976) and Goiás Massif (Almeida, 1984), with the latter most commonly used therein. However, the extention and meaning of ‘Goiás Massif’ has always been unclear as it is composed of several different terranes juxtaposed prior to the Brasiliano Cycle.

Nomenclature issues also occur within the domains/blocks/terranea that compose the Brasília Belt basement: a) Archean TTG complexes and Paleoproterozoic greenstone belts between the cities of Crixás, Guarinos and Goiás, b) Pau de Mel Suite Paleoproterozoic metatonalites and related metavolcano-sedimentary rocks of the Campinorte Sequence, c) Paleoproterozoic Aurumina Suite and the Mesoproterozoic Araí metavolcano-sedimentary unit, d) Paleoproterozoic Almas-Dianópolis TTG and greenstone belts.

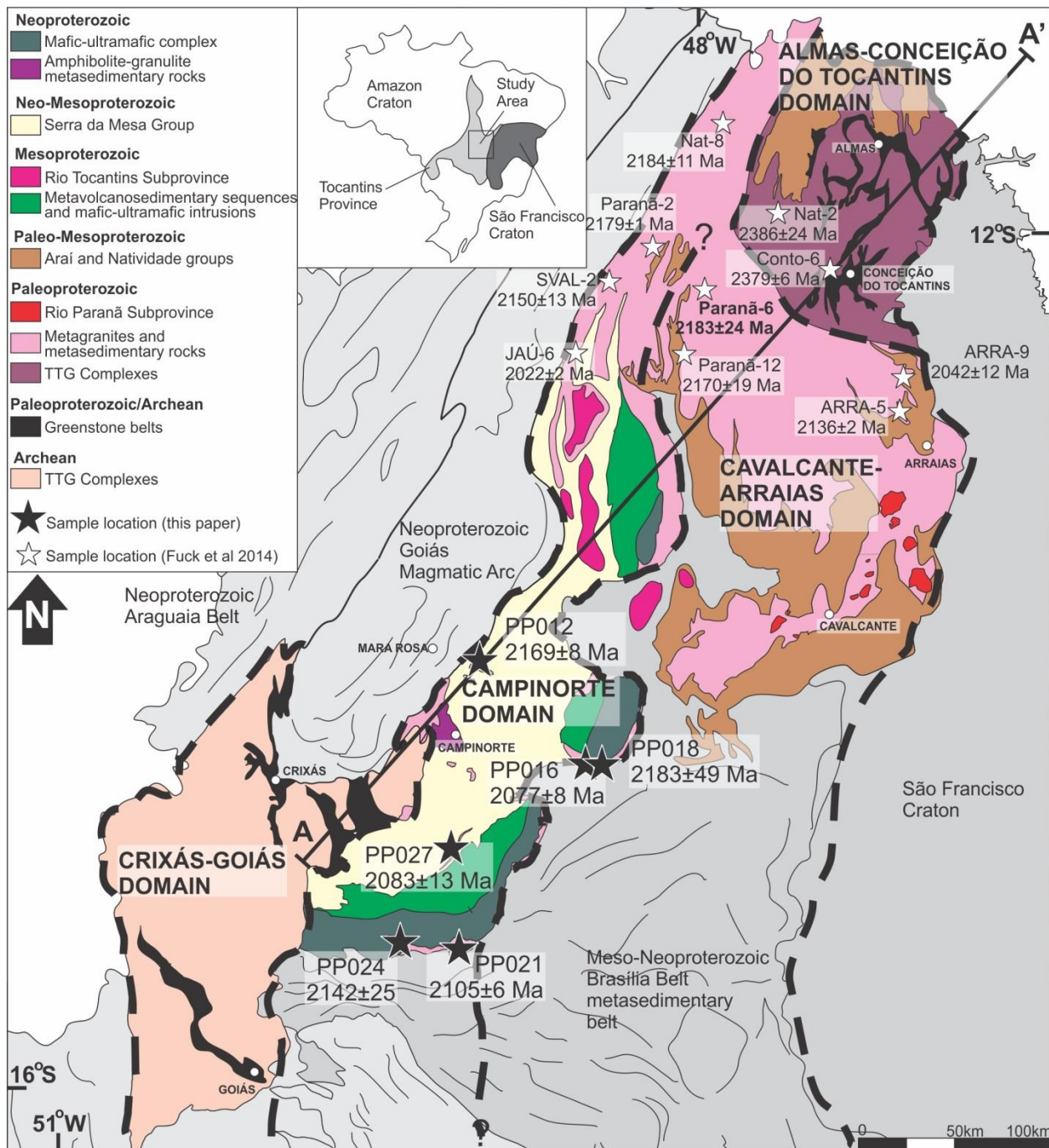


Figure 1 – Goiás Massif Archean to Paleoproterozoic domains separated by dashed lines and overlain by our samples locations and ages and those of Fuck et al. (2014) for comparison. The A-A' section is shown on Figure 8.

2.1. Northern Brasília Belt Basement - Goiás Massif

Goiás Massif was initially referred to all crystalline rocks of unknown age and origin in Central Brazil (Marini et al., 1984). At the time, it comprised most of the Archean-Paleoproterozoic basement and what was later defined as the Neoproterozoic Goiás Magmatic Arc (Pimentel and Fuck, 1994). After the definition of this Neoproterozoic orogenic event (Pimentel and Fuck, 1992; Viana et al., 1995), the Goiás Massif extention and meaning became vague and was used either with the old meaning, encompassing the Goiás Magmatic Arc, or to mean the combined terrane formed by Archean rocks of the Crixás-Goiás region and less-known Paleo-Mesoproterozoic crystalline rocks to the west. Later studies of Central Brazil large mafic-ultramafic complexes and related metavolcano-sedimentary sequences (Pimentel et al., 2006; Moraes et al., 2006) revealed Meso-Neoproterozoic ages that also set these rocks apart from the Goiás Massif basement. The lack of a regional compilation led authors to make inferences on the Goiás Massif regional tectonics based on local studies of certain deposits, suites or set of structures. These vast tracts of Archean to Mesoproterozoic rocks, however, are fundamental to determine the Brasília Belt basement architecture and its links with the São Francisco Craton. In this study Goiás Massif refers to the northern Brasília Belt terrane formed by exposed Archean to Mesoproterozoic crystalline belts east of the Neoproterozoic Goiás Magmatic Arc and the division into domains is adapted from Fuck et al. (2014)

From southwest to northeast, the Goiás Massif is divided into the Crixás-Goiás, Campinorte, Cavalcante-Arraias and Almas-Conceição do Tocantins domains (Figure 1). The massif is separated from the Goiás Magmatic Arc by the Rio dos Bois Thrust to the west, whereas it is buried under the Paleozoic Parnaíba Basin and Brasília Belt supracrustal units to the north and south, respectively. The massif is covered by Bambuí and Urucuia sedimentary rocks towards the São Francisco Craton, to the east.

Goiás Massif domains have been described as part of a microcontinent accreted to the São Francisco platform during the Brasiliano Cycle (Pimentel et al., 2000; Valeriano et al., 2008) or otherwise hinted as part of the São Francisco platform prior to the collision (Pimentel et al., 1996; D'el-Rey Silva et al., 2008). Geophysical data

interpretation have favored the microplate hypothesis based on strong gravimetric and seismic contrasts marked by the Rio Maranhão Thrust (Assumpção et al., 2004; Berrocal et al., 2004; Perosi, 2006; Ventura et al., 2011) and suggesting it as a collisional suture. Geological evidence such as Neoproterozoic ophiolites or collisional magmatism along the suture have never been described.

The proposal of a coherent Goiás Massif tectonic model is also hindered by its domains nomenclature issues. Most studies have focused on local mineralogical, geochronological, petrological and structural topics and relied on non-uniform, sometimes interpretative nomenclature. For example, the terrane defined by Central Goiás Archean TTG gneisses and Archean-Paleoproterozoic greenstone belts has received eight different names throughout the years. Geological papers on the domain formed by the Aurumina Suite and Ticunzal Formation rocks provided only patchy regional geology for lack of a more comprehensive tectonic framework on pre-Brasiliano terranes. Whereas the available framework (Fuck et al., 1994; Pimentel et al., 2000) is widely valid for the Brasília Belt, we believe a revised one is needed for the Goiás Massif. Our following proposed domains (Figure 1) have loose limits and will benefit from future regional/local refinement.

2.1.1. Crixás-Goiás Domain

The Goiás Archean-Paleoproterozoic terrane composed of TTG complexes wrapped by greenstone belts has been widely studied to provide insight on its gold deposits, particularly the Crixás gold deposit (Jost et al., 2010). Its positioning as the sole Central Brazil Archean terrane, afar from other coeval rocks, has been argued as additional evidence for a microcontinent origin (Jost et al., 2013). Although well studied, the terrane has been named ‘Crixás Granite-Greenstone Terrane’ (Queiroz et al., 2000), ‘Archean terranes of Crixás-Goiás’ (Pimentel et al., 2000), ‘Goiás Archean Nuclei’ (Jost et al., 2001), ‘Goiás-Crixás Archean Block’ (Pimentel et al., 2003), Crixás-Goiás Block (Delgado et al., 2003), ‘Archean Terrain of central Brazil’ (Jost et al., 2010), ‘Goiás Archean Block’ (Jost et al., 2012) and the most recent ‘Archean-Paleoproterozoic terrane of central Brazil’ (Jost et al., 2013).

Following the descriptive nomenclature approach, we propose that the central Brazil terrane composed of Archean TTG complexes wrapped by greenstone belt units should be hence referred as ‘Crixás-Goiás Domain’. Proper adjectives can be added whenever necessary as Archean-Paleoproterozoic Crixás-Goiás Domain or Central Brazil Crixás-Goiás Domain. The Crixás-Goiás Domain is separated from the Goiás Magmatic Arc through the Rio dos Bois Fault to the north and limited to the west by the Transbrasiliano Lineament. The domain is covered by Serra da Mesa Group rocks to the east and Serra Dourada Group to the South.

2.1.2. Campinorte Domain

The Campinorte Domain (Giustina et al., 2009; Cordeiro, 2014) is the most recent addition to the regional geological literature and probably the missing piece needed for a Paleoproterozoic tectonic reconstruction. Almost entirely covered by Meso-Neoproterozoic Serra da Mesa metasedimentary rocks this domain is defined by metavolcano-sedimentary Campinorte Sequence, Pau de Mel Suite rocks and a granulite unit within a Paleoproterozoic Arc setting (Cordeiro, 2014). The domain is limited to the west by the Rio dos Bois Fault and to the east by the Rio Maranhão Thrust whereas open to north and south. The Campinorte Domain is likely to represent the full extention of the Campinorte Arc and related basins.

2.1.3. Cavalcante-Arraias Domain

The Cavalcante-Arraias Domain is limited to the west by the Rio Maranhão Thrust and covered by Brasília Belt Meso-Neoproterozoic metasedimentary rocks to the west and south. The northern contact is loosely interpreted as in Figure 1. The Cavalcante-Arraias Domain has also been named Almas-Cavalcante Complex (Delgado et al., 2003) and Araí Block (Alvarenga et al., 2007). The most recent “Cavalcante-Arraias Domain” suggested by Fuck et al. (2014) is referred to in this paper.

This domain is dominantly composed of Paleoproterozoic Aurumina Suite peraluminous metagranitoids cutting Ticunzal Formation graphiite-bearing gneisses, migmatites and schists. These Paleoproterozoic rocks are covered by the Araí Group rift sedimentary rocks that include volcanics dated by Pimentel et al. (1991) at 1771 Ma.

Coeval Paraná Subprovince Soledade and Sucuri granites were dated with ages of 1767 ± 10 Ma and 1769 ± 2 Ma, respectively (Pimentel et al., 1991). Mesoproterozoic Paranoá Group passive margin sediments and the Neoproterozoic Bambuí Group foreland sequence deposited on top of the Paleoproterozoic domain. Fuck et al. (2014) provide ages from 2183 ± 24 Ma to 2136 ± 3 Ma to Aurumina Suite metagranites and a younger tonalite intrusion crystallization age of 2042 ± 12 Ma.

Aurumina Suite muscovite granites are strongly peraluminous and register a syntectonic geochemistry signature incompatible with that of the Campinorte Domain Pau de Mel Suite. The formation of the Cavalcante-Arraias Domain most likely involved the Ticunzal Formation as a possible source for the Arumina Suite magmatism in a syn-collisional setting (Botelho et al., 2006). A more refined regional tectonic Goiás Massif tectonic framework depends on additional studies on Cavalcante-Arraias Domain rocks.

2.1.4. Almas-Conceição do Tocantins Domain

The Almas-Conceição do Tocantins Domain has been also named Tocantins granite-greenstone terrane (Kuyumjian et al., 2012) and Almas-Dianópolis granite-greenstone terrane (Saboia, 2009). The Goiás Massif northeasternmost domain is covered by the Parnaíba Basin to the north and by the Bambuí and Urucuia groups to the east and is composed of Paleoproterozoic TTG complexes wrapped by greenstone belts of unknown age (Cruz and Kuyumjian, 1999).

Three granite suites occur within this domain: a) 2.35 Ga Ribeirão das Areias Complex TTG suite a) 2.2 Ga Suite 1 amphibole-bearing granites and b) 2.2 Ga Suite 2 biotite-bearing TTG (Cruz et al., 2003). Greenstone belt sequences can be summarized from bottom to top as basaltic flows with subordinate ultramafic rocks and phyllites with interbedded iron formations, quartzite, conglomerate and felsic volcanics (Cruz & Kuyumjian 1998). Fuck et al. (2014) provide ages of 2343 ± 11 Ma for a biotite tonalite gneiss and 2379 ± 6 Ma for a deformed granite gneiss that are within the Ribeirão das Areias Complex age range. The authors also report ages of 2180 ± 12 Ma for a tonalite and 2144 ± 21 Ma for a coarse-grained foliated biotite granite that could belong to either the Suite 1 or the Suite 2 described by Cruz and Kuyumjian (1999).

2.2. Campinorte Arc

As one of the least understood Goiás Massif terranes and an important piece of the regional tectonic framework, the Campinorte Arc eastern contact is detailed in this paper. The arc is composed of three main units, a) Campinorte Sequence meta volcanosedimentary rocks, b) Pau de Mel Suite metagranitoids, and c) mafic granulites and paragranulites.

The Campinorte Sequence in its type area (Oliveira et al., 2006; Giustina et al., 2009) is dominantly composed of quartz-muscovite schist with variable amounts of carbonaceous material, quartzite, chert and gondite lenses. Metapyroclastic rocks and felsic metavolcanics are subordinated. Giustina et al. (2009) gives a maximum depositional age of ~2.2 Ga for the Campinorte Sequence and a direct age of 2179 ± 4 Ga for a felsic metatuff.

Pau de Mel Suite metagranitoids are calc-alkaline and show volcanic arc signatures (Cordeiro, 2014). Although contact relations are hindered by thick weathering profiles the suite is interpreted as intrusive within the Campinorte Sequence. Giustina et al. (2009) provides granite and volcanic rocks crystallization ages around 2.15 Ga, thus marking the minimum age of deposition for the Campinorte Sequence. Pau de Mel Suite rocks were formed from at least three main parental magmas as interpreted from whole rock geochemistry (Cordeiro, 2014).

The granulite unit shows two roughly coincident granulite ages, one from a paragranulite and another from mafic rocks within the paragranulite, that mark the metamorphic peak from 2.11 to 2.09 Ga (Cordeiro, 2014). The granulite unit is interpreted to have formed in a short lived back arc basin that after island arc tectonic switching and consequent lithospheric thinning underwent granulite metamorphism in the Paleoproterozoic. These two studied rocks preserved Paleoproterozoic metamorphism peak ages even though retrometamorphism under the green-schist facies, likely during the Brasiliano Orogeny, is observed.

The Campinorte Arc lateral extention is not well established due to extensive Meso-Neoproterozoic cover. To the west, the Campinorte and Goiás arcs are separated

by the Rio dos Bois Thrust, whereas to the east it is limited by the Rio Maranhão Thrust. North of the Canabrava Complex this thrust contact is well marked and has been mapped by Marques (2010). To the south, at the Barro Alto and Niquelândia complexes footwall, the Rio Maranhão Thrust has been detailed by D'el-Rey Silva et al. (2008). In this region, the Campinorte Arc occurs as coarse granodioritic to tonalitic mylonite to ultramylonite that is zoned towards distal sillimanite-garnet-biotite gneiss of similar composition and interpreted as metamorphosed under upper amphibolite facies (Fuck et al., 1981). Campinorte Arc rocks have been thrusted over Aurumina Suite metagranites and Paranoá Group metasedimentary rocks in a Neoproterozoic intraplate compressional event marked at surface by the Rio Maranhão Thrust (D'el-Rey Silva et al., 2008).

However, several authors have argued in favor of the Rio Maranhão Thrust as a collisional suture widely based on a strong gravimetric contrast coincident with the thrust (Marangoni et al., 1995; Pimentel et al., 2004; Ferreira Filho et al., 2010; Jost et al., 2013). In order to refine the discussion we provide direct U-Pb ages and Hf isotopes of the Campinorte Arc eastern contact and a detailed regional geology discussion to support a regional tectonic model proposal.

3. Analytical Procedures

Six samples were chosen for LA-ICPMS investigation in the Geochronology Laboratory of the University of Brasília: a) PP012 metagranodiorite (of which the U-Pb age is reported by Cordeiro, 2014); b) PP016 garnet-muscovite gneiss; c) PP018 muscovite-gneiss; d) PP021 quartz-diorite; e) PP024 augen gneiss; f) PP027 granodiorite.

U–Pb isotopic analyses followed the analytical procedure described by Buhn et al. (2009). Extraction of zircon concentrates from rock samples of more than 10 kg as performed by crushing, milling and magnetic separation at the Geochronology Laboratory of the University of Brasília. Handpicked mineral fractions of similar color, shape and size were obtained by using a binocular microscope and then mounted in epoxy blocks and polished. Backscattering electron (BSE) images were obtained using a scanning electron microscope in the Geochronology Laboratory of the University of Brasília in order to investigate the internal structures of the zircon crystals prior to analysis. Mounts were cleaned with dilute (ca. 2%) HNO₃, mounted in an especially adapted laser cell and loaded into a New Wave UP213 Nd:YAG laser ($\lambda = 213$ nm), linked to a Thermo Finnigan Neptune Multi-collector ICPMS. Helium was the carrier gas and before entering the ICP was mixed with Ar. The laser was set at 10 Hz, energy of 34%, 70 mm total diameter with a spot size of 30 μm . The primary standard analyzed throughout the U–Pb analyses was GJ-1 (Jackson et al., 2004). Masses 204, 206 and 207 were measured with ion counters, and ²³⁸U was analyzed on a Faraday cup. The signal of ²⁰²Hg was monitored on an ion counter for the correction of the isobaric interference between ²⁰⁴Hg and ²⁰⁴Pb and taken in 40 cycles of 1 s each. At the end of each session, the Temora 2 standard (Black et al., 2004) was run yielding accuracy around 2% and precision around 1%.

A natural ²⁰²Hg/²⁰⁴Hg ratio of 4.346 was used to calculate and correct the ²⁰⁴Pb signal intensity and common Pb correction using the common lead composition by Stacey and Kramers (1975) was applied for zircon grains with 206Pb/204Pb lower than 1000. Plotting of U–Pb data was performed by ISOPLOT v.3 (Ludwig, 2003) and errors for isotopic ratios are presented as 2 σ . The statistical treatment used in Concordia

Ages calculations are more precise than any individual U/Pb or Pb/Pb ages (Ludwig, 1993) and, therefore, always correspond to less than the 2% accuracy obtained from the standards inter calibration. Consequently, the Isoplot calculated errors were modified to represent a more realistic age and to take into account the method analytical limitations and uncertainty.

Lu–Hf isotopes analyses were performed on grains from eight samples previously analyzed for U-Pb following the method described in Matteini et al. (2010). Replicate analyses of 200 pb Hf JMC 475 standard solution doped with Yb ($\text{Yb/Hf}=0.02$) were performed prior to Hf isotopes measurements on zircon ($^{176}\text{Hf}/^{177}\text{Hf} = 0.282162 \pm 13$ 2 s, $n=4$). Analyses of GJ-1 standard zircon were replicated during analyses obtaining a $^{176}\text{Hf}/^{177}\text{Hf}$ ratio of 0.282006 ± 16 2σ ($n=25$), in agreement with the reference value for GJ standard zircon (Morel et al., 2008). Ablation time using a 40 μm diameter spot size lasted 40 s.

The Hf isotope ratios were normalized to $^{179}\text{Hf}/^{177}\text{Hf}$ of 0.7325 (Patchett, 1983) and the ^{176}Yb and ^{176}Lu contribution were calculated using the Lu and Hf isotopic abundance proposed by Chu et al. (2002). We used Söderlund et al. (2004) ^{176}Lu decay constant $\lambda = 1.867 \times 10^{-11}$ to calculate $\epsilon\text{Hf}(t)$ and Bouvier et al. (2008) chondritic values of $^{176}\text{Lu}/^{177}\text{Hf} = 0.0336$ and $^{176}\text{Hf}/^{177}\text{Hf} = 0.282785$. The Hf TDM age is calculated from the zircon initial Hf isotopic composition with an average crustal Lu/Hf ratio (Gerdes and Zeh, 2006, 2009; Nebel et al., 2007) based on the previously calculated $^{176}\text{Hf}/^{177}\text{Hf}$ value at the time of zircon crystallization, calculated having the U-Pb age as base. The depleted mantle values of $^{176}\text{Lu}/^{177}\text{Hf} = 0.0388$ and $^{176}\text{Hf}/^{177}\text{Hf} = 0.28325$ from Andersen et al. (2009) and mafic and felsic crust $^{176}\text{Lu}/^{177}\text{Hf}$ values of 0.022 and 0.01 from Pietranik et al. (2008) were used to calculate the two stages depleted mantle TDM Hf. U-Pb ages were used to calculate ϵHf values for each single grain.

3.1. Samples and Results

The results of U-Pb and Lu-Hf data obtained on zircon grains previously studied using BSE images are listed on tables 1 and 2 and plotted on Concordia diagrams of figures 2 and 3. U-Pb ages vary within 2.15 Ga and 2.07 Ga in tandem with Campinorte Arc ages (Giustina et al. 2009; Cordeiro 2014). Lead loss is common to all studied samples and lead to Neoproterozoic lower intercept ages around 750 Ga.

Sample PP012, represents a Pau de Mel Suite metagranodiorite with interpreted crystallization age of 2169 ± 8 Ga and a well constrained lower intercept age of 751 ± 28 Ga (Cordeiro, 2014) compatible with the Barro Alto granulitization age (Giustina et al., 2011). Two zircon populations can be observed, one with prismatic, rounded and fractured zircon grains with inclusions and another with well-formed zircon grains without any internal structures and inclusions. However, there is no correlation among zircon population and the data obtained. Zircon from this metagranodiorite have moderate $\epsilon\text{Hf}_{(t)}$ between -3.3 and +5.18 around the CHUR line suggesting that they crystallized from a magma with mixed crustal and mantle sources. Their TDM values cover the range from 2.66 to 2.34 Ga

Sample PP016 represents a garnet-muscovite gneiss with a homogeneous zircon population of euhedral dark orange to brown crystals. Back scattering imaging shows no internal zonation. An alignment of thirty zircon grains gives the interpreted crystallization age of 2077 ± 8 Ga. This gneiss shows $\epsilon\text{Hf}_{(t)}$ around the CHUR, from -3.33 to 1.64, and TDM values within the restricted range from 2.55 to 2.39 Ga.

Sample PP018 is a muscovite gneiss with feldspar porphyroblasts and two distinct zircon populations, though no correlation among zircon population and the data obtained was determined. One population is pink to translucent, euhedral and prismatic whereas the other is composed of orange, yellow and brown euhedral prismatic to rounded zircon grains. Back scattering images show strong zonation, inherited cores and fractured grains with inclusions. A group of seventeen concordant zircon grains define a Concordia age of 2183 ± 49 Ma interpreted as the crystallization age of this gneiss. A poorly constrained lower intercept age ca. 612 is also provided. This sample has four zircon grains $\epsilon\text{Hf}_{(t)}$ between -4.7 and -6 suggesting crustal

influence whereas three grains are scattered between -1.86 and +2.15 and formed under a chondrite-like isotopic setting. TDM ages vary from 2.72 to 2.42 Ga.

Sample PP021 is a quartz-diorite with well-preserved igneous cumulus texture and a very homogeneous zircon population of light brown to translucent euhedral prismatic crystals with inclusions but limited compositional zonation as suggested by BSE images. Interpreted crystallization timing is given by the Concordia age of 2105 ± 6 in an alignment of forty two zircon grains. A poorly constrained lower intercept age of c.a. 740 Ma is also provided. Zircon $\epsilon\text{Hf}_{(t)}$ from this sample vary from +1.05 to +3.33 suggesting a slightly dominance of mantle-derived sources for this quartz-diorite. TDM ages vary from 2.40 to 2.32 Ga.

Sample PP024 is a granodioritic augen gneiss cropping out close to the town of Santa Isabel with a homogeneous yellow to orange, euhedral and prismatic zircon population. Fracturing and compositional overgrowth are highlighted in BSE images. A Concordia age of 2142 ± 25 is suggested by the alignment of thirty seven zircon analyses and interpreted as referring to zircon crystallization and a lower intercept age of 684 ± 74 due to a Pb loss event. This gneiss has $\epsilon\text{Hf}_{(t)}$ slightly higher than the CHUR line from 0.49 to 3.96 and TDM values within the restricted range from 2.52 to 2.29 Ga.

Sample PP027 is a granodiorite cropping out as a hill 10 km long next to the Juscelândia Sequence. This sample has two zircon populations, one with pink prismatic to rounded grains and another with orange to translucent rounded grains. Whereas the first population is compositionally homogenous in BSE images, orange to translucent rounded grains show strong zonation and overgrowth over homogeneous rounded cores. However, there is no correlation among zircon population and the data obtained. Thirty four zircon grains provide the interpreted crystallization age of 2083 ± 12 and a well constraint lower intercept age of 785 ± 24 due to a Neoproterozoic Pb loss event. This rock shows $\epsilon\text{Hf}_{(t)}$ around the CHUR, from -2.96 to 3.25 and TDM values from 2.31 to 2.53 Ga.

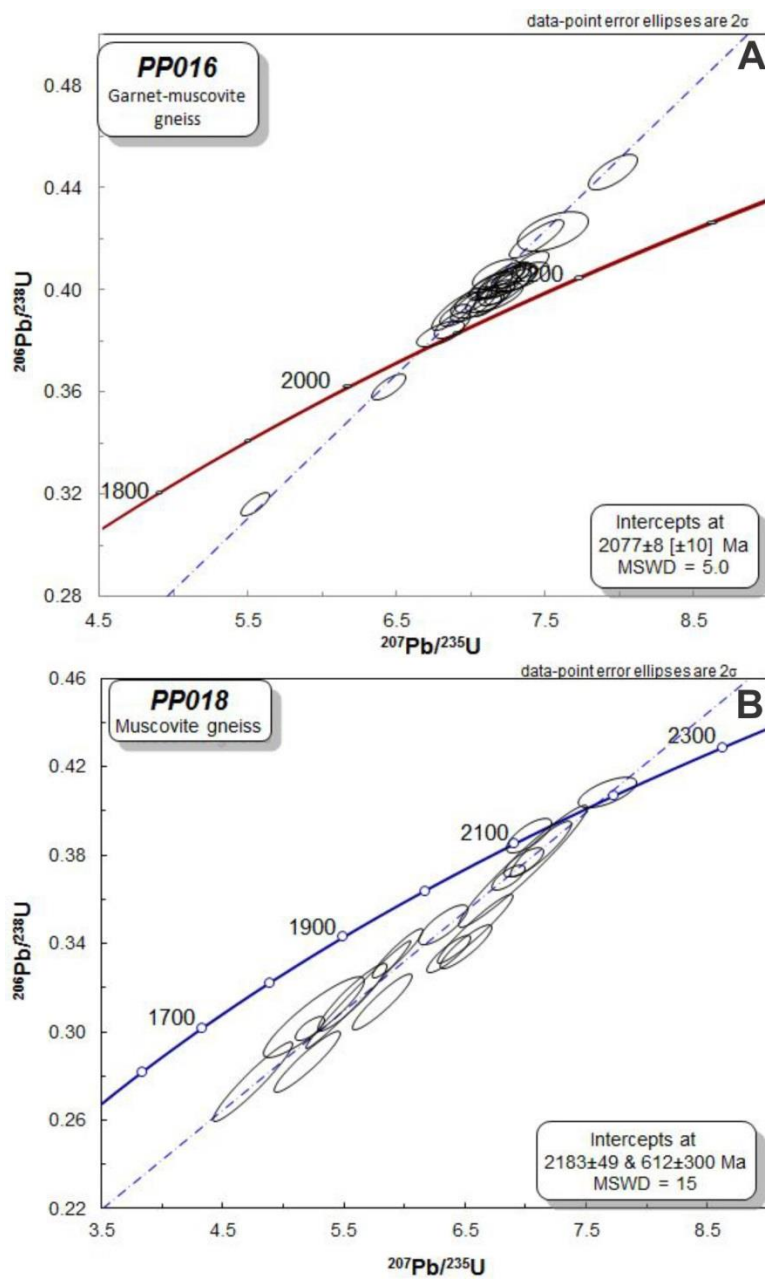


Figure 2 – U-Pb zircon Concordia ages for Niquelândia Complex footwall gneisses (Figure 1 for location); A) PP016 garnet-muscovite gneiss and; B) PP018 muscovite gneiss.

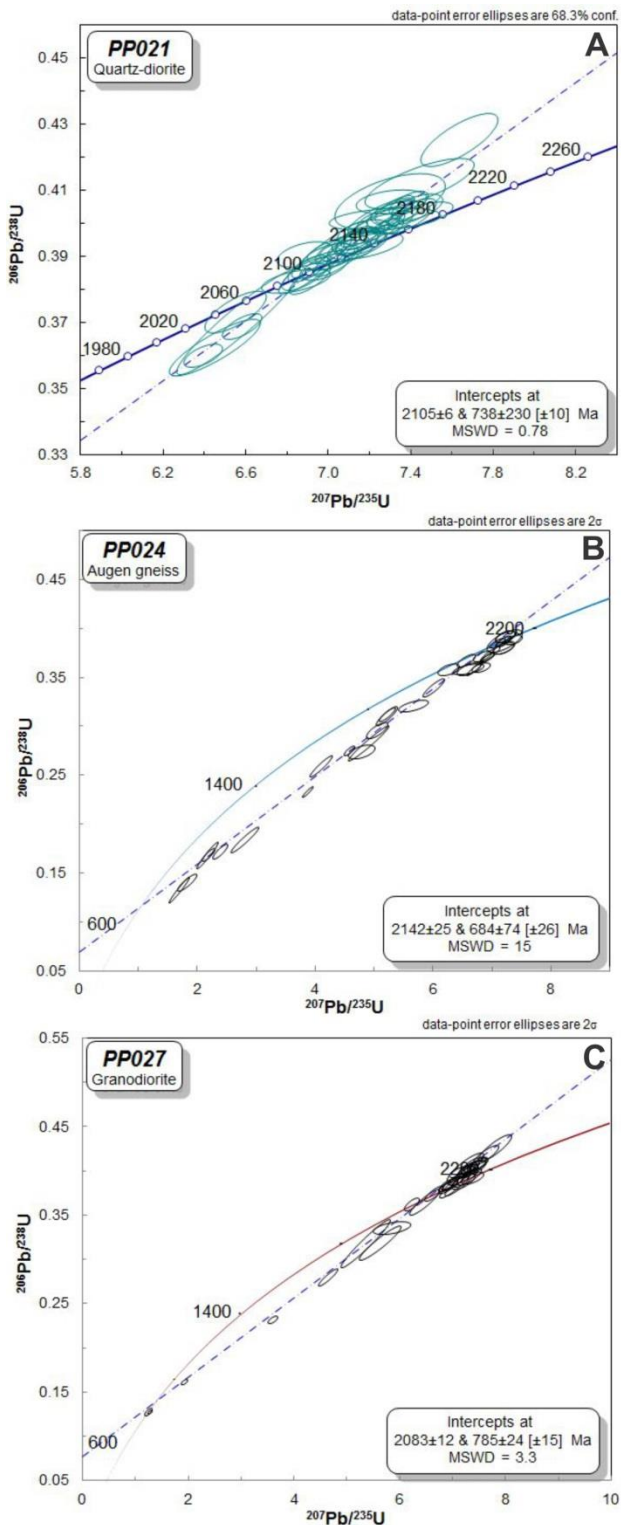


Figure 3 – U-Pb zircon Concordia ages for rocks at the footwall of the Barro Alto Complex for A) PP021 quartz-diorite ; B) PP024 augen gneiss and C) PP027 granodiorite emplaced along the Juscelândia Sequence western contact.

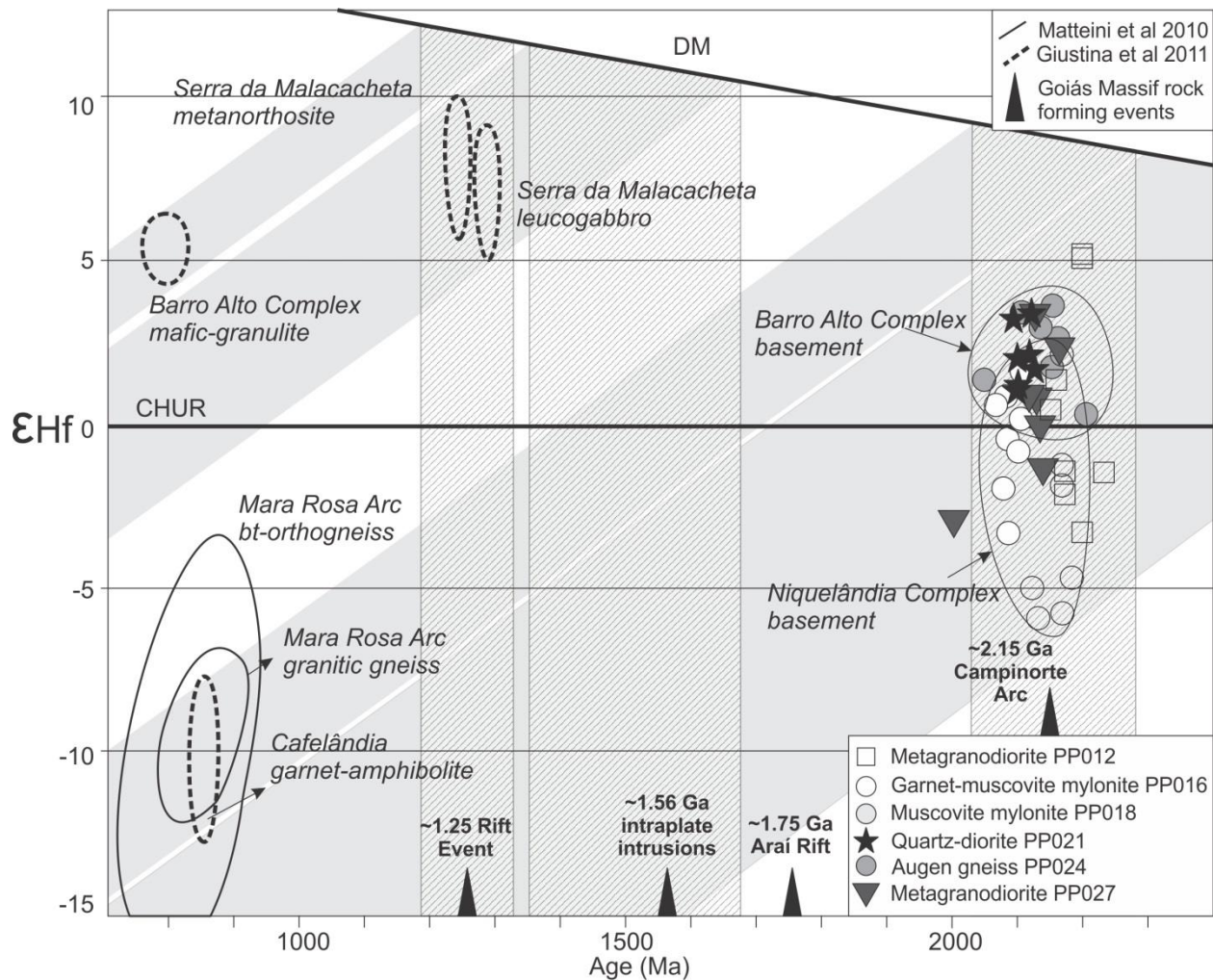


Figure 4 - ϵHf vs time diagram calculated based on our reported U-Pb ages and that of Cordeiro (2014) for sample PP012 overlain by fields from the Barro Alto Complex (Giustina et al., 2011) and the Mara Rosa Arc (Matteini et al., 2010).

4. Discussion

4.1. Campinorte Arc U-Pb and Hf isotopes data

A ϵ Hf vs time diagram was calculated from the same grain Lu-Hf and U-Pb data shows isotopic evolution trends of depleted mantle crustal rocks generated at ~2.15 Ga as shaded areas (Figure 4). These are calculated using average continental crust $^{176}\text{Lu}/^{177}\text{Hf}$ ratio of 0.0113 (Taylor and McLennan, 1985) for each group of rocks. Added in for comparison are the fields of samples from the Mesoproterozoic Serra da Malacacheta Complex, Neoproterozoic Barro Alto complex, Cafelândia amphibolite (Giustina et al., 2011) and Mara Rosa Arc gneisses (Matteini et al., 2010).

An evolutionary trend for the Campinorte Arc from mantle sources with ages from 2.3 Ga to 3.1 Ga can be observed from ϵ Hf data. The Pau de Mel Suite samples show average ϵ Hf around the CHUR composition and variable TDM ages, compatible with Nd TDM ages reported by Giustina et al. (2009). A wider ϵ Hf range from 2.4 Ga to 3.1 is observed in the Niquelândia basement samples when compared to Barro Alto basement samples ranging from 2.3 Ga to 2.7 Ga. This variation, highlighted by their respective fields on Figure 4 could be an artifice of limited sampling, indicate general older sources for the Campinorte Arc in the Niquelândia region or, most likely, variable degrees of crustal contamination during emplacement.

A comparison with ϵ Hf data from the younger Serra da Malacacheta and Barro Alto complexes provide interesting insights on post Campinorte Arc events where crystallization and model ages detail the Goiás Massif history from Paleoproterozoic through Neoproterozoic. As reported by Giustina et al. (2011), Serra da Malacacheta Complex leucogabbro and metanorthosite yielding interpreted crystallization ages of, respectively, 1288 ± 14 Ga and 1271 ± 78 Ga show Hf TDM ages from 1.30-1.65 Ga. These ages are compatible with ~1.58 Ga Tocantins Subprovince intraplate intrusions (Pimentel et al., 1999; Pimentel and Botelho, 2001; Lenharo et al., 2002) and might suggest that isotopic fractionation at a ~1.58 Ga event had bearings on the formation of rocks at ~1.25 Ga. This later Mesoproterozoic event is interpreted as a rift that generated MORB-like signatures in rocks of the Juscelândia Sequence (Moraes et al.,

2003; Ferreira Filho et al., 2010). In tandem with lack of coeval intrusions within the Campinorte Domain, no samples reported source ages compatible with the ~1.75Ga Araí Rift (Figure 4).

Data from Giustina et al. (2011) also show that coeval rocks within the same setting can be generated from very diverse sources. For instance, both Cafelândia and Barro Alto samples yielded U-Pb crystallization ages around ~780 Ga but with two groups of model ages. The first group is compatible with the ~1.25 Ga rift (Barro Alto Complex mafic-granulite). The second group falls within the 2.0-2.2 Ga range (Cafelândia garnet amphibolite) coeval with Campinorte Arc Pau de Mel Suite crystallization ages. Giustina et al. (2011) suggest the Cafelândia amphibolite discrepant ϵ Hf results point to a previously unidentified Neoproterozoic intrusion of uncertain origin.

4.2 Campinorte Arc data

The new U–Pb and Lu–Hf isotope data obtained on zircon permitted to recognize two Paleoproterozoic magmatic-metamorphic events and a later Neoproterozoic one, in agreement with previously published ages by Giustina et al. (2009) and Cordeiro (2014) in the Campinorte Arc. Ages from 2.19 to 2.15 Ga are in tandem with magmatism and coeval basin formation that defines the Pau de Mel Suite and mixed crustal-mantle sources as suggested by Hf isotopes. Intermediate magmatism represented by quartz-diorite PP021 (2105 ± 6) and granodiorite PP027 (2083 ± 12 Ga) seems to postdate the metamorphic peak between 2.11-2.09 Ga (Cordeiro, 2014). Post-peak deformation is expected as attested by the garnet-muscovite gneiss PP016 age of 2077 ± 8 Ma.

A well-constrained Neoproterozoic lower intercept age in granodiorite PP027 (785 ± 24 Ma) and less well constrained examples in the augen gneiss PP024 (ca. 690 Ma) and quartz-diorite PP021 (ca. 740 Ma) are in tandem with the Pau de Mel Suite metagranodiorite PP012 lower intercept of 751 ± 28 Ga (Cordeiro, 2014). These younger ages point to a regional Neoproterozoic lead loss event that has also affected the older Pau de Mel Suite zircon. Metamorphic ages around 750 Ma are observed in Barro Alto Complex high grade metamorphic rocks overprinting emplacement ages of ~790 Ma (Moraes et al., 2006; Pimentel et al., 2006; Giustina et al., 2011). Giustina et al. (2011) interpret the collision of a Neoproterozoic island arc (the Goiás Magmatic Arc) against a Paleoproterozoic continental block (Goiás Massif) around 750 Ma. Our suggestion is that this Neoproterozoic collision was able to induce lead loss in zircon of older basement rocks and generate the lower intercept ages observed in our samples. The influence of such event is expected to be greater in the Campinorte Domain given its contact with the Goiás Magmatic Arc than elsewhere in the Goiás Massif.

The geochronological data presented in this paper extend the Campinorte Arc to at least the Barro Alto and Niquelândia footwall and confirms a very complex post-Paleoproterozoic geological history for the Campinorte Domain. Our data in the Niquelândia and Barro Alto complexes footwall combined with those of Marques (2010) for the northern Canabrava complex basement confirm the Rio Maranhão Thrust as the most likely surface expression of the Campinorte/Cavalcante-Arraias domains contact.

4.3. The formation of the Goiás Massif and its links with the São Francisco Craton

The origin of the Goiás Massif and its relationship with the São Francisco Craton have been discussed by various authors (e.g. Brito Neves and Cordani, 1991; Pimentel et al., 2000, 2011; Valeriano et al., 2008; Ferreira Filho et al., 2010; Cordeiro, 2014). Two main geological settings have been proposed for the Goiás Massif one of which suggests the massif as a microcontinent amalgamated to the western margin of the São Francisco plate during the Neoproterozoic Brasiliano Cycle. This scenario was first suggested by Brito Neves and Cordani (1991) in a highly speculative sketch and assumed as well established henceforth (Pimentel et al., 2000; Blum et al., 2003; Pimentel et al., 2004; Queiroz et al., 2008; Valeriano et al., 2008; Ferreira Filho et al., 2010; Pimentel et al., 2011). Commonly cited variations of this scenario interpret the Rio Maranhão Thrust as a collisional suture between the Campinorte and Cavalcante-Arraias domains (Marangoni et al., 1995; Pimentel et al., 1999; Moraes et al., 2006; Jost et al., 2013) or that the microcontinent included only the Crixás-Goiás Domain (Pimentel et al., 2000; Valeriano et al., 2008). The allochthonous microcontinent scenario has become widely referred to as an explanation to the Archean-Paleoproterozoic Crixás-Goiás Domain positioning afar from coeval rocks. Sharp seismic, tomography and gravimetric contrasts between these domains have been argued to support the microcontinent hypothesis (Assumpção et al., 2004; Soares et al., 2006).

A second scenario envisages the Goiás Massif as a western extention of the São Francisco plate that was widely affected by Brasiliano Neoproterozoic events and therefore, not cratonized (Cordeiro, 2014). The almost 400 km wide Neoproterozoic foreland system covering the contact region between the exposed São Francisco Craton basement and the Goiás Massif hinders the assessment of this hypothesis by direct means of mapping and sampling. Seismic and stratigraphic (Martins-Neto, 2009), structural (D'el-Rey Silva et al., 2008) and gravimetric studies (Pereira and Fuck, 2005), however, fully support São Francisco plate basement under the Brasília Belt Meso-Neoproterozoic metasedimentary cover.

As suggested by the Goiás Massif placement theories, the Campinorte Domain is of paramount importance to propose regional tectonic models as it could represent the

very western edge of the São Francisco-Congo continent. In the following sections we discuss much of previously published data and interpretation presented to support both theories along with our own suggestions.

4.3.1. Crixás-Goiás Domain as a microcontinent

The Crixás-Goiás Domain is the sole Goiás Massif terrane with known Archean rocks and this uniqueness was probably one of the reasons it was proposed as an allochthonous terrane. However, common ages, lithologies, depositional setting and geochemical signature between the Campinorte Sequence and Crixás-Goiás metasedimentary rocks indicated that they were once part of the same Paleoproterozoic basin (Giustina et al., 2009; Jost et al., 2010; Cordeiro, 2014) and, therefore, amalgamated prior to the Neoproterozoic. Moreover, Paleoproterozoic/Archean magnetic structures transpose the Crixás-Goiás domain into the Campinorte Domain where they are covered by younger metasedimentary rocks and no magnetic features mark the contact between these domains (Cordeiro, 2014).

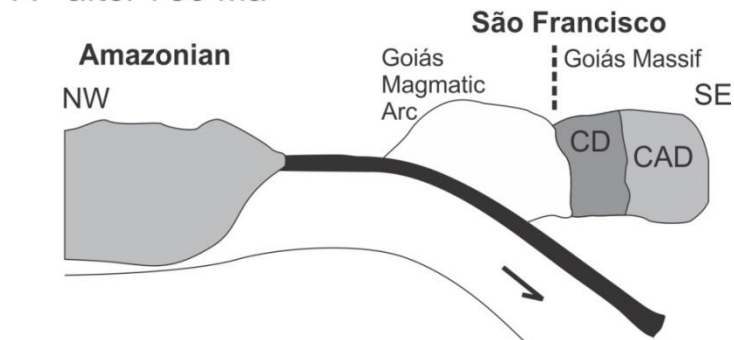
4.3.2. Crixás-Goiás and Campinorte domains as a microcontinent

The hypothesis that the Crixás-Goiás and Campinorte domains are a single microcontinent was proposed based on gravimetric data that suggests the Rio Maranhão Thrust as a regional discontinuity typical of suture zones (Marangoni et al., 1995; Pimentel et al., 2004). Later additional gravimetric data along with refractory seismics seemed to concur by indicating a Moho boundary upwelling under the Goiás Magmatic Arc and Campinorte Domain (Assumpção et al., 2004; Berrocal et al., 2004; Perosi, 2006; Ventura et al., 2011). The Rio Maranhão Thrust marks not only the Campinorte and Cavalcante-Arraias domains contact but also the footwall zone of Central Brazil > 80 km long mafic-ultramafic complexes. In the only detailed structural study of the Rio Maranhão Thrust, D'el-Rey Silva et al. (2008) argued that the lineament is a ~620-630 Ma intraplate fault developed through the São Francisco paleocontinent upper crust during D₃ WNW-ESE shortening.

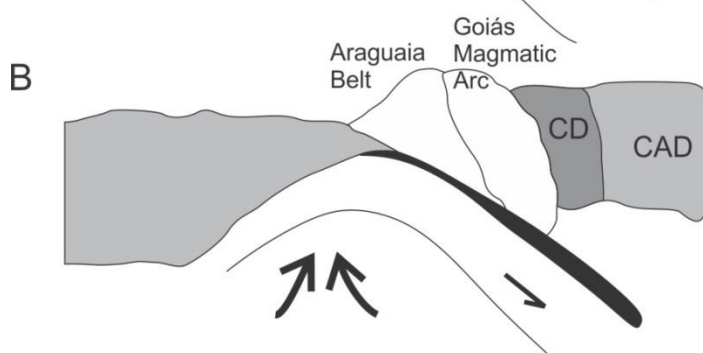
Seismic and gravimetric evidence used to support the microcontinent hypothesis can be reinterpreted under the suggestion of D'el-Rey Silva et al. (2008) for a Rio

Maranhão Thrust intraplate origin. Soares et al. (2006) argued that a sharp contrast in the Moho boundary should be expected between accreted terranes of different ages. Such contrast is not observed in seismic and gravimetric data from the Campinorte Domain and the Goiás Magmatic Arc contact, a clear collisional suture. A very sharp contrast exists, however, between the Campinorte and Cavalcante-Arraias domains, of which no Brasiliano syn-collisional magmatism has been reported. To explain this conundrum, Soares et al. (2006) proposed that the root of the Goiás Magmatic Arc was delaminated during the final Brasiliano Orogeny collision between Amazonian and São Francisco paleoplates which induced the observed Moho relief homogenization. Likewise, we believe that the root under the Campinorte Domain was delaminated in the same event along with that of the Goiás Magmatic Arc similarly to the model by Sacks and Secor (1990) for the southern Appalachians (Figure 5). The Cavalcante-Arraias Domain lower crust, comparatively more stable since the Mesoproterozoic, was preserved from the delamination event generating the Moho step marked in surface by the Rio Maranhão Thrust.

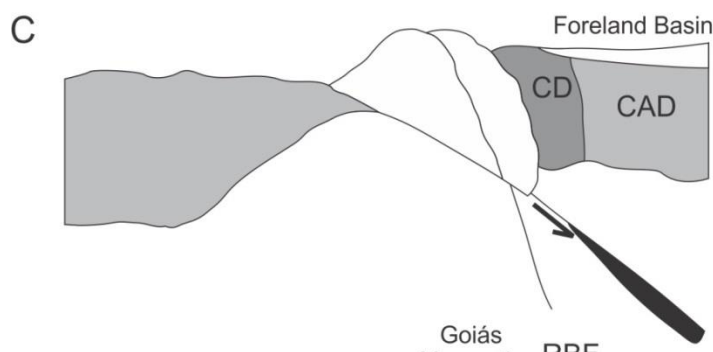
A - after 730 Ma



B



C



D - 630-600 Ma

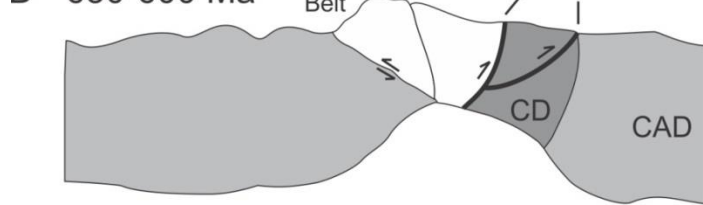


Figura 5 – Goiás Magmatic Arc and Campinorte Domain delamination model (based on Sacks and Secor, 1990; Soares et al., 2006; Ventura et al., 2011). A) Goiás Magmatic Arc formation; B) Amazonian Paleocontinent lithospheric and crustal extention under the Araguaia Belt due to oceanic crust delamination; C) Oceanic lithosphere detachment inducing asthenosphere upwelling between the paleocontinents; D) Progressive compression thrusts the Araguaia Belt over the Amazonian Plate and generates thin crust under both the Goiás Magmatic Arc and the Campinorte Domain, preserving the Cavalcante-Arraias Domain Moho boundary. RBF = Rio dos Bois Fault; RMT = Rio Maranhão Thrust, CD = Campinorte Domain; CAD = Cavalcante-Arraias Domain.

The interpretation that the Rio Maranhão Thrust represents an intraplate fault as proposed by D'el-Rey Silva et al. (2008) is also supported by the well-correlated metasedimentary rocks of the Araí and Serra da Mesa groups and which are placed in both sides of the thrust (Dardenne, 2000; Marques 2010). The stratigraphical and isotopic correlation study of Marques (2010) indicate that both successions are made of a mixed marine platform with two distinct fining upwards cycles that consist of a basal sequence of coarse sandstones, followed upwards by an intermediate sequence of pelites interbedded with marls representing a common carbonaceous platform, and by an upper turbidite facies sand-silt sequence. Marques (2010) geochronological provenance study indicated different sediments sources for these basins as the basal sandstones show ages from 2.4 to 2.0 Ga for the Araí Group Traíras Formation and from 2.22 to 1.5 Ga to the Serra da Mesa Group. The ages of ~1.5 Ga in Serra da Mesa Group detrital zircon were interpreted as derived from Tocantins Subprovince A-type granites.

Two northern Goiás granite subprovinces (Figure 6) with ages of ~1.58 Ga, referred as Tocantins Subprovince, and ~1.76 Ga, Paraná Subprovince (Pimentel et al., 1999; Pimentel and Botelho, 2001; Lenharo et al., 2002) hold evidence to refute the microcontinent hypothesis. While granites from the Paraná Subprovince are restricted to the Cavalcante-Arraias Domain, younger granites from the Tocantins Subprovince are found both in the Cavalcante-Arraias and in the Campinorte Domain. These A-type granites are believed to be related to rift events that affected the Goiás Massif in the Paleo-Mesoproterozoic. These domains are bound to have been amalgamated prior to the age of the subprovince itself if the Tocantins Subprovince granites intruded both of them.

Even though Tocantins Subprovince granites lack appropriate geochronological data, they show similar petrological features that were used to establish them as a single subprovince (Marini et al., 1992). To the north, the Peixe Alkaline Complex (Figure 6) shows a crystallization age of 1503 ± 3 Ma (Kitajima et al., 2001), but its genetic relation with the Tocantins Subprovince is unknown. The presence of roughly coeval A-type granites in both sides of the Rio Maranhão Thrust strongly supports our

hypothesis that the Campinorte and Cavalcante-Arraias domains were amalgamated before the Mesoproterozoic, not during the Neoproterozoic.

Since these domains were amalgamated since at least the Mesoproterozoic, thus the Goiás Massif itself was already formed, the relation of the massif and the São Francisco Craton needs to be addressed. Close genetic relation of ~1.76 Ga and ~1.58 Ga rift-related rocks is also observed elsewhere in the São Francisco Craton. Around 1.77 Ga both Araí Group basal volcanics (Pimentel et al., 1991) and Espinhaço Basin Rio dos Remédios formation volcanics (Babinski et al., 1994; 1999) were formed during crustal extention. Around 1.58 Ga, Tocantins Subprovince intraplate granites intruded the Goiás Massif and Bomba Formation volcanic rocks in the Espinhaço Basin representing a renewed rift event in the central São Francisco Craton as detailed by Danderfer et al. (2009). Coeval ages are registered within the Mineiro Belt Tiradentes Formation, south of the São Francisco Craton, where detrital zircon ages around 1.55 Ga are described as also pointing to a reactivation of the Espinhaço system (Ribeiro et al., 2013).

We believe that geological and geophysical data favor the Goiás Massif as the São Francisco paleocontinent western edge since the Paleoproterozoic instead of an allochthonous microcontinent hypothesis. Neoproterozoic lower crust delamination affecting both the Neoproterozoic Goiás Magmatic Arc and the Campinorte Domain render current seismic and gravimetric data ambiguous in interpreting suture boundaries. Geological and geochronological work on the Rio Maranhão Thrust, especially along trend to the north, should confirm the conspicuous lack of Neoproterozoic collisional magmatism evidence and help rule out the microcontinent hypothesis.

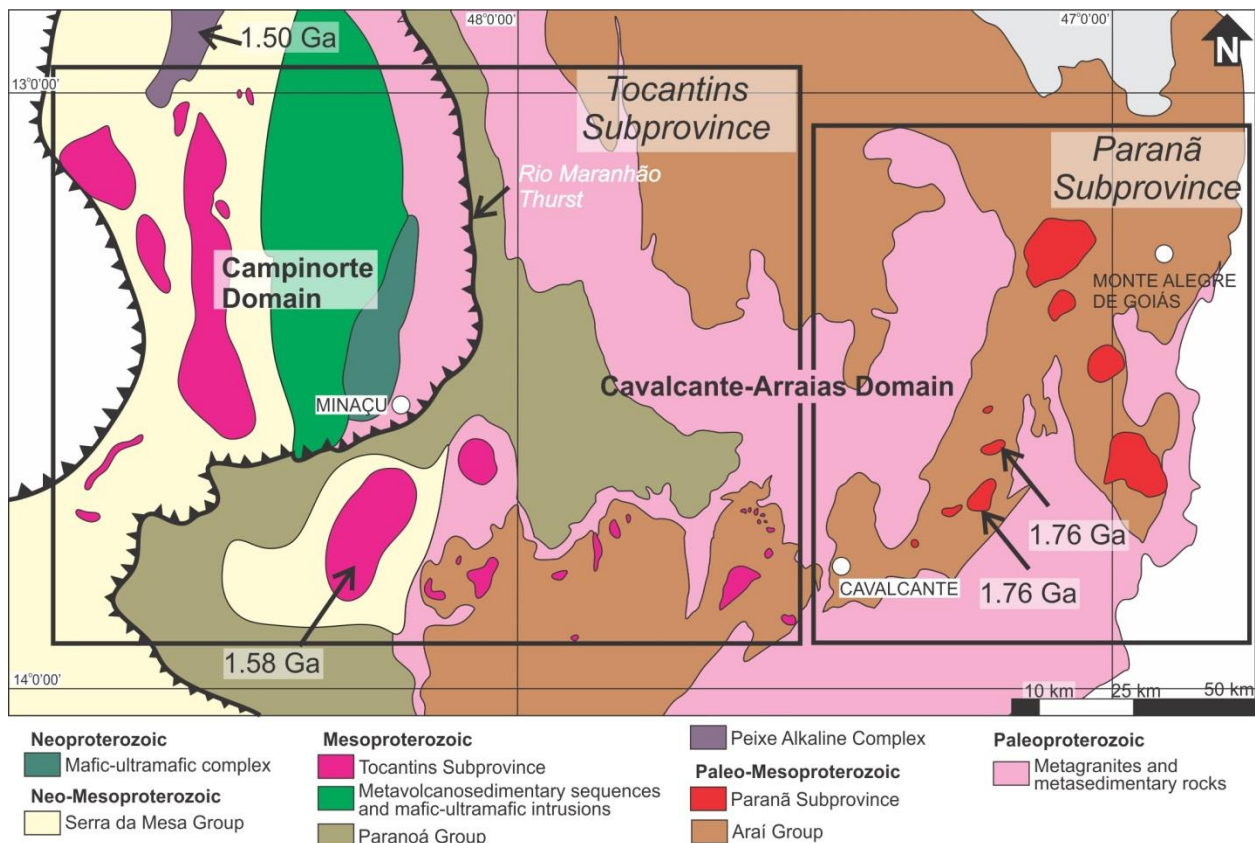


Figure 6 – Tocantins and Paraná subprovinces from Marini et al. (1992). Whereas the ~1.77 Ga A-type granites are described only in the Cavalcante-Arraias Domain, the Sn-mineralized ~1.58 Ga magmatic event occurred both in the Cavalcante-Arraias and in the Campinorte domains (Pimentel et al., 1999; Pimentel and Botelho, 2001). The Peixe Alkaline Complex age of ~1.50 Ga is given by Kitajima et al (2001).

The formation of the Goiás Massif is depicted on Figure 8. Its formation and post-assembling events can be summarized as:

3.10 to 2.70 Ga Crixás-Goiás Domain TTG suite rocks (Queiroz et al., 2000) were amalgamated into a single block.

2.40-2.35 Ga Almas-Conceição do Tocantins Domain TTG suite rocks from the Ribeirão das Areias Complex likely formed as a volcanic arc (Cruz, 2001; Fuck et al., 2014).

2.20-2.00 Ga Orogenic event with consequent arc and basin formation. This event generated the Crixás-Guarinos greenstone belts upper sedimentary units (Crixás-Goiás Domain), Campinorte Arc (Campinorte Domain), Arumina Suite (Cavalcante-Arraias Domain) and Suites 1 and 2 (Almas-Conceição do Tocantins Domain). A continent-continent collision was likely involved in the generation of the large volume Aurumina Suite syn-collisional peraluminous magmatism and, therefore, a hypothetical Ticunzal Block is invoked to represent an older poorly understood crustal fragment. Several other Paleoproterozoic arcs were formed elsewhere and assembled along with older Archean-Paleoproterozoic crustal blocks into the São Francisco Plate. The metamorphic peak registered by granulite metamorphism in the Campinorte Arc occurred from 2.11-2.08 Ga, marking the Goiás Massif final amalgamation stage. Post-peak magmatism is registered as granitoids and gneisses from 2.08 to 2.03 Ga.

1.78-1.75 Ga - The Goiás Massif underwent a regional rift event marked by the Araí Group volcanism and coeval Paraná Subprovince granites intrusions and later basin formation.

1.57-1.50 Ga – Tocantins and Paraná subprovinces A-type granites in a rift setting intruding the Campinorte and Cavalcante-Arraias domains as, respectively, large and small intrusions. Late-stage intrusion of the Peixe Alkaline Complex in the Campinorte Domain.

1.28-1.25 Ga – Continental break up and bimodal volcanism with oceanic lithosphere and basin formation (Juscelândia and Palmeirópolis sequences) and coeval mafic-ultramafic magmatism of the Serra da Malacacheta Complex (Moraes et al., 2003; 2006). Evidence of this rifting event is so far restricted to the Campinorte Domain.

0.80-0.77 Ga – Goiás Magmatic Arc collision against the Goiás Massif with mafic-ultramafic back-arc magmatism represented by the Barro Alto, Niquelândia and Canabrava complexes (Giustina et al., 2011). These complexes intruded along the 1.25-1.28 Ga rifting event crustal weakness.

0.77-0.73 Ga – Arc-continent collision metamorphic peak responsible for the Barro Alto and Niquelândia granulite formation (Giustina et al., 2011) and lead loss in Campinorte Arc zircon. The Neoproterozoic metamorphic peak is well constrained in two samples lower intercepts, a) our granodiorite PP027 785±24 Ga and b) the metagranodiorite PP012 751±28 Ga (Cordeiro, 2014).

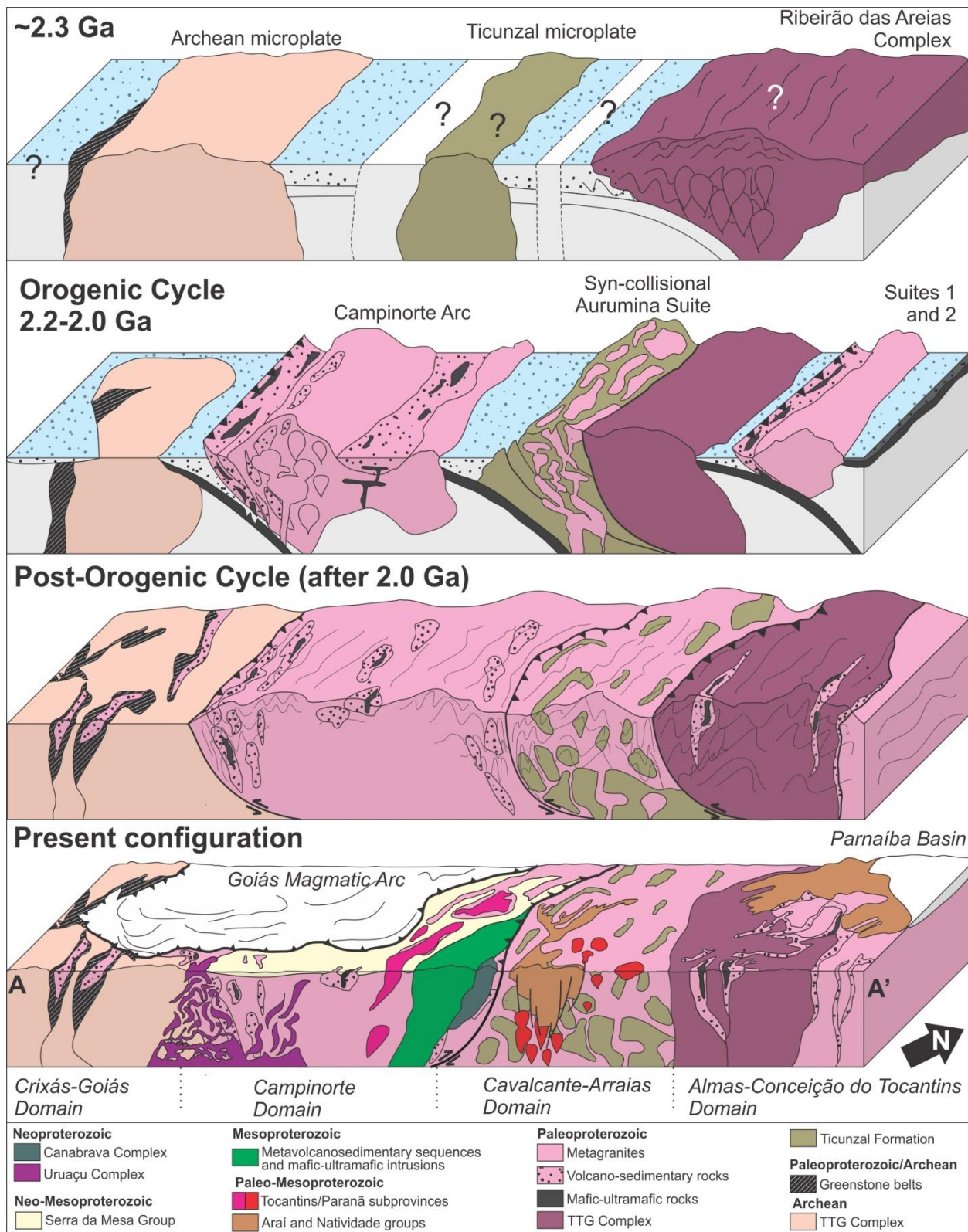


Figure 8 – Tectonic evolution model of the Goiás Massif during a Paleoproterozoic orogenic cycle. The A-A' section location is shown on Figure 1.

5. Conclusions

The Northern Brasília Belt basement is composed of Archean-Paleoproterozoic terranes with varying degrees of post-assembling reworking by Meso-Neoproterozoic rifting, basin formation and magmatism. Non-interpretative terrane nomenclature should be favored instead of loosely previously proposed local names that lacked regional tectonic framework discussion. We propose these terranes to be grouped within the Goiás Massif and divided from southwest to northeast into the Crixás-Goiás, Campinorte, Cavalcante-Arraias and Almas-Conceição do Tocantins domains (Figure 1).

U-Pb zircon ages and Hf isotopes for the eastern margin of the Campinorte Domain confirm the extention of the Campinorte Arc as basement of the Barro Alto and Niquelandia complexes. Similar ages within the Goiás Massif suggest a Paleoproterozoic amalgamation event from 2.19 to 2.04 Ga with metamorphic peak from 2.11 to 2.08 Ga.

The sharp gravimetric/seismic contrast marked in surface by the Rio Maranhão Thrust has been largely interpreted as a collisional feature and argued to support the combined Crixás-Goiás and Campinorte domains block as an allochthonous microcontinent accreted to the São Francisco plate in the Neoproterozoic Brasiliano Orogeny. Geological and geochronological evidence for this collision, however, have not been proposed so far. The sharp gravimetric/seismic contrast can be explained by lower crust delamination affecting both the Goiás Magmatic Arc and the terrane it was accreted against, the Campinorte Domain, leaving the Moho boundary of remainder domains unperturbed.

The Goiás Massif shares coeval features with São Francisco Craton terranes: a) Paleoproterozoic rift-related magmatism and basin formation approximately around 1.76 Ga at the Goiás Massif Araí Rift and São Francisco Craton Espinhaço Basin; b) Paleo-Mesoproterozoic intraplate magmatism around 1.58 Ga of the Tocantins/Paraná subprovinces at the Campinorte/Cavalcante-Arraias domains and the Espinhaço Basin Bomba Formation. These common features indicate that the Goiás Massif was affected by the same intraplate events as the São Francisco Craton. Common Goiás Massif and São Francisco Craton Paleo-Mesoproterozoic magmatic events allied to lack of sharp

internal gravimetric contrast lineaments could indicate that the Goiás Massif represented the São Francisco Paleocontinent western edge since the Paleoproterozoic.

References

- Alkmim, F.F., 2004. O que faz de um cráton um cráton? O Cráton do São Francisco e as revelações almeidianas ao delimitá-lo. In: Mantesso-Neto, V., Bartorelli, A., Carneiro, C.D.R., Brito Neves, B.B. (Eds.), Geologia do Continente Sul-American. Evolução da Obra de Fernando Flávio Marques de Almeida, São Paulo, Beca, pp. 17–35.
- Almeida, F. F. M. 1967. Origem e Evolução da plataforma brasileira. Rio de Janeiro, DNPM, 36 p. (Boletim 241).
- Almeida, F.F.M., 1976. Evolução tectônica do Centro-Oeste brasileiro no Proterozóico Superior. Anais da Academia Brasileira de Ciências 40, 285-295.
- Almeida, F.F.M., 1977. O Cráton São Francisco. Revista Brasileira de Geociências 7, 349-364.
- Almeida, F. F. M. 1984. Província Tocantins, setor sudoeste. In: Almeida, F. F. M., Hasui, Y. (eds.) O Pré-Cambriano do Brasil, São Paulo, E. Blucher, 265-281.
- Alvarenga, C.J.S., Dardenne, M.A., Botelho, N.F., Lima, O.N.B., Machado, M.A., Almeida, T., 2007. Nota Explicativa das folhas SD.23-V-C-III (Monte alegre de Goiás), SD.23-V-C-V (Cavalcante) , SD.23-V-C-VI (Nova Roma). CPRM, 2007. 65 pp.
- Andersen, T., Andersson, U.B., Graham, S., Åberg, G., Simonsen, S.L., 2009. Granitic magmatism by melting of juvenile continental crust: new constraints on the source of Palaeoproterozoic granitoids in Fennoscandia from Hf isotopes in zircon. Journal of the Geological Society 166, 233-247.
- Assumpção, M., An, M., Bianchi, M., França, G.S.L., Rocha, M., Barbosa, J.R., Berrocal, J., 2004. Seismic studies of the Brasília fold belt at the western border of the São Francisco Craton, Central Brazil, using receiver function, surface-wave dispersion and teleseismic tomography. Tectonophysics 388, 173-185.
- Babinski, M., Brito Neves, B.B., Machado, N., Noce, C.M., Uhlein, A., van Schmus,W.R., 1994. Problemas da metodologia U/Pb em zircões de vulcânicas continentais: caso do Grupo Rio dos Remédios, Supergrupo Espinhaço, no

- Estado da Bahia. In: Anais 42º Congresso Brasileiro de Geologia, Sociedade Brasileira de Geologia, Balneário Camboriú, vol. 2, pp. 409–410.
- Babinski, M., Pedreira, A.J., Brito Neves, B.B., van Schmus,W.R., 1999. Contribuição à geocronologia da Chapada Diamantina. In: Anais 7º Simpósio Nacional de Estudos Tectônicos, Sociedade Brasileira de Geologia, Lençóis, Section 2, pp. 118–120.
- Barbosa, J.S.F., Sabaté, P., 2002. Geological features and the Paleoproterozoic collision of four Archean crustal segments of the São Francisco Craton, Bahia, Brazil. A synthesis. Anais da Academia Brasileira de Ciências 74, 343-359.
- Barbosa, J.S.F., Sabaté, P., 2004. Archean and Paleoproterozoic crust of the São Francisco Craton, Bahia, Brazil: geodynamic features. Precambrian Research 133, 1-27.
- Berrocal, J., Marangoni, Y., Sá, N.C., Fuck, R., Soares, J.E.P., Dantas, E., Perosi, F., Fernandes, C., 2004. Deep seismic refraction and gravity crustal model and tectonic deformation in Tocantins Province, Central Brazil. Tectonophysics 388, 187-199.
- Black, L.P., Kamo, S.L., Allen, C.M., Davis, D.W., Aleinikoff, J.N., Valley, J.W., Mundil, R., Campbell, I.H., Korsch, R.J., William, I.S., Foudoulis, C., 2004. Improved $^{206}\text{Pb}/^{238}\text{U}$ microprobe geochronology by the monitoring of a trace-element related matrix effect: SHRIMP, ID-TIMS, ELA-ICP-MS and oxygen isotope documentation for a series of zircon standards. Chemical Geology 205, 115–140.
- Blum, M.L.B., Jost, H., Moraes, R.A.V., Pires, A.C.B., 2003. Caracterização dos complexos ortognáissicos arqueanos de Goiás por gamaespectrometria aérea. Revista Brasileira de Geociências 33, 147-152.
- Botelho, N.F., Fuck, R.A., Dantas, E.L., Laux, J.L., Junges, S.L., 2006 The Paleoproterozoic Aurumina granite Suite, Goiás and Tocantins, whole rock geochemistry and U-Pb and Sm-Nd isotopic constrain. The Paleoproterozoic Record of the São Francisco Craton. Brazil, IGCP 509, 9-21.
- Bouvier, A., Vervoort, J.D. & Patchett, P.J. 2008. The Lu–Hf and Sm–Nd isotopic composition of CHUR: Constraints from unequilibrated chondrites and

- implications for the bulk composition of terrestrial planets. *Earth and Planetary Science Letters* 273, 48–57.
- Brito Neves, B.B., 2011. The Paleoproterozoic in the South American continent: Diversity in the geologic time. *Journal of South American Earth Sciences* 32, 270-286.
- Brito Neves, B.B., Cordani, U.G., 1991. Tectonic evolution of South America during the Late Proterozoic. *Precambrian Research* 53, 23–40.
- Buhn, B., Pimentel, M.M., Matteini, M., Dantas, E., 2009. High spatial resolution analysis of Pb and U isotopes for geochronology by laser ablation multi-collector inductively coupled plasmamass spectrometry (LA-MC-ICP-MS). *Anais da Academia Brasileira de Ciências* 81, 99–114
- Chu, N.C., Taylor, R.N., Chavagnac, V., Nesbitt, R.W., Boella, R.M., Milton, J.A., German, C.R., Bayon, G., Burton, K., 2002. Hf isotope ratio analysis using multi-collector inductively coupled plasma mass spectrometry: an evaluation of isobaric interference corrections. *Journal of Analytical Atomic Spectrometry* 17, 1567–1574.
- Cordani, U.G., Hasui, Y., 1975. Comentários sobre os dados geocronológicos da Folha Goiás. In: Schobbenhaus, C. *Carta Geológica do Brasil ao Milionésimo – SD-22*. Brasília, DNPM.
- Cordeiro, P.F.O., 2014. Compartimentação Tectônica do Maciço de Goiás e o Arco de Campinorte. Unpublished PhD Thesis.
- Cruz, E.L.C.C., 2001. A gênese e o contexto tectônico da Mina Córrego do Paiol, terreno Almas-Conceição: um depósito de ouro hospedado em anfibolito do embasamento da Faixa de Dobramentos Brasília. Unpublished PhD thesis, Universidade de Brasília, 183 p.
- Cruz, E.L.C.C., Kuyumjian, R.M., 1998. The geology and tectonic evolution of the Tocantins granite-greenstone terrane: Almas-Dianópolis region, Tocantins State, Central Brazil. *Revista Brasileira de Geociências* 28, 173-182.
- Cruz, E.L.C.C., Kuyumjian, R.M., 1999. Mineralizações auríferas filoneanas do terreno granite-greenstone do Tocantins. *Revista Brasileira de Geociências* 29, 291-298.

- Cruz, E.L.C.C., Kuyumjian, R.M., Boaventura, G.R., 2003. Low-K calc-alkaline granitic series of southeastern Tocantins state: chemical evidence for two sources for the granite-gneissic complexes in the Paleoproterozoic Almas-Dianópolis terrane. *Revista Brasileira de Geociências* 33, 125-136.
- Dandefer, A., Waele, B., Pedreira, A.J., Nalini, H.A., 2009. New geochronological constraints on the geological evolution of Espinhaço basin within the São Francisco Craton-Brazil. *Precambrian Research* 170, 116-128.
- Dardenne, M.A., 2000. The Brasília Fold Belt. In: Cordani, U.G., Milani, E.J., Thomaz Filho, A., Campos, D.A. (eds) *Tectonic Evolution of South America*. 31st International Geological Congress, Rio de Janeiro, 231-263.
- Delgado, I.M., Souza, J.D., Silva, L.C., Silveira Filho, N.C., Santos, R.A., Pedreira, A.J., Guimarães, J.T., Angelim, L.A., Vasconcelos, A.M., Gomes, I.P., Lacerda Filho, J.V., Valente, C.R., Perrota, M.M., Heinick, C.A., 2003. Província Tocantins, in: Buzzi, L.A., Schobbenhaus, C., Vidotti, R.M., Gonçalves, J.H. (Eds.), *Geologia, Tectônica e Recursos Minerais do Brasil*. CPRM, Rio de Janeiro, pp. 281-292.
- Ferreira Filho, C.F., Pimentel, M.M., Araújo, S.M., Laux, J.H., 2010. Layered intrusions and volcanic sequences in Central Brazil: Geological and geochronological constraints for Mesoproterozoic (1.25 Ga) and Neoproterozoic (0.79 Ga) igneous associations. *Precambrian Research* 183, 617-634.
- Fuck, R.A., Danni, J.C.M., Winge, M., Andrade, G.F., Barreira, C.F., Leonards, O.H., Kuyumjian, R.M., 1981. Geologia da Região de Goianésia. Simpósio de Geologia do Centro-Oeste, Goiânia, p.447-469.
- Fuck, R.A., Pimentel, M.M., Silva, L.J.H.D-R., 1994. Compartimentação tectônica na porção oriental da Província Tocantins. In: Congresso Brasileiro de Geologia, 38, Anais., Balneário Camboriú, SBG. 215-216.
- Fuck, R.A., Dantas, E.L., Pimentel, M.M., Botelho, N.F., Armstrong, R., Laux, J.H., Junges, S.L., Soares, J.E., Praxedes, I.F., 2014. Paleoproterozoic crust-formation and reworking events in the Tocantins Province, central Brazil: A contribution for Atlantica supercontinent reconstruction. *Precambrian Research* (2014), <http://dx.doi.org/10.1016/j.precamres.2013.12.003>

- Gerdes, A., Zeh, A., 2006. Combined U–Pb and Hf isotope LA-(MC)-ICP-MS analyses of detrital zircons: comparison with SHRIMP and new constraints for the provenance and age of an Armorican metasediment in Central Germany. *Earth and Planetary Sciences Letters*, 249, 47–61.
- Gerdes, A., Zeh, A., 2009. Zircon formation versus zircon alteration - New insights from combined U– Pb and Lu–Hf in situ LA-ICP-MS analyses, and consequences for the interpretation of Archean zircon from the Central Zone of the Limpopo Belt. *Chemical Geology* 261, 230–243.
- Giustina, M.E.S.D., Oliveira, C.G., Pimentel, M.M., Melo, L.V., Fuck, R.A., Dantas, E.L., Buhn, B., 2009. U–Pb and Sm–Nd constraints on the nature of the Campinorte Sequence and related Paleoproterozoic juvenile orthogneisses, Tocantins Province, Central Brazil. *Geological Society of London Special Publication* 323, 255-269.
- Giustina, M.E.S.D., Pimentel, M.M., Ferreira Filho, C.F., Fuck, R.A., Andrade, S., 2011. U–Pb–Hf-trace element systematics and geochronology of zircon from a granulite-facies metamorphosed mafic–ultramafic layered complex in Central Brazil. *Precambrian Research* 189, 176-192.
- Grisolia, M.F., Oliveira, E.P., 2012. Sediment provenance in the Palaeoproterozoic Rio Itapicuru greenstone belt, Brazil, indicates deposition on arc settings with a hidden 2.17-2.25 Ga substrate. *Journal of South American Earth Sciences* 38, 89-109.
- Heilbron, M., Duarte, B.P., Valeriano, C.M., Simonetti, A., Machado, N., Nogueira, J.R., 2010. Evolution of reworked Paleoproterozoic basement rocks within the Ribeira belt (Neoproterozoic), SE-Brazil, based on U–Pb geochronology: Implications for paleogeographic reconstructions of the São Francisco-Congo paleocontinent. *Precambrian Research* 178, 136-148.
- Hurley, P.M., Melcher, G.C., Pinson, W.H., Fairbairn, H.W., 1968. Some orogenic episodes in South America by K-Ar and whole-rock Rb-Sr dating. *Canadian Journal of Earth Sciences* 5, 633-638.

- Jackson, S.E., Pearson, N.J., Griffin, W.L., Belousova, E.A., 2004. The application of laser ablation-inductively coupled plasma-mass spectrometry to in situ U-Pb zircon geochronology. *Chemical Geology* 211, 47–69.
- Jost, H., Fuck, R., Brod, J.A., Dantas, E.L., Meneses, P.R., Assad, M.L.P., Pimentel, M.M., Blum, M.L.B., Silva, A.M., Spigolon, A.L.D., Maas, M.V.R., Souza, M.M., Fernandez, B.P., Faulstich, F.R.L., Macedo Jr., P.M.M., Schobbenhaus, C.N., Almeida, L., Silva, A.A.C., Anjos, C.W.D., Santos, A.P.M.R., Bubenick, A.N., Teixeira, A.A., Lima, B.E.M., Campos, M.O., Barjud, R.M., Carvalho, D.R., Scislewski, L.R., Lucianisarli C., Oliveira, D.P.L., 2001. Geologia dos terrenos arqueanos e proterozóicos da região de Crixás-Cedrolina, Goiás. *Revista Brasileira de Geociências* 31, 315-328.
- Jost, H., Chemale, F., Dussin, I.A., Tassinari, C.C.G., Martins, R., 2010. A U-Pb zircon Paleoproterozoic age for the metasedimentary host rocks and gold mineralization of the Crixás greenstone belt, Goiás, central Brazil. *Ore Geology Reviews*, 37:127-139.
- Jost, H., Rodrigues, V.G., Carvalho, M.J., Chemale, F., Marques, J.C., 2012. Estratigrafia e geocronologia do greenstone belt de Guarinos, Goiás. *Geologia USP Série Científica* 12, 31-48.
- Jost, H., Chemale Jr., F., Fuck, R.A., Dussin, I.A., 2013. Uvá Complex, the oldest orthogneiss of the Archean-Paleoproterozoic terrane of central Brazil. *Journal of South American Earth Sciences* 47, 201-212.
- Kitajima, L.F.W., Ruiz, J., Gehrels, G., Gaspar, J.C., 2001. Uranium-Lead ages of zircon megacrysts and zircon included in corundum from Peixe Alkaline Complex (Brazil). In: III Simposio Sudamericano de Geología Isotópica, 2001, Pucón.
- Kuyumjian, R.M., Cruz, E.L.C.C., Araújo Filho, J.O., Moura, M.A., Guimarães, E.M., Pereira, K.M.S., 2012. Geologia e ocorrências de ouro do terreno granito-greenstone do Tocantins, TO: síntese do conhecimento e parâmetros para a exploração mineral. *Revista Brasileira de Geociências* 42, 213-228.
- Lenharo, S.L.R., Moura, M.A., Botelho, N.F., 2002. Petrogenetic and mineralization processes in Paleo- to Mesoproterozoic rapakivi granites: examples from Pitinga and Goiás, Brazil. *Precambrian Research* 119, 277-299.

- Ludwig, K.R., 1993. PBDAT. A computer program for processing Pb–U–Th isotope data. USGS Open File Report, 88-542, pp. 34.
- Ludwig, K.R., 2003, User's Manual for Isoplot/Ex v. 3.00. A Geochronological Toolkit for Microsoft Excel. BGC Special Publication 4, Berkeley, 71 pp.
- Marangoni, Y.R., Assumpção, M., Fernandes, E.P., 1995. Gravimetria em Goiás, Brasil. Revista Brasileira de Geofísica 13 (3), 205–219.
- Marini, O.J., Botelho, N.F., Rossi, P., 1992. Elementos terras raras em granitóides da Província Estanífera de Goiás. Revista Brasileira de Geociências 22, 61-72.
- Marini, O. J., Fuck, R. A., Dardenne, M. A., Danni, J. C. M. 1984. Província Tocantins: setores Central e Sudeste. In: Almeida, F. F. M., Hasui, Y. (coords.). O Pré-cambriano do Brasil. São Paulo, E. Blücher, 205-264.
- Marques, G.C., 2010. Geologia dos grupos Araí e Serra da Mesa e seu embasamento no sul do Tocantins. Unpublished MSc thesis, Universidade de Brasília, 122 pp.
- Martins-Neto, M.A., 2009. Sequence stratigraphic framework of Proterozoic successions in eastern Brazil. Marine and Petroleum Geology 26, 163-176.
- Matteini, M., Junges, S.S., Dantas, E.L., Pimentel, M.M., Bühn, B., 2010. In situ zircon U–Pb and Lu–Hf isotope systematic on magmatic rocks: Insights on the crustal evolution of the Neoproterozoic Goiás Magmatic Arc, Brasília belt, Central Brazil. Gondwana Research 17, 1-12.
- Meert, J.G., 2012. What's in a name? The Columbia (Paleopangea/Nuna) supercontinent. Gondwana Research 21, 987-993.
- Moraes, R., Fuck, R.A., Pimentel, M.M., Gioia, S.M.C.L., Figueiredo, A.M.G., 2003. Geochemistry and Sm-Nd isotopic characteristics of bimodal volcanic rocks of Juscelândia, Goiás, Brazil: Mesoproterozoic transition from continental rift to ocean basin. Precambrian Research 125, 317-336.
- Moraes, R., Fuck, A.R., Pimentel, M.M., Gioia, S.M.C.L., Hollanda, M.H.B.M., Armstrong, R., 2006. The bimodal rift-related volcanosedimentary sequence in Central Brazil: Mesoproterozoic extention and Neoproterozoic metamorphism. Journal of South American Earth Sciences 20, 287–301

- Morel, M.L.A., Nebel, O., Nebel-Jacobsen, Y.L., Miller, J.S., Vroon, P.Z., 2008. Hafnium isotope characterization of the GJ-1 zircon reference material by solution and laserablation MC-ICPMS. *Chemical Geology* 255, 231–235.
- Nebel, O., Nebel-Jacobsen, Y., Mezger, K., Berndt, J., 2007. Initial Hf isotope compositions in magmatic zircon from early Proterozoic rocks from the Gawler Craton, Australia: a test for zircon model ages. *Chemical Geology* 241, 23–37.
- Noce, C.M., Pedrosa-Soares, A.C., Silva, L.C., Armstrong, R., Piuzana, D., 2007. Evolution of polycyclic basement complexes in the Araçuaí Orogen, based on U–Pb SHRIMP data: Implications for Brazil–Africa links in Paleoproterozoic time. *Precambrian Research* 159, 60-78.
- Oliveira, C.G., Oliveira, F.B., Dantas, E.L., Fuck, R.A., 2006. Programa Geologia do Brasil – Folha Campinorte. FUB/CPRM, Brasília, 124.
- Oliveira, E.P., Souza, Z.S., McNaughton, N.J., Lafon, N.J., Costa, F.G., Figueiredo, A.M., 2011. The Rio Capim volcanic–plutonic–sedimentary belt, São Francisco Craton, Brazil: Geological, geochemical and isotopic evidence for oceanic arc accretion during Palaeoproterozoic continental collision. *Gondwana Research* 19, 735-750.
- Patchett, P.J., 1983. Importance of the Lu–Hf isotopic system in studies of planetary chronology and chemical evolution. *Geochimica and Cosmochimica Acta* 47, 81.
- Pereira, R.S., 2007. Cráton do São Francisco, kimberlitos e diamantes. University of Brasília, Unpublished PhD thesis, 200 p.
- Pereira, R.S., Fuck, R.A., 2005. Archean Nucleii and the distribution of kimberlite and related rocks in the São Francisco Craton, Brazil. *Revista Brasileira de Geociências* 35, 93-104.
- Perosi, F.A., 2006. Estrutura crustal do setor central da Província Tocantins utilizando ondas P, S e fases refletidas com dados de refração de sísmica profunda. Unpublished PhD thesis, Universidade de São Paulo, 162 p.
- Pietranik, A.B., Hawkesworth, C.J., Storey, C.D., Kemp, A.I.S., Sircombe, K.N., Whitehouse, M.J., Bleeker, W., 2008. Episodic, mafic crust formation from 4.5 to 2.8 Ga: New evidence from detrital zircons, Slave craton, Canada. *Geology* 36, 875-878.

- Pimentel, M.M., Botelho, N.F., 2001. Sr and Nd isotopic characteristics of 1.77-1.58 Ga rift-related granites and volcanics of the Goiás tin province, Central Brazil. *Anais da Academia Brasileira de Ciências* 73, 263-276.
- Pimentel, M.M., Fuck, R.A., 1992. Neoproterozoic crustal accretion in central Brazil. *Geology* 20, 375-379.
- Pimentel, M.M., Fuck, R.A., 1994. Geocronologia Rb-Sr da porção sudoeste do Maciço de Goiás. *Revista Brasileira de Geociências* 24, 104-111.
- Pimentel, M.M., Heaman, L., Fuck, R.A., Marini, O.J., 1991. U-Pb zircon geochronology of Precambrian tin-bearing continental-type acid magmatism in central Brazil. *Precambrian Research* 52, 321-335.
- Pimentel, M.M., Fuck, R.A., Silva, J.L.H., 1996. Dados Rb-Sr e Sm-Nd da região de Jussara- Goiás-Mossâmedes (GO), e o limite entre terrenos antigos do Maciço de Goiás e o Arco Magmático de Goiás. *Revista Brasileira de Geociências* 26, 61–70.
- Pimentel, M.M., Fuck, R.A., Botelho, N.F., 1999. Granites and the geodynamic history of the Neoproterozoic Brasília belt, Central Brazil: a review. *Lithos* 46, 463–483.
- Pimentel, M.M., Fuck, R.A., Ferreira Filho, C.F., Araújo, S.M., 2000. The basement of the Brasília Belt and the Goiás Magmatic Arc. In: Cordani, U.G., Milani, E.J., Thomaz Filho, A., Campos, D.A. (eds) *Tectonic Evolution of South America*. 31st International Geological Congress, Rio de Janeiro, 195–229.
- Pimentel, M.M., Dantas, E.L., Fuck, R.A., Armstrong, R.A., 2003. Shrimp and conventional U-Pb age, Sm-Nd isotopic characteristics and tectonic significance of the K-rich Itapuranga suite in Goiás, Central Brazil. *Anais da Academia Brasileira de Ciências* 75, 97-108.
- Pimentel, M.M., Ferreira Filho, C.F., Armstrong, R.A., 2004. SHRIMP U-Pb and Sm-Nd ages of the Niquelândia layered complex: Meso- (1.25 Ga) and Neoproterozoic (0.79 Ga) extentional events in central Brazil. *Precambrian Research* 132, 133-153.
- Pimentel, M.M., Ferreira Filho, C.F., Armele, A., 2006. Neoproterozoic age of the Niquelândia Complex, central Brazil: Further ID-TIMS U-Pb and Sm-Nd isotopic evidence. *Journal of South American Earth Sciences* 21, 228-238.

- Pimentel, M.M., Rodrigues, J.B., Giustina, M. E. S., Junges, S., Matteini, M., Armstrong, R., 2011. The tectonic evolution of the Neoproterozoic Brasília Belt, central Brazil, based on SHRIMP and LA-ICPMS U-Pb sedimentary provenance data: A review. *Journal of South American Earth Sciences* 31, 345-357.
- Queiroz, C.L., McNaughton, N.J., Fletcher, R., Jost, H., Barley, M.E., 2000. Polymetamorphic history of the Crixás-Açu Gneiss, Central Brazil: SHRIMP U-Pb evidence from titanite and zircon. *Revista Brasileira de Geociências* 30, 40-44.
- Queiroz, C.L., Jost, H., Silva, L.C., McNaughton, N.J., 2008. U-Pb SHRIMP and Sm-Nd geochronology of granite-gneiss complexes and implications for the evolution of the Central Brazil Archean Terrain. *Journal of South American Earth Sciences* 26, 100-124.
- Reddy, S.M., Evans, D.A.D., 2009. Paleoproterozoic supercontinents and global evolution: correlations from core to atmosphere. *Geological Society, London, Special Publications* 323, 1-26.
- Ribeiro, A., Teixeira, W., Dussin, I.A., Ávila, C.A., Nascimento, D., 2013. U-Pb LA-ICP-MS detrital zircon ages of the São João del Rei and Carandaí basins: New evidence of intermittent Proterozoic rifting in the São Francisco paleocontinent. *Gondwana Research* 24, 713-726.
- Rogers, J.J.W., 1996. A history of continents in the past three billion years. *Journal of Geology* 104, 91-107.
- Rosa-Costa, L.T., Lafon, J.M., Delor, C., 2006. Zircon geochronology and Sm-Nd isotopic study: Further constraints for the Archean and Paleoproterozoic geodynamical evolution of the southeastern Guiana Shield, north of Amazonian Craton, Brazil *Gondwana Research* 10, 277-300.
- Saboya, A.M., 2009. O vulcanismo em Monte do Carmo e litoestratigrafia do Grupo Natividade, Estado do Tocantins. University of Brasília, Unpublished MSc thesis, 96 pp.
- Sacks, P.E., Secor, D.T.Jr., 1990. Delamination in collisional orogens. *Geology* 18, 999-1002.

- D'el-Rey Silva, J.H., Vasconcelos, M.A.R., Silva, D.V.G., 2008. Timing and role of the Maranhão River Thrust in the evolution of the Neoproterozoic Brasília Belt and Tocantins Province, central Brazil. *Gondwana Research* 13, 352-374.
- Soares, J.E., Berrocal, J., Fuck, R.A., Mooney, W.D., Ventura, D.B.R., 2006. Seismic characteristics of central Brazil crust and upper mantle: a deep seismic refraction study. *Journal of Geophysical Research*. doi:10.1029/2005JB003769 III-B12302.
- Söderlund, U., Patchett, P.J., Vervoort, J.D., Isachsen, C.E., 2004. The ^{176}Lu decay constant determined by Lu-Hf and U-Pb isotope systematics of Precambrian mafic intrusions. *Earth and Planetary Science Letters* 219, 311-324.
- Stacey, J.S., Kramers, J.D., 1975. Approximation of terrestrial lead isotope evolution by a two-stage model. *Earth and Planetary Science Letters* 26, 207–221.
- Taylor, S.R., McLennan, S.M., 1985. *The Continental Crust: its Composition and Evolution*. Blackwell, Oxford. 312 pp.
- Valeriano, C.M., Pimentel, M.M., Heilbron, M., Almeida, J.C.H., Trouw, R.A.J., 2008. Tectonic evolution of the Brasília Belt, Central Brazil, and early assembly of Gondwana. *Geological Society, London, Special Publication* 294, 197-210.
- Ventura, D.B.R., Soares, J.E.P., Fuck, R.A., Caridade, L.C.C., 2011. Caracterização sísmica e gravimétrica da litosfera sob a linha de refração sísmica profunda de Porangatu, Província Tocantins, Brasil Central. *Revista Brasileira de Geociências* 41, 130-140.
- Viana, M.G., Pimentel, M.M., Whitehouse, M.J., Fuck, R.A., Machado, N., 1995. O Arco Magmático de Mara Rosa, Goiás: Geoquímica e geocronologia e suas implicações regionais. *Revista Brasileira de Geociências* 25, 111-123.
- Zhao, G., Cawood, P.A., Wilde, S.A., Sun, M., 2002. Review of global 2.1–1.8 Ga orogens: implications for a pre-Rodinia supercontinent. *Earth-Science Reviews* 59, 125-162.

Table 1 - Summary of in situ Lu-Hf analyses.

Sample	Spot	Rock	U-Pb Age (Ma)	$\pm 2\sigma$	$^{176}\text{Hf}/^{177}\text{Hf}$ (i)	$\pm 2\sigma$	$^{176}\text{Lu}/^{177}\text{Hf}$	$\pm 2\sigma$	$^{176}\text{Hf}/^{177}\text{Hf}$ (t)	$\epsilon\text{Hf(t)}$	$\pm 2\sigma$	TDM Ga
PP012	003-Z5	metagranodiorite	2169	9	0.2813654	0.0000289	0.0006934	0.0000238	0.2813367	-2.12	0.08	2.59
	004-Z17		2198	13	0.2815568	0.0000356	0.0008661	0.0000387	0.2815206	5.08	0.26	2.34
	005-Z40		2227	10	0.2813747	0.0000578	0.0013668	0.0001294	0.2813167	-1.49	0.15	2.62
	006-Z42		2145	24	0.2814680	0.0000403	0.0010832	0.0000242	0.2814238	0.42	0.01	2.47
	007-Z54		2156	14	0.2814988	0.0000430	0.0013868	0.0001140	0.2814418	1.31	0.12	2.45
	008-Z56		2165	9	0.2813926	0.0000490	0.0007983	0.0000815	0.2813597	-1.40	0.15	2.56
	009-Z59		2194	9	0.2813314	0.0000919	0.0010567	0.0000678	0.2812872	-3.30	0.23	2.66
	010-Z61		2200	11	0.2815531	0.0000467	0.0007432	0.0000094	0.2815220	5.18	0.09	2.34
PP016	003-Z4	garnet-muscovite gneiss	2083	14	0.2814714	0.0000299	0.0007835	0.0000600	0.2814403	-0.43	0.04	2.45
	004-Z5		2079	9	0.2815021	0.0000343	0.0005935	0.0000097	0.2814786	0.83	0.02	2.40
	005-Z9		2100	7	0.2814782	0.0000395	0.0007978	0.0000389	0.2814463	0.17	0.01	2.44
	006-Z15		2101	16	0.2815208	0.0000616	0.0008490	0.0000224	0.2814869	1.64	0.06	2.39
	007-Z16		2065	8	0.2815082	0.0000553	0.0007085	0.0000346	0.2814804	0.57	0.03	2.39
	008-Z17		2097	9	0.2814543	0.0000613	0.0008599	0.0000244	0.2814200	-0.83	0.03	2.48
	009-Z18		2074	14	0.2814290	0.0000602	0.0006622	0.0000369	0.2814029	-1.97	0.12	2.50
	010-Z23		2079	10	0.2813805	0.0000658	0.0004802	0.0000640	0.2813615	-3.33	0.46	2.55
PP018	003-Z2	muscovite-gneiss	2169	10	0.2814382	0.0000412	0.0018711	0.0000778	0.2813609	-1.26	0.06	2.57
	004-Z3		2082	354	0.2813143	0.0000420	0.0010840	0.0000192	0.2812713	-6.46	1.21	2.68
	005-Z6		2160	9	0.2812887	0.0000461	0.0011910	0.0000725	0.2812397	-5.78	0.38	2.72
	006-Z12		2167	15	0.2814068	0.0000445	0.0014855	0.0001195	0.2813455	-1.86	0.16	2.58
	007-Z21		2120	13	0.2813185	0.0000346	0.0007699	0.0000508	0.2812875	-5.01	0.36	2.65
	008-Z23		2177	19	0.2812952	0.0000374	0.0008703	0.0001642	0.2812591	-4.70	0.93	2.69
	009-Z38		2162	11	0.2815078	0.0000560	0.0011209	0.0001666	0.2814616	2.15	0.33	2.42
	010-Z57		2126	12	0.2813006	0.0000362	0.0010719	0.0000713	0.2812572	-5.94	0.43	2.70
PP021	003-Z7	quartz-diorite	2112	14	0.2815298	0.0000420	0.0009553	0.0000779	0.2814914	2.05	0.18	2.38
	004-Z19		2132	27	0.2813533	0.0000423	0.0012695	0.0000198	0.2813018	-4.22	0.12	2.64
	005-Z14		2093	11	0.2815800	0.0000688	0.0010975	0.0000282	0.2815363	3.21	0.10	2.32
	006-Z37		2116	12	0.2815461	0.0000446	0.0005294	0.0000039	0.2815248	3.33	0.04	2.33
	007-Z38		2100	18	0.2815081	0.0000541	0.0008089	0.0000536	0.2814757	1.22	0.09	2.40
	008-Z44		2117	8	0.2815089	0.0000481	0.0007940	0.0000569	0.2814769	1.65	0.12	2.40
	009-Z50		2096	26	0.2814949	0.0000702	0.0005339	0.0000038	0.2814736	1.05	0.02	2.40
	010-Z51		2098	13	0.2815344	0.0000598	0.0008960	0.0000315	0.2814986	1.98	0.08	2.37

Table 1 - continuation

Sample	Spot	Rock	U-Pb Age (Ma)	$\pm 2\sigma$	$^{176}\text{Hf}/^{177}\text{Hf}$ (i)	$\pm 2\sigma$	$^{176}\text{Lu}/^{177}\text{Hf}$	$\pm 2\sigma$	$^{176}\text{Hf}/^{177}\text{Hf}$ (t)	$\epsilon\text{Hf(t)}$	$\pm 2\sigma$	TDM Ga
PP024	003-Z3	augen gneiss	2134	9	0.2815748	0.0000493	0.0010838	0.0000373	0.2815307	3.96	0.15	2.33
	004-Z6		2087	10	0.2816001	0.0000689	0.0010802	0.0000327	0.2815572	3.81	0.13	2.29
	005-Z12		2140	12	0.2815503	0.0000445	0.0012204	0.0000244	0.2815005	3.03	0.08	2.37
	006-Z13		2117	11	0.2815610	0.0000455	0.0009060	0.0000081	0.2815245	3.34	0.05	2.34
	007-Z33		2133	7	0.2815414	0.0000403	0.0014861	0.0002037	0.2814810	2.17	0.30	2.40
	008-Z34		2033	14	0.2815959	0.0000480	0.0015892	0.0001051	0.2815344	1.75	0.13	2.33
	009-Z38		2195	8	0.2814705	0.0000653	0.0018476	0.0002566	0.2813932	0.49	0.07	2.52
	010-Z51		1999	9	0.2814736	0.0000360	0.0008827	0.0000072	0.2814401	-2.39	0.03	2.45
PP027	003-Z1	metagranodiorite	2123	12	0.2815502	0.0000549	0.0007959	0.0000472	0.2815180	3.25	0.21	2.34
	004-Z6		2225	10	0.2815840	0.0000677	0.0009411	0.0000183	0.2815440	6.55	0.16	2.31
	005-Z17		2124	11	0.2814495	0.0000574	0.0000693	0.0000007	0.2814467	0.74	0.01	2.43
	006-Z23		2162	17	0.2815096	0.0000760	0.0010574	0.0000276	0.2814661	2.31	0.08	2.41
	007-Z28		2137	15	0.2813959	0.0000497	0.0004690	0.0000105	0.2813768	-1.44	0.04	2.53
	008-Z36		2113	30	0.2814826	0.0000714	0.0006285	0.0000150	0.2814573	0.86	0.03	2.42
	009-Z37		2132	12	0.2814519	0.0000869	0.0008514	0.0000424	0.2814173	-0.12	0.01	2.48
	010-Z40		2000	11	0.2814501	0.0000628	0.0007066	0.0000238	0.2814232	-2.96	0.12	2.47

Table 2 - Summary of in situ U-Pb analyses.

Sample	Isotopic ratios								Apparent ages							
	f(206) %	Th/U	$^{206}\text{Pb}/^{204}\text{Pb}$	$^{207}\text{Pb}/^{206}\text{Pb}$	1s (%)	$^{207}\text{Pb}/^{235}\text{U}$	1s (%)	$^{206}\text{Pb}/^{238}\text{U}$	1s (%)	$^{207}\text{Pb}/^{206}\text{Pb}$	2 σ	$^{207}\text{Pb}/^{235}\text{U}$	2 σ	$^{206}\text{Pb}/^{238}\text{U}$	2 σ	Conc (%)
Garnet-muscovite gneiss PP016																
PP016-Z1	0.00	0.12	507479	0.12875	0.4	7.1721	0.7	0.4040	0.5	2080.9	7.5	2133.0	5.8	2187.6	9.2	105
PP016-Z2	0.05	0.31	31128	0.12579	0.4	6.5706	0.6	0.3789	0.5	2039.9	6.8	2055.4	5.5	2070.9	8.7	102
PP016-Z3	0.00	0.17	496088	0.12937	0.7	7.1929	0.8	0.4032	0.5	2089.5	12.1	2135.6	7.4	2183.9	8.6	105
PP016-Z4	0.01	0.22	186113	0.12886	0.8	7.0403	1.0	0.3962	0.6	2082.5	14.3	2116.5	8.9	2151.7	10.5	103
PP016-Z5	0.01	0.22	216214	0.12858	0.5	6.8771	0.7	0.3879	0.5	2078.7	8.6	2095.7	6.3	2113.1	9.3	102
PP016-Z6	0.00	0.42	335327	0.12991	0.5	7.1798	0.7	0.4008	0.5	2096.7	7.9	2134.0	6.0	2172.9	9.2	104
PP016-Z7	0.01	0.34	176199	0.12805	0.7	7.4502	1.0	0.4220	0.7	2071.4	12.2	2167.0	9.0	2269.4	14.0	110
PP016-Z8	0.01	0.64	120995	0.12884	0.6	7.9625	0.8	0.4482	0.6	2082.1	9.8	2226.8	7.6	2387.4	12.6	115
PP016-Z9	0.00	0.21	349175	0.13014	0.4	7.1076	0.6	0.3961	0.5	2099.8	6.7	2125.0	5.7	2151.1	9.3	102
PP016-Z10	0.01	0.38	209415	0.12748	0.7	7.1758	0.9	0.4083	0.6	2063.5	12.8	2133.5	8.3	2207.0	11.1	107
PP016-Z11	0.03	0.43	53317	0.13083	0.8	7.3477	1.0	0.4073	0.6	2109.2	14.7	2154.6	9.0	2202.6	10.4	104
PP016-Z12	0.01	0.54	276877	0.13014	0.7	7.2990	0.9	0.4068	0.6	2099.8	12.1	2148.7	7.9	2200.2	10.3	105
PP016-Z13	0.00	0.49	467575	0.13044	0.5	7.2531	0.9	0.4033	0.7	2103.9	9.3	2143.1	8.0	2184.1	13.3	104
PP016-Z14	0.01	0.38	270033	0.12793	0.5	7.0214	0.7	0.3981	0.5	2069.7	8.7	2114.1	6.4	2160.2	9.5	104
PP016-Z15	0.01	0.64	169689	0.13020	0.9	7.1607	1.1	0.3989	0.6	2100.7	16.4	2131.6	9.9	2163.8	11.2	103
PP016-Z16	0.00	0.22	362413	0.12761	0.4	6.8986	0.6	0.3921	0.4	2065.3	7.6	2098.5	5.5	2132.5	8.1	103
PP016-Z17	0.01	0.53	250440	0.12994	0.5	7.1487	0.7	0.3990	0.5	2097.2	8.7	2130.1	6.5	2164.4	9.7	103
PP016-Z18	0.01	0.23	219027	0.12825	0.8	6.7993	1.0	0.3845	0.5	2074.1	14.1	2085.6	8.6	2097.4	9.8	101
PP016-Z19	0.00	0.29	594613	0.12707	0.5	6.8928	0.9	0.3934	0.8	2057.8	8.8	2097.7	8.3	2138.7	14.3	104
PP016-Z20	0.00	0.27	348148	0.12855	0.4	6.4526	0.7	0.3640	0.6	2078.3	7.7	2039.5	6.3	2001.3	9.8	96
PP016-Z21	0.01	0.63	147909	0.12898	0.5	7.2401	0.7	0.4071	0.6	2084.1	8.2	2141.5	6.6	2201.8	10.6	106
PP016-Z22	0.00	0.29	1615475	0.12850	0.7	7.1476	0.9	0.4034	0.6	2077.6	13.2	2130.0	8.3	2184.7	10.3	105
PP016-Z23	0.01	0.49	232041	0.12861	0.6	7.0229	0.9	0.3961	0.7	2079.0	9.7	2114.3	8.1	2150.9	13.3	103
PP016-Z24	0.03	80.12	54922	0.12650	0.4	5.5445	0.7	0.3179	0.6	2049.9	7.6	1907.5	6.3	1779.4	9.2	87
PP016-Z25	0.01	0.31	152403	0.13031	0.4	7.3995	0.7	0.4118	0.5	2102.2	7.8	2160.9	6.2	2223.3	10.0	106
PP016-Z26	0.01	0.61	154866	0.12940	1.1	7.2233	1.3	0.4049	0.7	2089.8	19.6	2139.4	11.5	2191.4	12.2	105
PP016-Z27	0.00	0.33	333639	0.12414	0.4	6.5046	0.7	0.3800	0.6	2016.6	7.9	2046.5	6.5	2076.3	10.4	103
PP016-Z28	0.01	0.69	245543	0.12890	1.1	7.5531	1.3	0.4250	0.7	2083.1	18.7	2179.3	11.6	2283.0	14.1	110
PP016-Z29	0.00	0.40	526622	0.12972	0.4	7.2925	0.6	0.4077	0.5	2094.2	6.8	2147.9	5.6	2204.5	9.2	105
PP016-Z30	0.00	0.19	380317	0.12962	0.5	7.2820	0.7	0.4075	0.5	2092.8	9.3	2146.6	6.4	2203.3	8.9	105

Table 2 - continuation

Sample	Isotopic ratios									Apparent ages								
	f(206) %	Th/U	$^{206}\text{Pb}/^{204}\text{Pb}$	$^{207}\text{Pb}/^{206}\text{Pb}$	1s (%)	$^{207}\text{Pb}/^{235}\text{U}$	1s (%)	$^{206}\text{Pb}/^{238}\text{U}$	1s (%)	$^{207}\text{Pb}/^{206}\text{Pb}$	2 σ	$^{207}\text{Pb}/^{235}\text{U}$	2 σ	$^{206}\text{Pb}/^{238}\text{U}$	2 σ	Conc (%)		
Garnet-muscovite gneiss PP016																		
Muscovite-gneiss PP018																		
PP018-Z02	0.13	0.25	11501	0.13406	0.6	6.9822	0.9	0.3778	0.7	2151.8	10.3	2109.2	8.3	2065.8	12.8	96		
PP018-Z04	0.25	0.26	6459	0.13067	0.8	5.1809	2.1	0.2876	2.0	2106.9	13.3	1849.5	17.9	1629.4	28.5	77		
PP018-Z06	0.04	0.21	36214	0.13423	0.5	6.8574	0.8	0.3705	0.6	2154.0	8.7	2093.2	7.1	2031.9	10.9	94		
PP018-Z08	0.33	0.15	4794	0.12335	0.9	4.7317	2.8	0.2782	2.7	2005.2	15.3	1772.9	23.3	1582.4	37.4	79		
PP018-Z10	0.00	0.18	1711032	0.12469	0.6	5.2025	1.0	0.3026	0.7	2024.5	10.8	1853.0	8.1	1704.2	10.9	84		
PP018-Z12	0.05	0.21	31309	0.13470	0.8	6.9769	3.1	0.3757	3.0	2160.1	14.6	2108.5	27.4	2055.9	52.8	95		
PP018-Z21	0.04	0.05	37869	0.13119	0.8	6.3124	1.3	0.3490	1.1	2113.9	13.4	2020.2	11.4	1929.7	17.7	91		
PP018-Z23	0.01	0.29	123767	0.13592	1.1	7.6674	1.3	0.4091	0.7	2175.8	18.9	2192.8	11.4	2211.0	12.4	102		
PP018-Z26	0.26	0.18	5979	0.12807	0.5	5.6085	3.2	0.3176	3.1	2071.6	8.9	1917.4	27.1	1778.1	48.6	86		
PP018-Z27	0.18	0.10	8546	0.12338	2.2	5.2356	3.3	0.3078	2.4	2005.6	38.9	1858.4	27.6	1729.7	36.4	86		
PP018-Z28	0.16	0.03	9554	0.12822	0.5	5.9458	1.4	0.3363	1.4	2073.7	8.8	1968.0	12.5	1869.0	22.0	90		
PP018-Z38	0.01	0.21	108637	0.13471	0.6	7.1241	1.5	0.3836	1.3	2160.3	10.6	2127.1	13.0	2092.8	23.8	97		
PP018-Z53	0.21	0.12	7258	0.13726	0.5	6.3558	1.1	0.3358	1.0	2192.9	9.2	2026.2	9.9	1866.6	16.3	85		
PP018-Z56	0.06	0.21	24645	0.13905	0.6	6.5049	1.3	0.3393	1.2	2215.5	10.4	2046.6	11.6	1883.2	19.2	85		
PP018-Z57	0.11	0.15	13087	0.13088	0.7	7.0268	1.1	0.3894	0.8	2109.8	12.0	2114.8	9.4	2120.0	14.6	100		
PP018-Z60	0.30	0.22	5137	0.13728	0.6	6.5756	1.9	0.3474	1.8	2193.2	10.3	2056.1	17.0	1922.1	30.7	88		
Quartz-diorite PP021																		
PP021-Z01	0.02	0.22	96598	0.13021	2.0	7.2997	2.4	0.4066	1.4	2100.9	35.2	2148.8	21.6	2199.2	25.3	105		
PP021-Z02	0.01	0.22	245975	0.12998	0.5	7.0257	0.8	0.3920	0.7	2097.7	8.5	2114.7	7.4	2132.2	12.2	102		
PP021-Z03	0.01	0.21	164405	0.13091	0.6	6.9114	1.0	0.3829	0.8	2110.2	10.0	2100.1	8.5	2089.9	13.8	99		
PP021-Z04	0.00	0.27	360044	0.13092	1.1	7.2565	1.5	0.4020	0.9	2110.4	20.1	2143.5	13.1	2178.2	16.9	103		
PP021-Z05	0.01	0.27	234137	0.13172	0.9	7.1581	1.1	0.3941	0.6	2121.1	15.6	2131.3	9.8	2141.9	11.8	101		
PP021-Z14	0.00	0.24	327187	0.12960	0.6	6.9016	0.9	0.3862	0.7	2092.6	11.0	2098.9	8.3	2105.3	12.4	101		
PP021-Z16	0.00	0.18	308417	0.13095	0.7	7.1389	0.9	0.3954	0.6	2110.8	11.7	2128.9	8.0	2147.8	10.9	102		
PP021-Z17	0.01	0.19	260573	0.13134	0.8	7.1414	1.0	0.3944	0.7	2115.9	13.2	2129.2	9.1	2143.0	12.7	101		
PP021-Z18	0.01	0.23	258656	0.13117	0.9	7.1301	1.0	0.3942	0.6	2113.7	15.0	2127.8	9.2	2142.5	10.5	101		
PP021-Z19	0.01	0.16	110062	0.13251	1.5	7.1809	1.7	0.3930	0.7	2131.5	26.9	2134.1	14.9	2136.8	12.2	100		
PP021-Z20	0.00	0.19	342130	0.13088	1.0	7.1699	1.1	0.3973	0.6	2109.9	17.0	2132.8	10.2	2156.6	11.3	102		
PP021-Z21	0.00	0.19	1046560	0.13028	1.0	7.0009	1.2	0.3897	0.7	2101.7	17.3	2111.5	10.7	2121.7	12.5	101		
PP021-Z22	0.02	0.18	89122	0.13157	0.9	7.2101	1.2	0.3975	0.9	2119.0	15.2	2137.7	11.0	2157.3	16.2	102		
PP021-Z23	0.01	0.24	137329	0.12910	1.6	6.4499	2.3	0.3623	1.6	2085.8	28.3	2039.1	19.7	1993.3	26.8	96		
PP021-Z29	0.00	0.19	433772	0.13126	1.1	7.0856	1.2	0.3915	0.6	2114.9	18.4	2122.2	10.6	2129.8	10.2	101		
PP021-Z30	0.00	0.17	391375	0.12735	1.0	6.5509	1.5	0.3731	1.1	2061.6	17.6	2052.8	13.2	2043.9	19.6	99		

Table 2 - continuation

Sample	Isotopic ratios								Apparent ages							
	f(206) %	Th/U	$^{206}\text{Pb}/^{204}\text{Pb}$	$^{207}\text{Pb}/^{206}\text{Pb}$	1s (%)	$^{207}\text{Pb}/^{235}\text{U}$	1s (%)	$^{206}\text{Pb}/^{238}\text{U}$	1s (%)	$^{207}\text{Pb}/^{206}\text{Pb}$	2σ	$^{207}\text{Pb}/^{235}\text{U}$	2σ	$^{206}\text{Pb}/^{238}\text{U}$	2σ	Conc (%)
Augen-gneiss PP024																
PP024-Z03	0.11	0.22	13476	0.13147	0.5	7.0852	0.8	0.3909	0.6	2117.6	9.3	2122.2	7.1	2126.9	10.7	100
PP024-Z05	0.59	0.20	2516	0.13554	0.6	7.3696	0.8	0.3944	0.5	2170.9	11.0	2157.3	7.3	2143.0	9.2	99
PP024-Z06	0.26	0.22	5905	0.12649	0.5	6.0061	1.2	0.3444	1.1	2049.8	9.6	1976.7	10.7	1907.7	18.4	93
PP024-Z08	0.08	0.22	19236	0.13518	0.8	7.1859	1.0	0.3855	0.7	2166.3	13.2	2134.7	9.1	2102.1	12.2	97
PP024-Z09	0.74	0.21	2164	0.12521	1.6	4.7891	1.9	0.2774	1.1	2031.7	28.0	1783.0	16.0	1578.3	14.8	78
PP024-Z21	2.22	0.10	767	0.09202	0.8	2.1688	3.4	0.1709	3.2	1467.9	16.0	1171.1	23.5	1017.3	31.1	69
PP024-Z23	0.83	0.12	1909	0.12407	1.0	4.8964	2.8	0.2862	2.6	2015.5	18.1	1801.6	23.5	1622.7	37.5	81
PP024-Z27	0.16	0.15	9202	0.13155	1.5	6.6015	1.6	0.3640	0.6	2118.8	25.6	2059.6	14.1	2000.9	11.2	94
PP024-Z33	0.14	0.25	10857	0.13266	0.4	7.1864	0.7	0.3929	0.6	2133.5	7.5	2134.8	6.5	2136.2	10.8	100
PP024-Z36	0.14	0.18	10678	0.13528	0.7	6.8124	0.9	0.3652	0.6	2167.6	12.6	2087.3	8.1	2006.9	9.7	93
PP024-Z38	0.38	0.24	3942	0.13321	0.5	6.9679	1.0	0.3794	0.8	2140.8	7.9	2107.3	8.5	2073.3	15.0	97
PP024-Z42	0.78	0.21	2077	0.10753	1.4	3.8724	1.8	0.2612	1.0	1758.0	25.5	1608.0	14.1	1495.9	14.1	85
PP024-Z45	0.45	0.21	3286	0.13190	0.8	7.2259	1.0	0.3973	0.6	2123.5	13.4	2139.7	8.7	2156.7	11.0	102
PP024-Z46	2.96	0.13	508	0.12506	0.9	6.2667	1.2	0.3634	0.7	2029.6	16.4	2013.8	10.2	1998.5	12.0	98
PP024-Z47	0.63	0.15	2352	0.13832	2.3	7.6130	2.5	0.3992	0.9	2206.3	40.2	2186.4	22.2	2165.2	15.7	98
PP024-Z51	0.31	0.22	5092	0.11972	0.5	5.2196	1.1	0.3162	1.0	1952.1	8.6	1855.8	9.2	1771.2	15.0	91
Metagranodiorite PP027																
PP027-Z1	0.06	0.26	25809	0.13127	0.7	7.0531	1.8	0.3897	1.6	2115.0	12.4	2118.1	15.8	2121.4	29.6	100
PP027-Z4	0.03	0.07	45740	0.12878	0.6	6.8591	0.8	0.3863	0.6	2081.4	9.9	2093.4	7.0	2105.6	9.9	101
PP027-Z6	1.11	0.29	1354	0.12711	0.6	6.6408	1.1	0.3789	0.9	2058.4	10.0	2064.8	9.6	2071.2	16.6	101
PP027-Z8	0.85	0.16	1821	0.12049	0.9	5.3528	3.6	0.3222	3.4	1963.6	16.4	1877.3	30.3	1800.4	54.4	92
PP027-Z9	0.00	0.03	312329	0.12980	0.6	6.9904	1.0	0.3906	0.8	2095.3	10.8	2110.2	9.2	2125.5	15.2	101
PP027-Z10	0.04	0.25	46807	0.06600	2.3	1.1906	2.6	0.1308	1.3	806.4	46.8	796.2	14.3	792.6	9.7	98
PP027-Z13	0.00	0.27	384531	0.12720	0.7	6.4674	1.8	0.3688	1.6	2059.6	12.7	2041.5	15.6	2023.6	28.2	98
PP027-Z16	0.01	0.11	121431	0.13193	0.6	7.1451	0.9	0.3928	0.7	2123.8	11.0	2129.7	8.1	2135.8	12.0	101
PP027-Z21	0.03	0.19	50165	0.12994	0.7	7.0808	1.0	0.3952	0.7	2097.1	11.5	2121.6	8.7	2147.0	13.3	102
PP027-Z23	0.01	0.25	101508	0.13467	1.0	7.3740	1.2	0.3971	0.7	2159.8	17.2	2157.8	10.6	2155.8	12.0	100
PP027-Z24	0.69	0.12	2378	0.11098	0.7	3.6064	1.0	0.2357	0.7	1815.5	13.2	1550.9	8.2	1364.2	9.1	75
PP027-Z25	0.29	0.40	5195	0.13316	0.8	7.3114	1.3	0.3982	1.0	2140.0	14.5	2150.2	11.7	2160.9	18.5	101
PP027-Z27	0.01	0.19	275090	0.13019	0.8	7.3169	1.1	0.4076	0.8	2100.5	13.6	2150.9	9.7	2204.0	14.3	105
PP027-Z28	0.03	0.60	43263	0.13293	0.9	7.2003	1.2	0.3928	0.9	2137.1	15.2	2136.5	11.1	2136.0	16.3	100
PP027-Z38	0.01	0.23	188452	0.13033	0.8	7.2722	1.1	0.4047	0.7	2102.4	14.7	2145.4	10.0	2190.6	13.6	104
PP027-Z40	0.01	0.27	259267	0.12302	0.6	6.2224	1.0	0.3668	0.8	2000.5	11.1	2007.6	8.7	2014.5	13.4	101

CAPÍTULO 4 – DISCUSSÃO, CONCLUSÕES E RECOMENDAÇÕES DE TRABALHOS FUTUROS

4.1 – Discussão

4.1.1 – Definição do Arco Campinorte e formação de granulitos (Capítulo 2)

O estudo de geoquímica de rocha total de metagranitóides da Suíte Pau de Mel ao longo do Domínio Campinorte forneceu informações a respeito do ambiente tectônico de formação dessa suite. Essa avaliação permitiu sua divisão em três grupos de metagranitóides (tipos 1, 2 e 3) baseado em variações de elementos maiores e traço. A Suíte Pau de Mel mostra assinaturas cárneo-alcalina e cárnea, baixo conteúdo de potássio e natureza fracamente peraluminosa. Em diagrama Rb versus Y+Nb a maior parte das análises cai no campo de granitos de arco vulcânico (VAG) e uma minoria tendendo a composições de granitos intra-placa (WPG).

Baseado nessas observações e nas de outros autores (Kuyumjian et al., 2004; Oliveira et al., 2006; Giustina et al., 2009) esta tese apresenta a proposta de que o terreno a leste da Falha Rio dos Bois composto por rochas metavulcano-sedimentares e granitos associados formou-se em ambiente de arco de ilhas e deve ser referido como Arco Campinorte. O Arco Campinorte formou-se em ambiente tectônico dinâmico onde formação de orógeno, erosão, deposição, metamorfismo em fácies granulito e inversão ocorreu em menos de 100 Ma.

A existência de granulitos no Arco Campinorte também foi explorada nessa tese. Granulitos podem ser gerados por espessamento crustal durante subducção ou por extensão crustal que produz granulitos de alta-, ultra-alta temperatura (Gibson e Ireland, 1995; Brown, 2007; Touret and Huizenga, 2012). A paragênese hercynita + quartzo com cordierita, granada e silimanita observada nos paragranulitos do Arco Campinorte é argumentada como indicativa de metamorfismo de alta temperatura em fácies granulito (Waters, 1991), mas estudos paragenéticos são necessários nessas amostras para definir melhor o seu processo metamórfico e condições de formação. Idades U-Pb em zircão mostram dados concordantes entre núcleo e borda com idades por volta de 2.1 Ga. A conclusão do estudo desses granulitos é que eles marcam

evento paleoproterozoico de granulitação de alta-temperatura e baixa pressão aproximadamente 60 Ma após o evento principal de formação do Arco Campinorte.

Modelo tectônico que seja capaz de explicar formação de granulitos de alta temperatura em arcos acrecionários também deve reconciliar evidências estruturais de espessamento crustal no pico metamórfico com extensão litosférica (Collins, 2002; Brown, 2007; Touret and Huizenga, 2012). Afinamento crustal em função de ascensão da Moho ou grande volume de magmatismo poderiam prover fonte de calor para gerar o metamorfismo granulítico. A amostra de paragranulito (PP02) e de granulito máfico (RMR04) representariam formação de bacia concomitante a magmatismo básico, enquanto rochas intrusivas félsicas representadas pelos granodioritos PP030 e PP027 sugerem magmatismo pós-colisional de extensão desconhecida.

4.1.2 – Correlação da Sequência Campinorte com rochas metassedimentares dos Greenstone Belts de Guarinos e Crixás

As sequências metassedimentares do topo dos *greenstone belts* de Crixás e Guarinos são descritas por Jost et al. (2010) e Jost e Scandolara (2012) como originalmente depositadas em ambiente de back-arc sobre basaltos e komatiitos arqueanos. Esses produtos sedimentares e as idades de grãos de zircão detritico entre 2.2-2.06 Ga fornecido pelos autores sugerem deposição contemporânea àquela da Sequência Campinorte, se não parte da mesma bacia.

Várias evidências ligam a Sequência Campinorte às rochas metassedimentares do topo dos *greenstone belts* de Crixás e Guarinos e ao Domínio Crixás-Goiás como um todo.

- 1) O magmatismo que gerou rochas metavulcanoclásticas félsicas, metatufo-riolíticos e lápili metatufo da Sequência Campinorte poderia ser a fonte de fragmentos de púmice félsico descrito nos xistos de Crixás.
- 2) O magmatismo da Suíte Pau de Mel é contemporâneo ao do diorito paleoproterozoico (Jost et al., 1993) e de corpos félsicos (Queiroz et al., 1999) intrusivos no Domínio Crixás-Goiás.

- 3) Ausência de anomalias de Eu em diagramas de ETR de metagranitóides da Suíte Pau de Mel concorda com assinatura similar das sequências metassedimentares do Domínio Crixás-Goiás.
- 4) O soerguimento da Moho e o contraste gravimétrico interpretado como uma feição de colisão continental não distingue os limites dos domínios Crixás-Goiás e Campinorte.
- 5) Mapas de dados magnetométricos da CPRM mostram a continuidade do baixo magnético do Domo de Hidrolina e do alto magnético do *greenstone* de Guarinos por sob o Grupo Serra da Mesa, provavelmente representando continuidade dessas rochas Arqueanas sob o Domínio Campinorte.

Considerando a continuidade de anomalias magnéticas, ausência de contraste gravimétrico entre os domínios e tipos similares de rochas sedimentares e de mesma idade em ambos os domínios, esta tese propõe que os domínios Crixás-Goiás e Campinorte estavam amalgamados antes do Ciclo Brasiliiano e foram afetados por ele como um bloco crustal único.

4.1.3 – A formação do Maciço de Goiás (Capítulo 3)

A origem do Maciço de Goiás e sua relação com o Cráton do São Francisco foram discutidas por vários autores (e.g. Brito Neves and Cordani, 1991; Pimentel et al., 2000, 2011; Valeriano et al., 2008; Ferreira Filho et al., 2010). Dois ambientes tectônicos foram propostos para o Maciço de Goiás:

1) A primeira proposta é a de que o Maciço de Goiás é um microcontinente amalgamado à porção oeste do Paleocontinente São Francisco durante a Orogenia Brasiliiana. Este cenário foi inicialmente sugerido por Brito Neves e Cordani (1991) em um esboço altamente especulativo sem uma discussão associada e assumido como bem estabelecida em publicações posteriores (Pimentel et al., 2000; Blum et al., 2003; Pimentel et al., 2004; Queiroz et al., 2008; Valeriano et al., 2008; Ferreira Filho et al., 2010; Pimentel et al., 2011). Variações comumente citadas desta hipótese interpretam o Empurrão Rio Maranhão como uma sutura colisional entre os domínios Campinorte e Arraias-Cavalcante (Marangoni et al., 1995; Pimentel et al., 1999; Moraes et al., 2006;

Jost et al., 2013) ou que o microcontinente incluía apenas o Domínio Crixás-Goiás (Pimentel et al., 2000; Valeriano et al., 2008). Este cenário de um microcontinente alóctone arqueano-paleoproterozoico tornou-se uma forma de explicar a presença de rochas arqueanas sem qualquer terreno contemporâneo adjacente. Contrastos sísmicos e gravimétricos entre esses domínios têm sido argumentados como evidência em favor da hipótese do microcontinente (Assumpção et al., 2004; Soares et al., 2006).

2) A segunda proposta sugere o Maciço de Goiás como a extensão oeste do Paleocontinente São Francisco que foi amplamente afetado por eventos Brasilianos e, portanto, não cratonizada. Os quase 400 km do sistema de antepaís neoproterozoico cobrindo a região entre cráton e Maciço de Goiás (Grupo Bambuí) impede a avaliação dessa hipótese por meios diretos de mapeamento e amostragem. Dados sísmicos e estratigráficos (Martins-Neto, 2009), estruturais (D'el-Rey Silva et al., 2008) e gravimétricos (Pereira e Fuck, 2007), suportam o paleocontinente São Francisco como embasamento da cobertura sedimentar da Faixa Brasília (figuras 3, 4 e 5)

Após a sugestão de que os domínios Crixás-Goiás e Campinorte formavam um microcontinente por Brito Neves e Cordani (1991), dados gravimétricos que pareciam sugerir o Empurrão Rio Maranhão como uma descontinuidade típica de suturas colisionais foram apresentados por Marangoni et al. (1995). Dados gravimétricos e sísmicos posteriores foram interpretados como concordando com a hipótese ao indicar o soerguimento do limite Moho sob o Arco Magmático de Goiás e o Domínio Campinorte (Assumpção et al., 2004; Berrocal et al., 2004; Perosi, 2006; Ventura et al., 2011).

O Empurrão Rio Maranhão marca não apenas o limite entre os domínios Campinorte e Cavalcante-Arraias como também é a lapa dos complexos máfico-ultramáfico acamadados do Brasil central. Em um trabalho de geologia estrutural detalhado do Empurrão Rio Maranhão, D'el-Rey Silva et al. (2008) argumentam que o lineamento representa falha intraplaca desenvolvida entre 620-630 Ma através da crosta superior do Paleocontinente São Francisco durante encurtamento WNW-ESE do evento D₃.

Considerando a sugestão de que o Empurrão Rio Maranhão é uma feição intracontinental, não uma sutura colisional neoproterozoica, dados sísmicos e gravimétricos podem ser reinterpretados. Soares et al. (2006) argumentam que fortes contrastes de profundidade da Moho refletem a acresção de terrenos de idades diferentes. Esse contraste não é observado nos dados geofísicos entre o Domínio Campinorte e o Arco Magmático de Goiás, uma sutura colisional bem estabelecida na literatura (Pimentel et al., 2000). Forte contraste existe, no entanto, entre os domínios Campinorte e Cavalcante-Arraias, onde magmatismo sin-colisional Brasiliano não foi descrito até o momento. Para explicar esta incongruência, Soares et al. (2006) propuseram que a raiz do Arco Magmático de Goiás foi delaminada durante o evento final de colisão entre os paleocontinentes Amazônico e São Francisco. De forma semelhante, esta tese defende que a delaminação neoproterozoica proposta por Soares et al. (2006) afetou também a espessura crustal sob o Domínio Campinorte, enquanto o Domínio Cavalcante-Arraias foi preservado.

Granitos das subprovíncias Tocantins (~1.58 Ga) e Paraná (~1.76 Ga) (Pimentel et al., 1999; Pimentel and Botelho, 2001; Lenharo et al., 2002), contém evidências adicionais para refutar a hipótese do microcontinente alóctone. Enquanto granitos da Subprovíncia Paraná ocorrem somente no domínio Cavalcante-Arraias, granitos mais jovens da Subprovíncia Tocantins intrudiram ambos os domínios Cavalcante-Arraias e Campinorte. Esses granitos tipo-A são interpretados como relacionados a eventos de rifteamento que afetaram o Maciço de Goiás no Meso-Paleoproterozoico. Se ambos os domínios foram intrudidos pela Subprovíncia Tocantins, isso significa que eles estavam amalgamados antes do Mesoproterozoico.

Pimentel et al. (1991) fornecem idade U-Pb entre 1.57-1.61 Ga para o Granito Serra da Mesa da Subprovíncia Tocantins, aflorando a leste do Empurrão Rio Maranhão. Dados geocronológicos de granitos da Subprovíncia Tocantins no Domínio Campinorte estão limitados a uma “errócrona” Sr-Sr no Granito Serra Dourada de 1430 ± 24 Ma. Apesar de os granitos da Subprovíncia Tocantins não possuírem idades apropriadas no Domínio Campinorte, eles mostram feições petrológicas semelhantes entre si suficientes para serem estabelecidos como uma unidade única (Marini et al., 1992). Ao norte, o Complexo Alcalino de Peixe possui idade de cristalização de 1503 ± 3

Ma (Kitajima et al., 2001) mas suas relações genéticas com a Subprovíncia Tocantins são desconhecidas. A ocorrência de granitos tipo-A contemporâneos em ambos os lados do Empurrão Rio Maranhão favorece a hipótese desta tese de que os domínios Campinorte e Cavalcante-Arraias foram amalgamados antes do Mesoproterozoico e não no Neoproterozoico.

Uma vez que esses domínios estavam amalgamados desde pelo menos o Mesoproterozoico, e por conseguinte o Maciço de Goiás também já havia sido amalgamado, a relação do maciço com o Cráton São Francisco merece ser revista. Por exemplo a relação espacial de rochas de rifte com idades por volta de 1.76 Ga e 1.58 Ga também é observada em rochas do cráton. Por volta de 1.76 Ga tanto rochas vulcânicas basais do Grupo Araí no Maciço de Goiás (Pimentel et al., 1991) como da Formação Rio dos Remédios da Bacia do Espinhaço no Cráton São Francisco (Babinski et al., 1994; 1999) formaram-se durante extensão crustal. Por volta de 1.58 Ga, granitos intraplaca da Subprovíncia Tocantins intrudiram o Maciço de Goiás e rochas vulcânicas da Formação Bomba formaram-se na Bacia do Espinhaço, representando outro evento de rifteamento no centro do Cráton São Francisco (Danderfer et al., 2009). Essas mesmas idades também são registradas na Formação Tiradentes do Cinturão Mineiro, ao sul do Cráton São Francisco, onde idades por volta de 1.55 Ga em rochas metassedimentares são descritas como reativação do sistema do Rifte do Espinhaço (Ribeiro et al., 2013).

Esta tese defende que dados geológicos favorecem a interpretação de que o Maciço de Goiás representa a porção oeste do Paleocontinente São Francisco desde o Paleoproterozoico em vez de a hipótese mais aceita de que o maciço era um bloco alóctone durante o Ciclo Brasiliano. Delaminação da crosta inferior no Neoproterozoico afetou tanto o Arco Magmático de Goiás quanto o Domínio Campinorte e os presentes dados gravimétricos e sísmicos são ambíguos na interpretação de limites de suturas. Trabalhos geológicos e geocronológicos ao longo do Empurrão Rio Maranhão, particularmente a norte, devem confirmar a notória ausência de evidências de magmatismo colisional Neoproterozoico e favorecer o descarte da hipótese do microcontinente.

4.1.4 O Evento Franciscano de 2.2-2.0 Ga

O atual limite do Cráton São Francisco foi refinado por Alkmim (2004) baseado no traço original de Almeida (1977) de rochas arqueano-paleoproterozoicas cratonizadas margeadas por cinturões móveis neoproterozoicos (Figura 6). Os limites do paleocontinente, entretanto, eram certamente muito mais amplos que os cratônicos como sugerido por dados gravimétricos reinterpretados para exploração de diamantes (Pereira e Fuck 2005). Certos cinturões do cráton e a maior parte do embasamento bordejando-o são compostos por faixas Paleoproterozoicas formadas e amalgamadas entre 2.2 e 2.0 Ga. A correlação entre faixas paleoproterozoicas cratonizadas e deformadas e como elas se amalgamaram a blocos mais antigos para formar o paleocontinente requer detalhamento.

Um ciclo orogênico riaciano-orosiriano é amplamente reconhecido no Cráton São Francisco e é referido como Ciclo Trans-Amazônico. “Trans-Amazônico” foi inicialmente proposto por Hurley et al. (1968) em referência a um ciclo orogênico a partir de idades Rb-Sr de rocha total entre 2.25 e 2.0 Ga que registraram dois eventos tectono-magmáticos na porção oeste do Cráton Amazônico. A partir de então o termo passou a ser utilizado também para eventos orogênicos contemporâneos no Cráton São Francisco. O posicionamento relativo entre os paleocontinentes Amazônico e São Francisco, no entanto, é desconhecido pois eles somente vieram a ser acrescionados no Neoproterozoico. Apesar de rochas e idades do Escudo das Guianas, na porção norte do Cráton Amazônico, serem muito semelhantes às do Paleocontinente São Francisco (Rosa-Costa et al., 2006), o termo Trans-Amazônico tornou-se erroneamente uma generalização e sua referência no Cráton São Francisco e áreas pericratônicas deve ser evitada (Brito Neves, 2011).

Por outro lado, há abundantes evidências de evento Paleoproterozoico contemporâneo ao Trans-Amazônico no Cráton São Francisco e faixas adjacentes. Alguns exemplos são a Faixa Itabuna-Salvador-Curaçá (Barbosa e Sabaté, 2002; 2004), a Faixa Rio Capim (Oliveira et al., 2011), e os greenstone belts do Rio Itapicuru (Grisolia e Oliveira, 2012). Ao sul do cráton esses terrenos paleoproterozoicos são representados pelo Cinturão Mineiro e pelos complexos Mantiqueira e Juiz de Fora (Noce et al., 2007, Heilbron et al., 2010). Idades de pico metamórfico entre 2.04-2.07

Ga são descritas tanto ao norte quanto ao sul do Cráton São Francisco, respectivamente no Complexo Mantiqueira e Bloco Jequié (Barbosa and Sabaté, 2004; Heilbron et al., 2010). O ambiente tectônico dessas faixas paleoproterozoicas, seu intervalo de formação e suas idades de pico metamórfico são praticamente idênticos aos descritos nesta tese para o Maciço de Goiás. Da mesma forma, o Maciço de Goiás poderia ter se formado no mesmo ciclo orogenético proposto para o norte e sul do Cráton São Francisco (Barbosa e Sabaté, 2004; Heilbron et al., 2010).

Esta tese propõe que o ciclo orogenético entre 2.2-2.0 Ga responsável pelo amalgamamento do Paleocontinente São Francisco seja referido como Orogenia Franciscano. Este evento representa:

- a) a formação de orógenos acrecionários paleoproterozoicos (Campinorte, Rio Capim, Rio Itapicuru, Mantiqueira e Juiz de Fora),
- b) sistemas orogênicos colisionais entre blocos crustais mais antigos arqueano-paleoproterozoicos e arcos vulcânicos recém-formados (Suite Aurumina),
- c) amalgamamento desses arcos de ilha, arcos continentais e microcontinentes no Paleocontinente São Francisco.

Em função da Orogenia Franciscano, a porção brasileira do Paleocontinente São Francisco-Congo já era uma massa continental estável parte de Atlântica durante o amalgamamento do Supercontinente Columbia entre 1.9-1.8 Ga (Zhao et al., 2002).

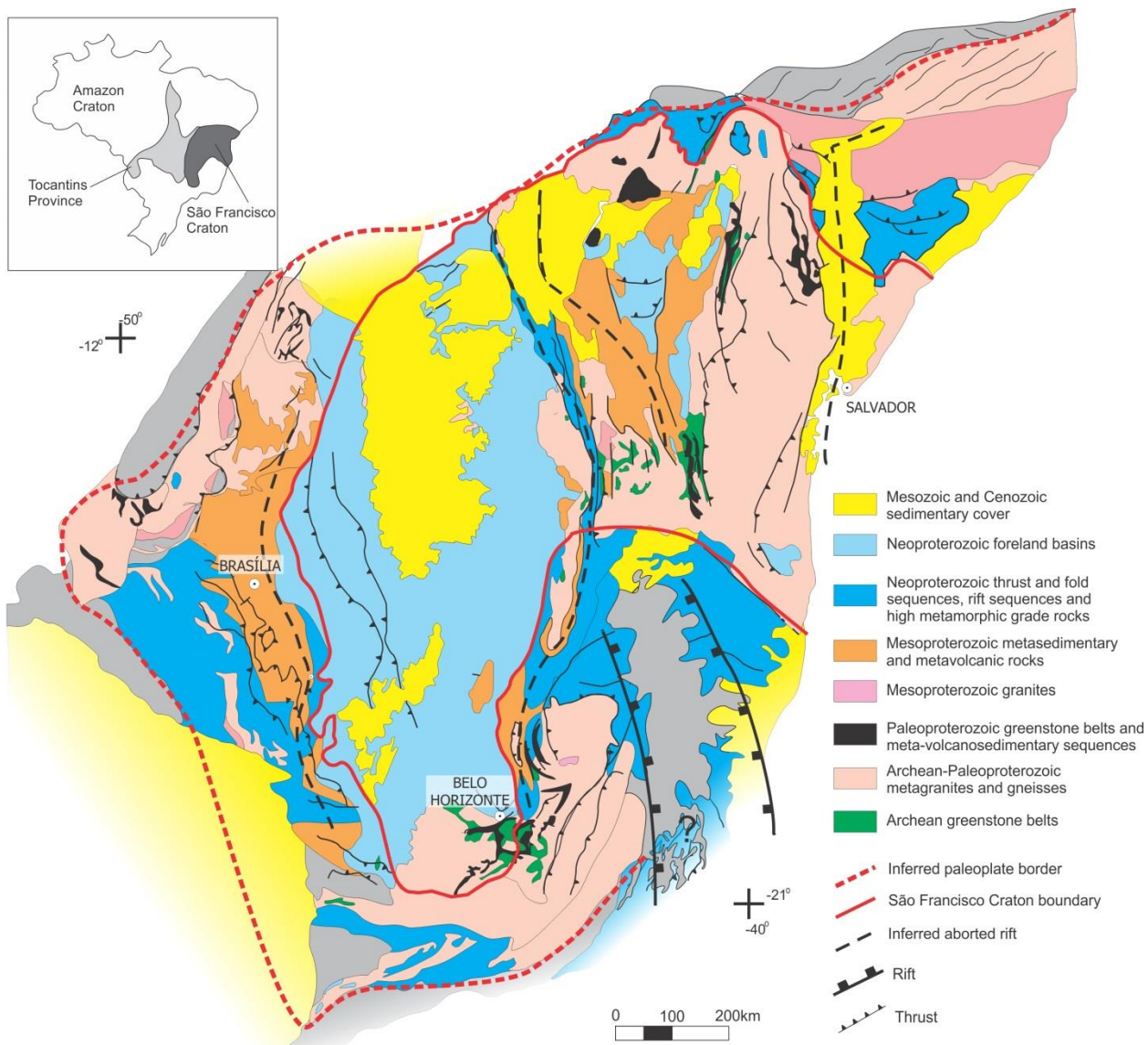


Figure 6 – Mapa geológico do Cráton São Francisco e cinturões pericratônicos sobrepostos por traço do limite inferido do craton e traço do limite inferido do paleocontinente baseado em dados magnéticos e gravimétricos (adaptado de Pereira e Fuck 2005 e Pereira, 2007).

4.2 - Conclusões

Os estudos desenvolvidos nesta tese contribuíram com a determinação de um arco magmático paleoproterozoico (Arco Campinorte) e a proposição de um modelo de formação para esse ambiente de arco de ilhas. A sugestão desse modelo também permitiu inferência a respeito da própria formação do Maciço de Goiás e do Paleocontinente São Francisco. As principais conclusões desta tese de doutoramento podem ser resumidas como se segue:

O embasamento norte da Faixa Brasília é predominantemente composto por terrenos paleoproterozoicos com graus variados de retrabalhamento pós amalgamamento por rifteamento, formação de bacias e magmatismo do Paleoproterozoico ao Neoproterozoico. Nomenclatura não-interpretativa deve ser favorecida em vez de nomes locais previamente propostos que careciam de discussão de componente tectônico regional. A proposta desta tese é que os terrenos arqueanos-paleoproterozoicos da Faixa Brasília norte sejam considerados parte do Maciço de Goiás e divididos de sudoeste a nordeste nos domínios Crixás-Goiás, Campinorte, Cavalcante-Arraias e Almas-Conceição do Tocantins.

Dados geoquímicos, ambientes tectônicos compatíveis e idades contemporâneas de cristalização concordam com definição desta tese de um arco de intraoceânico paleoproterozoico de extensão ainda desconhecida denominado Arco Campinorte e formado em sua maior parte entre 2.19 e 2.14 Ga. Este arco está em contato a oeste com o Arco Magmático de Goiás pela Falha Rio dos Bois e a leste com o Domínio Cavalcante-Arraias pelo Empurrão Rio Maranhão. O Arco Campinorte e terrenos contemporâneos do Domínio Cavalcante-Arraias não possuem relação genética clara, apesar de formados no mesmo período geológico.

Evidências texturais de influência de vulcanismo félscico, proximidade geográfica, tipos semelhantes de rocha, contemporaneidade de idade máxima de sedimentação e

idades modelo indicam que as sequências metassedimentares de Campinorte e dos *greenstone belts* de Crixás/Guarinos dividem a mesma fonte de sedimentos e provavelmente foram parte da mesma bacia. Dados sísmicos e gravimétricos estão de acordo com a teoria apresentada de uma bacia comum para os dois terrenos. Adicionalmente, assinaturas magnéticas de baixo de sinal analítico a partir do Domo de Hidrolina e alto sinal analítico do *Greenstone Belt* de Guarinos sob o Grupo Serra da Mesa podem implicar na existência de complexos TTG e *greenstone belts* na região presentemente mapeada como parte do Domínio Campinorte. Apesar dessas semelhanças, dada a predominância de rochas arqueanas TTG no Domínio Crixás-Goiás em comparação com metagranitos e rochas metassedimentares paleoproterozoicas no Domínio Campinorte, eles devem ser considerados dois terrenos distintos para fins de compartimentação tectônica.

Granulitos formaram-se em uma bacia no *back arc* do Arco Campinorte entre 2.14 e 2.09 Ga devido a *tectonic switching* e consequente afinamento da litosfera durante o pico do metamorfismo entre 2.11-2.08 Ga. O arco foi então rapidamente contraído e preservou paragêneses minerais do pico metamórfico Paleoproterozoico enquanto permitiu a formação de volume ainda desconhecido de magmatismo granítico mais jovem que 2.08 Ga.

O forte contraste sísmico/gravimétrico marcado em superfície pelo Empurrão Rio Maranhão tem sido amplamente interpretado como uma feição colisional e usado como evidência para apoiar a hipótese dos domínios Crixás-Goiás e Campinorte como um bloco alóctone acresionado ao Paleocontinente São Francisco no Ciclo Brasiliano. Evidências geológicas e geocronológicas para esta colisão, entretanto, não foram apresentadas até o momento. O contraste sísmico/gravimétrico pode ser explicado por um evento neoproterozoico de delaminação da crosta inferior que afetou tanto o Arco Magmático de Goiás quanto o terreno contra o qual ele foi acresionado, i.e., o

Domínio Campinorte, enquanto o limite Moho dos demais domínios permaneceu protegido e sem perturbações.

O Maciço de Goiás tem em comum com terranos contemporâneos do Cráton São Francisco:

- a) Magmatismo e formação de bacia associados a rifteamento Paleoproterozoico por volta de 1.77 Ga no Rift do Araí do Maciço de Goiás e na Bacia do Espinhaço do Cráton São Francisco;
- b) Magmatismo intraplaca Mesoproterozoico por volta de 1.58 Ga das suprovíncias Tocantins/Paraná nos domínios Campinorte e Cavalcante-Arraias e na Formação Bomba da Bacia do Espinhaço.

Essas feições comuns sugerem que o Maciço de Goiás foi afetado pelo mesmo evento intraplaca que o restante do Cráton São Francisco. Eventos magmáticos mesopaleoproterozoicos comuns ao Maciço de Goiás e ao cráton aliados à ausência de fortes lineamentos gravimétricos intracratônicos podem indicar que o Maciço de Goiás representa a borda oeste do Paleocontinente São Francisco desde o Paleoproterozoico.

Orógenos formados entre 2.2 e 2.0 Ga com pico metamórfico entre 2.12 e 2.05 Ga são outra feição comum entre domínios do Maciço de Goiás e terrenos do Cráton São Francisco e da borda sul do cráton. Este ciclo tectônico foi referido na literatura geológica como Trans-Amazônico, apesar do posicionamento relativo dos paleocontinentes Amazônico e São Francisco ser desconhecido. Esta tese propõe que o ciclo orogênico de 2.2 a 2.0 Ga comum ao Cráton São Francisco e faixas adjacentes seja referido como Ciclo Franciscano que representa a formação de arcos acrecionários Paleoproterozoicos como Campinorte, Juiz de Fora e Rio Capim e seu amalgamamento a blocos pré-Franciscano. O Ciclo Franciscano foi responsável pela formação do Paleocontinente São Francisco (-Congo?) que eventualmente tornou-se parte da Atlântica como bloco estável durante o amalgamamento do Supercontinente Columbia de 1.9 a 1.8 Ga.

A formação do Maciço de Goiás com detalhe para o Arco Campinorte pode ser resumida nas etapas:

~3.10 to 2.70 Ga Rochas TTG do Domínio Crixás-Goiás foram amalgamadas em bloco único.

~2.40-2.35 Ga Rochas TTG do Complexo Ribeirão das Areias no Domínio Almas-Conceição do Tocantins formaram-se provavelmente como um arco intraoceânico.

~2.2-2.0 Ciclo Franciscano e formação consequente de arcos e bacias. O Ciclo Franciscano gerou as sequências metassedimentares do topo dos *greenstone belts* de Crixás-Guarinos (Domínio Crixás-Goiás), Sequência Campinorte, Suíte Pau de Mel e granulitos (Domínio Campinorte), Suíte Aurumina (Domínio Cavalcante-Arraias) e Suítes 1 e 2 (Domínio Almas-Conceição do Tocantins). Uma colisão continente-continente provavelmente estava envolvida na geração do grande volume de magmatismo peraluminoso sin-colisional da Suite Aurumina e, portanto, um hipotético Bloco Ticunzal foi invocado no modelo tectônico para representar um fragmento crustal mais antigo e desconhecido. Vários outros arcos paleoproterozoicos formaram-se e foram amalgamados entre blocos arqueano-paleoproterozoicos para construir o Paleocontinente São Francisco. O pico metamórfico registrado pelo metamorfismo granulítico do Arco Campinorte, entre 2.11-2.08 Ga, marcou o estágio final de amalgamamento do Maciço de Goiás. Magmatismo pós-pico metamórfico está registrado em granitóides e gnaisses com idades entre 2.08-2.03 Ga.

1.78-1.75- O Maciço de Goiás passou por evento de rifteamento marcado pelo vulcanismo do Grupo Araí e intrusão de granitos contemporâneos da Subprovíncia Paranã. Um evento de idade semelhante é descrito no Cráton São Francisco e marcado em sua porção leste pelo Rifte do Espinhaço.

1.57-1.50 – Formação de granitos tipo-A da Subprovíncia Tocantins em ambiente de rifte que afetou o Domínio Campinorte e, em menor escala, o Domínio Cavalcante-Arraias. Este evento é observado na porção leste do Cráton São Francisco como o vulcanismo da Formação Bomba.

1.28-1.25 Ga – Rifteamento crustal e vulcanismo bimodal com consequente formação de crosta oceânica e bacia sedimentar (sequências Juscelândia e Palmeirópolis) e magmatismo máfico-ultramáfico contemporâneo do Complexo Sera da

Malacacheta. Evidências desse evento de rifteamento no Maciço de Goiás são restritas ao Domínio Campinorte.

0.80-0.77 Ga – Colisão do Arco Magmático de Goiás contra o Maciço de Goiás e consequente magmatismo máfico-ultramáfico de *back-arc* representado pelos complexos Barro Alto e Niquelândia. Esses complexos intrudiram ao longo de fraquezas crustais geradas no evento de rifte de ~1.28 Ga.

0.76-0.73 Ga – Pico metamórfico da colisão Arco-Continente responsável pela formação de granulitos nos complexos de Barro Alto e Niquelândia e perda de chumbo marcada pelo intersepto inferior de idades de rochas paleoproterozoicas do Arco Campinorte apresentadas nesta tese, bem marcados no granodiorito PP027 (785 ± 24 Ga) e no metagranodiorito PP012 (751 ± 28 Ga).

4.3 - Recomendações de trabalhos posteriores

O trabalho iniciado nesta tese focou-se no Arco Campinorte e nos terrenos adjacentes. Como parte do modelo tectônico proposto, houve a necessidade de invocar um hipotético bloco pré 2.2 Ga (Bloco Ticunzal) para explicar o magmatismo peraluminoso sin-colisional da Suíte Aurumina. Em função da ausência de dados petrológicos e geocronológicos publicados, essa sugestão é especulativa e se beneficiaria de uma discussão detalhada em um artigo sobre a suíte e seu significado tectônico.

As suprovíncias Tocantins e Paranã são ainda pobramente compreendidas e um trabalho mais detalhado de sua distribuição, zoneamento e feições petrológicas poderia ajudar a contribuir para o entendimento deste importante evento de rifte por volta de 1.56 Ga e que foi responsável pela formação de depósitos hidrotermais no Domínio Cavalcante-Arraias. Um estudo geocronológico de detalhe poderia ajudar a confirmar a ocorrência dessas rochas em ambos os lados do Empurrão Rio Maranhão.

Imagens RGB K-Th-U sugerem rochas ao redor dos granitos da Subprovíncia Tocantins com assinatura distinta tanto dos granitos quanto das rochas metassedimentares do Grupo Serra da Mesa e que poderiam representar rochas do Arco Campinorte. O estudo dessas rochas poderia fornecer maior compreensão sobre a extensão norte do Domínio Campinorte.

Trabalhos futuros poderiam enfocar o delineamento melhor dos contatos entre os domínios do Maciço de Goiás e determinar o traço dessas zonas de sutura.

Pouca informação existe disponível na literatura geológica sobre o Domínio Almas-Conceição do Tocantins e estudos futuros poderiam estudar melhor este terreno com implicações para formação de depósitos de ouro associados a *greenstone belts*.

A proposta de um ciclo orogênico entre 2.2-2.0 Ga responsável pela formação do Paleocontinente São Francisco encontra suporte na literatura do leste e do sul do cráton. O escopo desta tese não foi amplo o suficiente para explorar em detalhe as similaridades de todos os cinturões paleoproterozoicos que bordejam ou fazem parte do cráton e seria fundamental para literatura regional que essa comparação fosse traçada.

Referências

- Alkmim, F.F., 2004. O que faz de um cráton um cráton? O Cráton do São Francisco e as revelações almeidianas ao delimitá-lo. In: Mantesso-Neto, V., Bartorelli, A., Carneiro, C.D.R., Brito Neves, B.B. (Eds.), Geologia do Continente Sul-Americano. Evolução da Obra de Fernando Flávio Marques de Almeida, São Paulo, Beca, pp. 17–35.
- Almeida, F. F. M. 1967. Origem e Evolução da plataforma brasileira. Rio de Janeiro, DNPM, 36 p. (Boletim 241).
- Almeida, F.F.M., 1976. Evolução tectônica do Centro-Oeste brasileiro no Proterozóico Superior. Anais da Academia Brasileira de Ciências 40, 285-295.
- Almeida, F.F.M., 1977. O Cráton São Francisco. Revista Brasileira de Geociências 7, 349-364.
- Almeida, F. F. M. 1984. Província Tocantins, setor sudoeste. In: Almeida, F. F. M., Hasui, Y. (eds.) O Pré-Cambriano do Brasil, São Paulo, E. Blucher, 265-281.
- Alvarenga, C.J.S., Dardenne, M.A., Botelho, N.F., Lima, O.N.B., Machado, M.A., Almeida, T., 2007. Nota Explicativa das folhas SD.23-V-C-III (Monte alegre de Goiás), SD.23-V-C-V (Cavalcante) , SD.23-V-C-VI (Nova Roma). CPRM, 2007. 65 pp.
- Assumpção, M., An, M., Bianchi, M., França, G.S.L., Rocha, M., Barbosa, J.R., Berrocal, J., 2004. Seismic studies of the Brasília fold belt at the western border of the São Francisco Craton, Central Brazil, using receiver function, surface-wave dispersion and teleseismic tomography. Tectonophysics 388, 173-185.
- Babinski, M., Brito Neves, B.B., Machado, N., Noce, C.M., Uhlein, A., van Schmus,W.R., 1994. Problemas da metodologia U/Pb em zircões de vulcânicas continentais: caso do Grupo Rio dos Remédios, Supergrupo Espinhaço, no Estado da Bahia. In: Anais 42º Congresso Brasileiro de Geologia, Sociedade Brasileira de Geologia, Balneário Camboriú, vol. 2, pp. 409–410.
- Babinski, M., Pedreira, A.J., Brito Neves, B.B., van Schmus,W.R., 1999. Contribuição à geocronologia da Chapada Diamantina. In: Anais 7º Simpósio Nacional de

Estudos Tectônicos, Sociedade Brasileira de Geologia, Lençóis, Section 2, pp. 118–120.

- Barbosa, J.S.F., Sabaté, P., 2002. Geological features and the Paleoproterozoic collision of four Archean crustal segments of the São Francisco Craton, Bahia, Brazil. A synthesis. Anais da Academia Brasileira de Ciências 74, 343-359.
- Barbosa, J.S.F., Sabaté, P., 2004. Archean and Paleoproterozoic crust of the São Francisco Craton, Bahia, Brazil: geodynamic features. Precambrian Research 133, 1-27.
- Berrocal, J., Marangoni, Y., Sá, N.C., Fuck, R., Soares, J.E.P., Dantas, E., Perosi, F., Fernandes, C., 2004. Deep seismic refraction and gravity crustal model and tectonic deformation in Tocantins Province, Central Brazil. Tectonophysics 388, 187-199.
- Blum, M.L.B., Jost, H., Moraes, R.A.V., Pires, A.C.B., 2003. Caracterização dos complexos ortognáissicos arqueanos de goiás por gamaespectrometria aérea. Revista Brasileira de Geociências 33, 147-152.
- Botelho, N.F., Fuck, R.A., Dantas, E.L., Laux, J.L., Junges, S.L., 2006 The Paleoproterozoic Aurumina granite Suite, Goiás and Tocantins, whole rock geochemistry and U-Pb and Sm-Nd isotopic constrain. The Paleoproterozoic Record of the São Francisco Craton. Brazil, IGCP 509, 9-21.
- Brito Neves, B.B., Cordani, U.G., 1991. Tectonic evolution of South America during the Late Proterozoic. Precambrian Research 53, 23–40.
- Brito Neves, B.B., 2011. The Paleoproterozoic in the South American continent: Diversity in the geologic time. Journal of South American Earth Sciences 32, 270-286.
- Brown, M., 2007. Metamorphism, plate tectonics, and the supercontinent cycle. Earth Science Frontiers 14, 1-18.
- Collins, W.J., 2002. Hot orogens, tectonic switching, and creation of continental crust. Geology, 30, 535-538.
- Cordani, U.G., Hasui, Y., 1975. Comentários sobre os dados geocronológicos da Folha Goiás. In: Schobbenhaus et al., C. Carta Geológica do Brasil ao Milionésimo – SD-22 – Folha Goiás. Brasília, DNPM.

- Cruz, E.L.C.C., Kuyumjian, R.M., 1993. O embasamento da porção norte da Faixa Brasilia na região de Almas-Dianopolis (TO) e seu contexto geodinâmico durante o Brasiliano. In: SBG, Simpósio sobre o Cráton do São Francisco, 2, Salvador, Anais, 302-304.
- Cruz, E.L.C.C., Kuyumjian, R.M., 1998. The geology and tectonic evolution of the Tocantins granite-greenstone terrane: Almas-Dianópolis region, Tocantins State, Central Brazil. Revista Brasileira de Geociências 28, 173-182.
- Cruz, E.L.C.C., Kuyumjian, R.M., 1999. Mineralizações auríferas filoneanas do terreno granite-greenstone do Tocantins. Revista Brasileira de Geociências 29, 291-298.
- Cruz, E.L.C.C., Kuyumjian, R.M., Boaventura, G.R., 2003. Low-K calc-alkaline granitic series of southeastern Tocantins state: chemical evidence for two sources for the granite-gneissic complex in the Paleoproterozoic Almas-Dianópolis terrane. Revista Brasileira de Geociências 33, 125-136.
- Danderfer, A., Waele, B., Pedreira, A.J., Nalini, H.A., 2009. New geochronological constraints on the geological evolution of Espinhaço basin within the São Francisco Craton-Brazil. Precambrian Research 170, 116-128.
- Dardenne, M.A., 2000. The Brasília Fold Belt. In: Cordani, U.G., Milani, E.J., Thomaz Filho, A., Campos, D.A. (eds) Tectonic Evolution of South America. 31st International Geological Congress, Rio de Janeiro, 231-263.
- Delgado, I.M., Souza, J.D., Silva, L.C., Silveira Filho, N.C., Santos, R.A., Pedreira, A.J., Guimarães, J.T., Angelim, L.A., Vasconcelos, A.M., Gomes, I.P., Lacerda Filho, J.V., Valente, C.R., Perrota, M.M., Heinick, C.A., 2003. Província Tocantins, in: Buzzi, L.A., Schobbenhaus, C., Vidotti, R.M., Gonçalves, J.H. (Eds.), Geologia, Tectônica e Recursos Minerais do Brasil. CPRM, Rio de Janeiro, pp. 281-292.
- Ferreira Filho, C.F., Pimentel, M.M., Araújo, S.M., Laux, J.H., 2010. Layered intrusions and volcanic sequences in Central Brazil: Geological and geochronological constraints for Mesoproterozoic (1.25 Ga) and Neoproterozoic (0.79 Ga) igneous associations. Precambrian Research 183, 617-634.

- Fuck, R.A., Pimentel, M.M., Silva, L.J.H.D-R., 1994. Compartimentação Tectônica na porção oriental da Província Tocantins. In: Congresso Brasileiro de Geologia, 38, Anais., Balneário Camboriú, SBG. 215-216.
- Fuck, R.A., Dantas, E.L., Pimentel, M.M., Botelho, N.F., Armstrong, R., Laux, J.H., Junges, S.L., Soares, J.E., Praxedes, I.F., 2014. Paleoproterozoic crust-formation and reworking events in the Tocantins Province, central Brazil: A contribution for Atlantica supercontinent reconstruction. *Precambrian Research* (2014), <http://dx.doi.org/10.1016/j.precamres.2013.12.003>
- Gibson, G.M., Ireland, T.R., 1995. Granulite formation during continental extention in Fiordland, New Zealand. *Nature* 375, 479-482.
- Giustina, M.E.S.D., Oliveira, C.G., Pimentel, M.M., Melo, L.V., Fuck, R.A., Dantas, E.L., Buhn, B., 2009. U–Pb and Sm–Nd constraints on the nature of the Campinorte Sequence and related Paleoproterozoic juvenile orthogneisses, Tocantins Province, Central Brazil. *Geological Society of London Special Publication* 323, 255-269.
- Grisolia, M.F., Oliveira, E.P., 2012. Sediment provenance in the Palaeoproterozoic Rio Itapicuru greenstone belt, Brazil, indicates deposition on arc settings with a hidden 2.17-2.25 Ga substrate. *Journal of South American Earth Sciences* 38, 89-109.
- Heilbron, M., Duarte, B.P., Valeriano, C.M., Simonetti, A., Machado, N., Nogueira, J.R., 2010. Evolution of reworked Paleoproterozoic basement rocks within the Ribeira belt (Neoproterozoic), SE-Brazil, based on U–Pb geochronology: Implications for paleogeographic reconstructions of the São Francisco-Congo paleocontinent. *Precambrian Research* 178, 136-148.
- Hasui, Y., Almeida, F.F.M., 1970. Geocronologia do Centro-Oeste Brasileiro. *Boletim da Sociedade Brasileira de Geologia* 19, 5-26.
- Hurley, P.M., Melcher, G.C., Pinson, W.H., Fairbairn, H.W., 1968. Some orogenic episodes in South America by K-Ar and whole-rock Rb-Sr dating. *Canadian Journal of Earth Sciences* 5, 633-638.

- Jost, H., Pimentel, M.M., Fuck, R.A., Danni, J.C.M., Heaman, L., 1993. Idade U-Pb do diorito Posselândia, Hidrolina, Goiás. Revista Brasileira de Geociências 23, 352-355.
- Jost, H., Fuck, R., Brod, J.A., Dantas, E.L., Meneses, P.R., Assad, M.L.P., Pimentel, M.M., Blum, M.L.B., Silva, A.M., Spigolon, A.L.D., Maas, M.V.R., Souza, M.M., Fernandez, B.P., Faulstich, F.R.L., Macedo Jr., P.M.M., Schobbenhaus, C.N., Almeida, L., Silva, A.A.C., Anjos, C.W.D., Santos, A.P.M.R., Bubenick, A.N., Teixeira, A.A., Lima, B.E.M., Campos, M.O., Barjud, R.M., Carvalho, D.R., Scislewski, L.R., Lucianisarli C., Oliveira, D.P.L., 2001. Geologia dos terrenos arqueanos e proterozóicos da região de Crixás-Cedrolina, Goiás. Revista Brasileira de Geociências 31, 315-328.
- Jost, H., Chemale, F., Dussin, I.A., Tassinari, C.C.G., Martins, R., 2010. A U-Pb zircon Paleoproterozoic age for the metasedimentary host rocks and gold mineralization of the Crixás greenstone belt, Goiás, central Brazil. Ore Geology Reviews, 37:127-139.
- Jost, H., Rodrigues, V.G., Carvalho, M.J., Chemale, F., Marques, J.C., 2012. Estratigrafia e geocronologia do greenstone belt de Guarinos, Goiás. Geologia USP Série Científica 12, 31-48.
- Jost, H., Chemale Jr., F., Fuck, R.A., Dussin, I.A., 2013. Uvá Complex, the oldest orthogneiss of the Archean-Paleoproterozoic terrane of central Brazil. Journal of South American Earth Sciences 47, 201-212.
- Kitajima, L.F.W., Ruiz, J., Gehrels, G., Gaspar, J.C., 2001. Uranium-lead ages of zircon megacrysts and zircon included in corundum from Peixe Alkaline Complex (Brazil). In: III Simposio Sudamericano de Geología Isotópica, 2001, Pucón.
- Kuyumjian, R.M., Oliveira, C.G., Campos, J.E.G., Queiroz, C.L., 2004. Geologia do limite entre os terrenos Arqueanos e o Arco Magmático de Goiás na região de Chapada-Campinorte, Goiás. Revista Brasileira de Geociências 34, 329-334.
- Kuyumjian, R.M., Cruz, E.L.C.C., Araújo Filho, J.O., Moura, M.A., Guimarães, E.M., Pereira, K.M.S., 2012. Geologia e ocorrências de ouro do terreno granito-greenstone do Tocantins, TO: síntese do conhecimento e parâmetros para a exploração mineral. Revista Brasileira de Geociências 42, 213-228.

- Lenharo, S.L.R., Moura, M.A., Botelho, N.F., 2002. Petrogenetic and mineralization processes in Paleo- to Mesoproterozoic rapakivi granites: examples from Pitinga and Goiás, Brazil. *Precambrian Research* 119, 277-299.
- Marangoni, Y.R., Assumpção, M., Fernandes, E.P., 1995. Gravimetria em Goiás, Brasil. *Revista Brasileira de Geofísica* 13 (3), 205–219.
- Marini, O.J., Botelho, N.F., Rossi, P., 1992. Elementos terras raras em granitóides da Província Estanífera de Goiás. *Revista Brasileira de Geociências* 22, 61-72.
- Marques, G.C., 2010. Geologia dos grupos Araí e Serra da Mesa e seu embasamento no sul do Tocantins. Unpublished MSc thesis, Universidade de Brasília, 122 pp.
- Martins-Neto, M.A., 2009. Sequence stratigraphic framework of Proterozoic successions in eastern Brazil. *Marine and Petroleum Geology* 26, 163-176.
- Moraes, R., Fuck, A.R., Pimentel, M.M., Gioia, S.M.C.L., Hollanda, M.H.B.M., Armstrong, R., 2006. The bimodal rift-related volcanosedimentary sequence in Central Brazil: Mesoproterozoic extention and Neoproterozoic metamorphism. *Journal of South American Earth Sciences* 20, 287–301.
- Noce, C.M., Pedrosa-Soares, A.C., Silva, L.C., Armstrong, R., Piuzana, D., 2007. Evolution of polycyclic basement complexes in the Araçuaí Orogen, based on U-Pb SHRIMP data: Implications for Brazil–Africa links in Paleoproterozoic time. *Precambrian Research* 159, 60-78.
- Oliveira, C.G., Oliveira, F.B., Dantas, E.L., Fuck, R.A., 2006. Programa Geologia do Brasil – Folha Campinorte. FUB/CPRM, Brasília, 124.
- Oliveira, E.P., Souza, Z.S., McNaughton, N.J., Lafon, N.J., Costa, F.G., Figueiredo, A.M., 2011. The Rio Capim volcanic–plutonic–sedimentary belt, São Francisco Craton, Brazil: Geological, geochemical and isotopic evidence for oceanic arc accretion during Palaeoproterozoic continental collision. *Gondwana Research* 19, 735-750.
- Pereira, R.S., 2007. Cráton do São Francisco, kimberlitos e diamantes. University of Brasília, Unpublished PhD thesis, 200 p.
- Pereira, R.S., Fuck, R.A., 2005. Archean Nucleii and the distribution of kimberlite and related rocks in the São Francisco Craton, Brazil. *Revista Brasileira de Geociências* 35, 93-104.

- Perosi, F.A., 2006. Estrutura crustal do setor central da Província Tocantins utilizando ondas P, S e fases refletidas com dados de refração de sísmica profunda. Unpublished PhD thesis, Universidade de São Paulo, 162 p.
- Pimentel, M.M., Whitehouse, M.J., Viana, M.G., Fuck, R.A., Machado, N., 1997. The Mara Rosa Arc in the Tocantins Province: further evidence for Neoproterozoic crustal accretion in Central Brazil. *Precambrian Research* 81, 299-310.
- Pimentel, M.M., Botelho, N.F., 2001. Sr and Nd isotopic characteristics of 1.77-1.58 Ga rift-related granites and volcanics of the Goiás tin province, Central Brazil. *Anais da Academia Brasileira de Ciências* 73, 263-276.
- Pimentel, M.M., Fuck, R.A., 1992. Neoproterozoic crustal accretion in central Brazil. *Geology* 20, 375-379.
- Pimentel, M.M., Heaman, L., Fuck, R.A., Marini, O.J., 1991. U-Pb zircon geochronology of Precambrian tin-bearing continental-type acid magmatism in central Brazil. *Precambrian Research* 52, 321-335.
- Pimentel, M.M., Fuck, R.A., Silva, J.L.H., 1996. Dados Rb-Sr e Sm-Nd da região de Jussara- Goiás-Mossâmedes (GO), e o limite entre terrenos antigos do Maciço de Goiás e o Arco Magmático de Goiás. *Revista Brasileira de Geociências* 26, 61–70.
- Pimentel, M.M., Fuck, R.A., Botelho, N.F., 1999. Granites and the geodynamic history of the Neoproterozoic Brasília belt, Central Brazil: a review. *Lithos* 46, 463–483.
- Pimentel, M.M., Fuck, R.A., Ferreira Filho, C.F., Araújo, S.M., 2000. The basement of the Brasília Belt and the Goiás Magmatic Arc. In: Cordani, U.G., Milani, E.J., Thomaz Filho, A., Campos, D.A. (eds) *Tectonic Evolution of South America*. 31st International Geological Congress, Rio de Janeiro, 195–229.
- Pimentel, M.M., Dantas, E.L., Fuck, R.A., Armstrong, R.A., 2003. Shrimp and conventional U-Pb age, Sm-Nd isotopic characteristics and tectonic significance of the K-rich Itapuranga suite in Goiás, Central Brazil. *Anais da Academia Brasileira de Ciências* 75, 97-108.
- Pimentel, M.M., Ferreira Filho, C.F., Armstrong, R.A., 2004. SHRIMP U-Pb and Sm-Nd ages of the Niquelândia layered complex: Meso- (1.25 Ga) and Neoproterozoic

(0.79 Ga) extentional events in central Brazil. *Precambrian Research* 132, 133-153.

Pimentel, M.M., Rodrigues, J.B., Giustina, M. E. S., Junges, S., Matteini, M., Armstrong, R., 2011. The tectonic evolution of the Neoproterozoic Brasília Belt, central Brazil, based on SHRIMP and LA-ICPMS U-Pb sedimentary provenance data: A review. *Journal of South American Earth Sciences* 31, 345-357.

Queiroz C.L., Jost H., McNaughton N.J., 1999. U/Pb - SHRIMP ages of Crixás granite-greenstone belt terranes: from Archaean to Neoproterozoic. Extended abstract, Simpósio Nacional de Estudos Tectônicos, Lençóis, Anais, p. 35-37.

Queiroz, C.L., McNaughton, N.J., Fletcher, R., Jost, H., Barley, M.E., 2000. Polymetamorphic history of the Crixás-Açu Gneiss, Central Brazil: SHRIMP U-Pb evidence from titanite and zircon. *Revista Brasileira de Geociências* 30, 40-44.

Queiroz, C.L., Jost, H., Silva, L.C., McNaughton, N.J., 2008. U-Pb SHRIMP and Sm-Nd geochronology of granite-gneiss complexes and implications for the evolution of the Central Brazil Archean Terrain. *Journal of South American Earth Sciences* 26, 100-124.

Ribeiro, A., Teixeira, W., Dussin, I.A., Ávila, C.A., Nascimento, D., 2013. U-Pb LA-ICP-MS detrital zircon ages of the São João del Rei and Carandaí basins: New evidence of intermittent Proterozoic rifting in the São Francisco paleocontinent. *Gondwana Research* 24, 713-726.

Rosa-Costa, L.T., Lafon, J.M., Delor, C., 2006. Zircon geochronology and Sm-Nd isotopic study: Further constraints for the Archean and Paleoproterozoic geodynamical evolution of the southeastern Guiana Shield, north of Amazonian Craton, Brazil. *Gondwana Research* 10, 277-300.

Saboya, A.M., 2009. O vulcanismo em Monte Carmo e litoestratigrafia do Grupo Natividade, Estado do Tocantins. University of Brasília, Unpublished MSc thesis, 96 pp.

D'el-Rey Silva, J.H., Vasconcelos, M.A.R., Silva, D.V.G., 2008. Timing and role of the Maranhão River Thrust in the evolution of the Neoproterozoic Brasília Belt and Tocantins Province, central Brazil. *Gondwana Research* 13, 352-374.

- Soares, J.E., Berrocal, J., Fuck, R.A., Mooney, W.D., Ventura, D.B.R., 2006. Seismic characteristics of central Brazil crust and upper mantle: a deep seismic refraction study. *Journal of Geophysical Research*. doi:10.1029/2005JB003769 III-B12302.
- Touret, J.L.R., Huizenga, J.M., 2012. Fluid-assisted granulite metamorphism: a continental journey. *Gondwana Research* 21, 224-235.
- Valeriano, C.M., Pimentel, M.M., Heilbron, M., Almeida, J.C.H., Trouw, R.A.J., 2008. Tectonic evolution of the Brasília Belt, Central Brazil, and early assembly of Gondwana. *Geological Society, London, Special Publication* 294, 197-210.
- Ventura, D.B.R., Soares, J.E.P., Fuck, R.A., Caridade, L.C.C., 2011. Caracterização sísmica e gravimétrica da litosfera sob a linha de refração sísmica profunda de Porangatu, Província Tocantins, Brasil Central. *Revista Brasileira de Geociências* 41, 130-140.
- Waters, D.J., 1991. Hercynite-quartz granulites: phase relations, and implications for crustal processes. *European Journal of Mineralogy* 3, 367-386.
- Zhao, G., Cawood, P.A., Wilde, S.A., Sun, M., 2002. Review of global 2.1–1.8 Ga orogens: implications for a pre-Rodinia supercontinent. *Earth-Science Reviews* 59, 125-162.

